Switched observers and input-delay compensation for anti-lock brake systems

Trong Bien Hoang

UNIVERSITÉ PARIS-SUD

ÉCOLE DOCTORALE : STITS
Laboratoire des signaux et systèmes

DISCIPLINE : Physique

THÈSE DE DOCTORAT

soutenue le 04/04/2014

par

Trọng Biên HOÀNG

Switched observers and input-delay compensation for anti-lock brake systems

Directeur de thèse :	William Pasillas-Lépine	Chargé de recherche CNRS (L2S-Supélec)
Co-directeur de thèse :	Mariana Netto	Chargée de recherche IFSTTAR (IFSTTAR COSYS-LIVIC)
	Alexandre De Bernardinis	Chargé de recherche IFSTTAR (IFSTTAR COSYS-LTN)

Composition du jury :

Président du jury :	Hugues MOUNIER	Professeur à l'Université Paris Sud (L2S-Supélec)
Rapporteurs :	Gildas BESANÇON	Professeur à Grenoble INP (Gipsa-Lab)
	Mohammed M'SAAD	Professeur à l'ENSI Caen (GREYC-ENSICAEN)
Examinateurs :	Saïd MAMMAR	Professeur à l'Université d'Evry (IBISC-Evry Val d'Essonne)
	Alessandro CORREA-VICTORINO	Maître de Conférence à l'UTC (HEUDIASYC-UTC)

Xin dành tặng cho bố Bạo, mẹ Thành yêu quí,
chị Thảo, anh Minh, cháu Hải Đăng thân yêu,
người anh em Vĩnh và Tâm thân mến,
vợ yêu Duy Minh của anh,
và những đứa con yêu dấu trong tương lai của chúng mình.

Table des matières

Acknowledgments **1**

Preamble **3**

General introduction **9**

1 The Anti-lock Brake System **9**
1.1 History of ABS . . . 9
1.2 Structure of ABS . . . 10
1.3 Functional description of ABS . . . 11
1.4 Academic research on ABS . . . 13
1.5 Single-wheel dynamics . . . 14

2 Switching observation of singular systems **19**
2.1 A motivating example coming from ABS . . . 19
2.2 Observing a class of singular systems . . . 23
2.3 State of the art: Nonlinear observers and XBS estimation . . . 27
2.4 Main contributions of Part I . . . 32

3 Input-delay compensation for linearizable systems **37**
3.1 Brake actuator delay compensation . . . 37
3.2 Input delay compensation for nonlinear systems . . . 40
3.3 Existing methods for input delay compensation . . . 41
3.4 Main contributions of Part II . . . 44

I Switching observation of singular systems **47**

4 Switching observer for systems with linearizable error dynamics via singular time-scaling **49**
4.1 Introduction . . . 49
4.2 Switchings and singular observer design . . . 50
4.3 Conditions for singular linearizability . . . 55
4.4 Simulations on a simple example . . . 57
4.5 Proofs of main results . . . 59
Appendix A - Alternative proof of Lemma 4.2 . . . 68
Appendix B - Alternative proof of Theorem 4.1 . . . 71

5 Application for ABS: Extended braking stiffness estimation 77
5.1 Introduction . . . 77
5.2 System modelling . . . 79
5.3 Observer design (known road conditions) . . . 82
5.4 Observer design (unknown road conditions) . . . 87
5.5 Control design . . . 91
5.6 Conclusion . . . 95
Appendix A - Proof of Theorem 5.1 . . . 96
Appendix B - Stability conditions for the four-dimensional observer . . . 97

II Input-delay compensation for linearizable systems 103

6 Output tracking for restricted feedback linearizable systems with input time-delay 105
6.1 Introduction . . . 105
6.2 Scalar systems . . . 107
6.3 Restricted-feedback linearizable systems . . . 110
6.4 Simulations on a simple example . . . 115
6.5 Conclusion . . . 116
Appendix: Proof of main results . . . 117

7 Actuator delay compensation for ABS systems 119
7.1 System modelling . . . 120
7.2 Control design . . . 120
7.3 Simulation results . . . 126

8 Dynamic notch filter 129
8.1 Introduction . . . 129
8.2 Modelling of the dynamic notch filter . . . 130
8.3 Application to ABS . . . 133
8.4 Delay margin analysis . . . 136
8.5 Conclusion . . . 141
Appendix A - Alternative modelling of the notch filter . . . 142
Appendix B - Padé approximation technique . . . 143

Conclusion & Perspectives 151

Bibliography 155

Acknowledgments

First of all, I am deeply grateful to Dr. William Pasillas-Lépine, without whom this thesis would not have been possible. I'm very lucky to have a thesis advisor, who is so kind, brilliant and passionate. I greatly appreciated his invaluable guidance, his precious support and his consistent encouragement to my research work throughout these years.

I would also like to express my gratitude and appreciation to Dr. Mariana Netto and Dr. Alexandre De Bernardinis, for their presence at any time of my work, for their expert advice and listening that have been paramount for the success of this thesis. It was a great pleasure to work with them.

As well, I sincerely thank Prof. Witold Respondek and Dr. Antonio Loría for interesting and productive collaborations, which have been of great importance for my research work and have largely broaden my knowledge and my interests.

I would like to thank Prof. Gildas Besançon and Prof. Mohammed M'Saad for having accepted to review this document and for giving me interesting and precious comments to improve this work. I would also like to thank the examiners of my committee, Prof. Said Mammar, Prof. Hugues Mounier, and Dr. Alessandro Correa-Victorino, for having accepted to participate in the evaluation of this work.

A very warm thank you to all my colleagues and to the staff of Laboratoire des Signaux et Systèmes and Supélec for their help and support during my thesis. I would also like to thank all my friends for their friendship, brotherhood and continuous support in work and life.

My biggest thanks goes to my family, mẹ Thành, bố Bạo, chị Thảo, anh Minh, cháu Hải Đăng, người anh em Vĩnh và Tâm, for always standing by my side through the good times and the bad in my life. Finally, I want to express my deepest love and thanks to my loving wife, Duy Minh, for her support and encouragement during this important phase of my life. It's my pleasure to dedicate this thesis to them.

Preamble

In the automotive industry, safety is an aspect of paramount importance that has considerably evolved in recent decades. Beginning with passive safety systems, such as air bags, seat belt pretensioners or head restraints, the automobile safety increased considerably with the introduction of active safety systems, such as the Anti-lock Braking System (ABS), the Traction Control System (TCS), the Electronic Brake-force Distribution (EBD) and the Electronic Stability Program (ESP). Compared to passive safety systems, active safety systems are more effective since they not only help the driver to better control the vehicle, in order to avoid collisions, but also enhance the driving experience under various road conditions.

In the area of active safety systems, the ABS is perhaps the most important system since it is used by many other active safety systems. The purpose of the ABS is twofold. On the one hand, its objective is to avoid wheel lock-up in order to preserve the ability of the tyre to produce a lateral force, and thus to ensure vehicle maneuverability. On the other hand, the ABS aims at keeping the braking force in a neighborhood of its maximum to, as a result, minimize the braking distance.

Many control algorithms for ABS systems have been proposed in the literature since the introduction of the first ABS system by Bosch in 1978. In general, one can divide these control algorithms into two different types: those based on a regulation logic with wheel acceleration thresholds that are used by most commercial ABS systems; and those based on wheel slip control that are preferred in the large majority of academic algorithms. Each approach has its pros and cons [Shida 2010]. Oversimplifying, one can say that the strength of the first ones is their robustness; while that of the latter ones their short braking distances (on dry grounds) and their absence of limit cycles. At the midpoint of this industry/academy dichotomy, based on the concept of *extended braking stiffness* (XBS), a quite different class of ABS control strategies has been proposed by several researchers (see, e.g., [Sugai 1999] and [Ono 2003]). This concept combines the advantages from both the industrial and academic approaches. Nevertheless, since the slope of the tyre characteristic is not directly measurable, it introduces the question of real-time XBS estimation. The first part of this thesis is devoted to the study of this estimation problem and to a generalization of the proposed technique to a larger class of systems.

From the technological point of view, the design of ABS control systems is highly dependent on the ABS system characteristics and actuator performance. Current ABS control algorithms on passenger cars, for instance the Bosch ABS algorithm, are based on heuristics that are deeply associated to the hydraulic nature of the actuator. An interesting observation is that they seem to work properly only in the presence of a specific delay coming from the hydraulic actuation [Gerard 2012]. For brake systems that have different delays compared to those of hydraulic actuators,

like electric in-wheel motors (with a smaller delay) or pneumatic trailer brakes (with a bigger delay), they might be no longer suitable [Miller 2013]. Therefore, adapting standard ABS algorithms to other advanced actuators becomes an imperative goal in the automobile industry. This goal can be reached by the compensation of the delays induced by actuators. The second part of this thesis is focused on this issue, and to the generalization of the proposed technique to a particular class of nonlinear systems.

Throughout this thesis, we employ two different linearization techniques: the linearization of the error dynamics in the construction of model-based observers [Krener 1983] and the linearization based on restricted state feedback [Brockett 1979]. The former is one of the simplest ways to build an observer for dynamical systems with output and to analyze its convergence. The main idea is to transform the original nonlinear system via a coordinate change to a special form that admits an observer with a linear error dynamics and thus the observer gains can be easily computed to ensure the observer convergence. The latter is a classical method to control nonlinear systems by converting them into a controllable linear state equation via the cancellation of their nonlinearities.

It is worth mentioning that existing results for observer design by error linearization in the literature are only applied to the case of regular time scalings ([Guay 2002] and [Respondek 2004]). The thesis shows how to extend them to the case of singular time scalings. Besides, the thesis combines the classical state feedback linearization with a new method for the input delay compensation to resolve the output tracking problem for restricted feedback linearizable systems with input delays.

The thesis has been divided into three parts in order to make it more accessible for readers. The purpose of the introductive part, which is composed of the first three chapters (Chapters 1, 2, and 3), is to introduce the most important concepts and summarize the main contribution of the thesis. Chapter 1 provides some basic knowledge of ABS systems, such as its history, structure, operation and some research publications on ABS systems. At the end of Chapter 1, the single-wheel dynamics is briefly presented for the aim of facilitating the reading of Chapters 2 and 3. While in Chapter 2 the observation problem for a class of singular nonlinear systems is introduced, in Chapter 3 the input delay compensation of restricted feedback linearizable systems is discussed. These two chapters have the same structure with four subsections: a motivating example coming from ABS systems, a more complex and general problem that generalizes this example, a state of the art, and the main contributions of the chapter.

Part I of the thesis is devoted to showing our first main results in the observation of singular systems. Chapter 4 discusses the design and stability analysis of switching observers for a class of singular nonlinear systems [5]. Chapter 5 presents a concrete example of singular systems observation: the XBS estimation in the case of ABS systems [4].

Part II of the thesis is composed of Chapters 6, 7, and 8. Chapter 6 presents our second main results about the input delay compensation problem for restricted feedback linearizable systems [3], whereas Chapter 7 shows the compensation of the delays induced by actuators in ABS systems, in the context of wheel acceleration control. Although no theoretical results are given, numerical simulations show the effectiveness of the proposed method. Finally, Chapter 8 introduces a new method to reduce the impact of wheel-frequency oscillations for ABS systems in order to improve its robustness [1].

This thesis is the result of the collaboration between three different research laboratories: Laboratoire des signaux et systèmes (L2S), Supélec - CNRS - Université Paris-Sud; Laboratoire des technologies nouvelles (LTN), IFSTTAR; and Laboratoire sur les interactions véhicules-infrastructure-conducteurs (LIVIC), IFSTTAR. It has been supported by the Region Ile-de-France through the REGENEO project (RTRA Digiteo and DIM LSC). It has also received funding from the European Union Seventh Framework Programme [FP7/2007-2013] under grant agreement no 257462 HYCON2 Network of excellence.

[1] T.-B. Hoang, W. Pasillas-Lépine, and A. De Bernardinis. Reducing the impact of wheel-frequency oscillations in continuous and hybrid ABS strategies. In *Proceedings of the International Symposium on Advanced Vehicle Control*, Seoul (Korea), 2012.

[2] T.-B. Hoang, W. Pasillas-Lépine, and M. Netto. Closed-loop wheel-acceleration control based on an extended braking stiffness observer. In *Proceedings of the IEEE American Control Conference*, Washington (District of Columbia, USA), 2013.

[3] W. Pasillas-Lépine, A. Loría, and T.-B. Hoang. Output tracking for restricted feedback linearizable systems with input delay. In *Proceedings of the IEEE Conference on Decision and Control*, Florence (Italy), 2013.

[4] T.B. Hoang, W. Pasillas-Lépine, A. De Bernardinis, M. Netto. Extended braking stiffness estimation based on a switched observer. Accepted for publication in *IEEE Transactions on Control Systems Technology*.

[5] T.-B. Hoang, W. Pasillas-Lépine, and W. Respondek. A switching observer for systems with linearizable error dynamics via singular time-scaling. Accepted for the *International Symposium on Mathematical Theory of Networks and Systems*, Groningen (The Netherlands), 2014.

General introduction

Chapter 1

The Anti-lock Brake System

1.1 History of ABS

The history of ABS systems began in 1908 when the first hydraulic anti-skid braking controller was conceived for trains [Schinkel 2002]. During and after the Second World War, ABS systems gained new prominence with their implementation on aircraft brakes [Savaresi 2010]. In 1946, the Crane company pioneered the anti-skid braking industry with the development of the Hydro-Aire Hytrol Mark I for the Boeing/USAF B47 to avoid tyre blowout on dry concrete and spin-outs on icy runways. Soon after, in the 1950s, mechanical skid prevention devices were commonly installed on both military and commercial planes ([Madison 1969] and [Wellstead 1997]).

It wasn't until 1954 that the first ABS system was used in the automobile industry by Ford. This vehicle manufacturer offered an anti-skid system from a French aircraft as an option on the Lincoln Continental MK II [Savaresi 2010]. Nevertheless, it is worth mentioning that the first patents for skid preventing devices on cars have been introduced in the early 1930s [Johnson 2001]. In Europe, the patent [Mom 1932] was issued in 1932, while in the US a similar patent [Thomas 1936] was filed in 1936. By the late 1950s, the British Road Research Laboratory (RRL) tried to adapt a Dunlop aircraft anti-skidding device called Maxaret on a 1950 Morris 6 car. Then, the Maxaret was officially installed on Jensen FF sport car [Johnson 2009]. In the late 1960's and early 1970's, several vehicle manufacturers like Ford, Chrysler and General Motors offered different ABS brakes for their cars [Limpert 1992]. Since these early automotive ABS systems are based on analogue electronics and vacuum-actuated hydraulic modulators, they couldn't react quickly enough to prevent effectively wheel locking. As a result, they weren't able to provide greater vehicle control in a panic situation [Savaresi 2010].

In Europe, during the mid and late 1970's, digital electronics with integrated circuits and microprocessors have been adapted to ABS [Limpert 1992]. The first electronically controlled ABS, named *Tekline* was put on the market by Teldix (affiliate of Telefunken and Bendix Corporation) [Ohyay 2011]. In 1975, Bosch acquired Teldix and then in 1978 introduced the first completely electronic four-wheel multi-channel ABS system in the Mercedes-Benz S-Class [Bosch Automotive Technology 2013], starting the spread of the ABS technology in the automotive field. The modern age of ABS had begun.

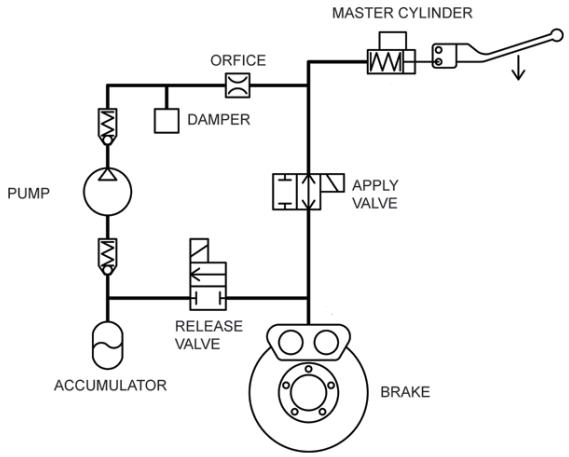

Figure 1.1: Hydraulic braking system [Daytona Tin Tec 2013]

Since the mid 1980s, vehicle manufacturers have introduced dozens of different anti-lock braking systems [Savaresi 2010]. These systems differ in their hardware configurations as well as in their control strategies. Today, 50 years after their first appearance on a commercial car, ABS is a standard equipment for passenger cars in the EU, the U.S., and Japan [Robert Bosch GmbH Press Release 2013]. Nevertheless, the research and development of ABS is far from complete. Each technological innovation on braking actuators or in the available sensors asks for a significant redesign of ABS systems. In particular, the advent of electric vehicles, for instance the in-wheel motor based electric vehicle, is likely to trigger a complete redesign of ABS strategies.

1.2 Structure of ABS

Depending on the hardware configurations, one can distinguish three different types of ABS architectures: hydraulic actuated brakes (HAB), electro-hydraulic brakes (EHB) and electro-mechanical brakes (EMB). The most used ABS system on commercial cars is the hydraulic actuated brake [Savaresi 2010]. The structure of a HAB system is shown in Figure 1.1. The master cylinder and the brake cylinder are connected by a pressure modulator that is composed of an apply valve, a release valve, a pump and a low pressure accumulator. The HAB has three different control actions: increase, hold and decrease of the brake pressure ([Savaresi 2010] and [Rajamani 2012]). These control actions are actuated by an electronic control unit (ECU) that uses information provided by wheel speed sensors. In the pressure increasing phase, the brake pressure exerted by the driver on the pedal is directly transmitted to the brake cylinder via the apply valve. The release valve is closed in

this phase. To decrease the brake pressure on the brake cylinder, the apply valve is closed and the release valve is open. The brake pressure is discharged via the release valve to the low pressure accumulator. The brake pressure is hold when the two valves are closed. The hydraulic fluid is pumped up from the accumulator to the master cylinder that is connected to the pedal. It is worth mentioning that modern ABS brakes use the so-called Pulse Width Modulation (PWM) to control the release and apply valves and therefore can obtain any increasing and decreasing slope of brake pressure. This leads to the introduction of some continuous controls for ABS brakes. Besides, the use of PWM allows the switchings between the three control actions to be faster and more accurate.

The other two brake system architectures: EHB and EMB have been introduced recently. EHB simplifies the design of the conventional HAB with the use of an electronic brake pedal. Unlike HAB, in which the driver directly activates the master cylinder by pressing on the brake pedal, the master cylinder in EHB is activated by an electric motor or pump that is regulated by a control unit [Bosch 2004]. The ECU uses information from a number of sensors to determine how much braking force on each wheel is needed. The system can then apply the necessary amount of hydraulic pressure to each caliper. The EMB system is fully electronic. The brake calipers are controlled by electronic actuators instead of hydraulic brake cylinders and the whole system is governed directly by a control unit instead of a high pressure master cylinder.

Even though EHB and EMB improve clearly the performance of automotive brakes in terms of the driver's comfort (no vibrations) or environment issues (no toxic oil), HAB is still the most used brake system in the automotive industry due to its long life-cycle and its high reliability [Savaresi 2010].

1.3 Functional description of ABS

Most ABS systems operate using the same general principles. When the driver brakes, the ECU uses the sensors to detect any wheel lock-up and rapidly provides the appropriate brake forces to prevent it from locking. Roughly speaking, if the ECU detects a deceleration in a certain wheel, indicating that a wheel lock-up may occur, it will reduce the brake force. As a consequence, the wheel will reaccelerate. Conversely, if the ECU detects a wheel turning significantly faster than the others, it will increase the brake force to the wheel to slow it down. This process is repeated continuously up to fifteen times per second to help the tyre maintain grip, so that the vehicle can turn around or stop with a shorter distance.

One of the most famous ABS algorithms is the Bosch algorithm whose functionality is based on the wheel acceleration thresholds (see, e.g., [Kiencke 2000], [Bosch 2004] and [Rajamani 2012]). Depending on the value of the wheel acceler-

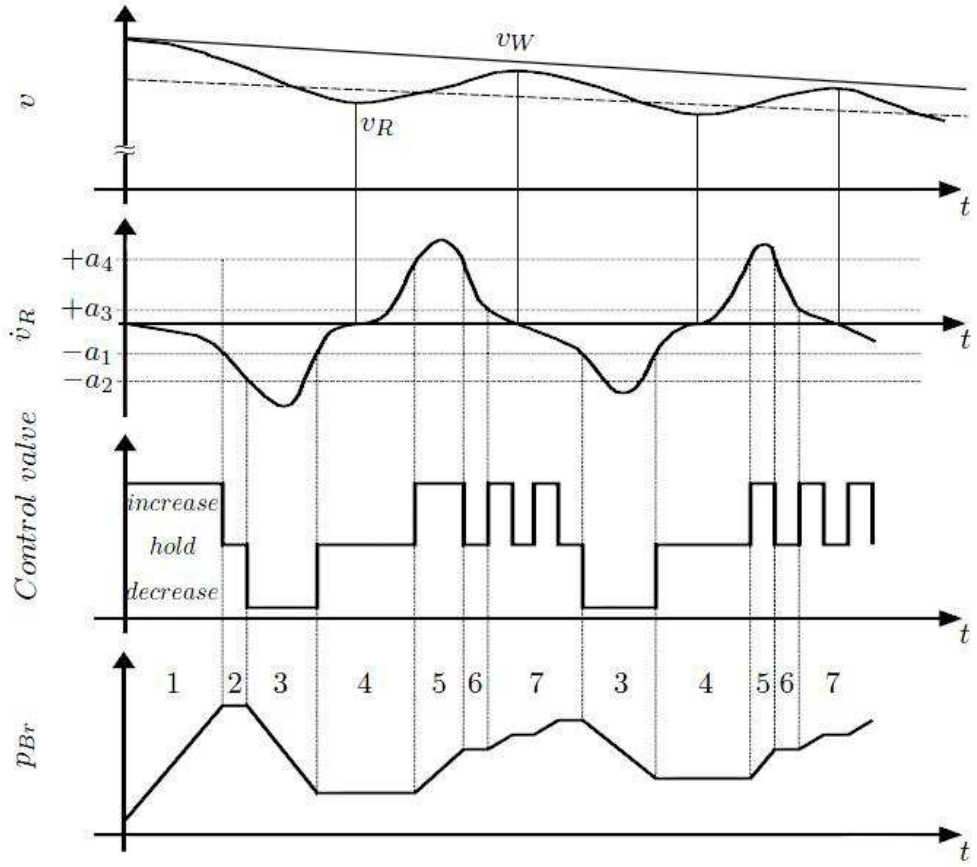

Figure 1.2: Cycle working of the ABS system with hydraulic brakes [Kiencke 2000]

ation, the ECU decides which control will be applied to the brake calipers. During the initial phase of braking, when the driver presses on the pedal, the driver's braking action is directly passed through to the brakes and the wheel deceleration increases (more negative). When the wheel deceleration $\dot{v}_R$ passes a threshold $-a_1$ (i.e. $\dot{v}_R < -a_1 < 0$), the ABS algorithm activates. The brake pressure is hold constant at the pressure value achieved when the wheel deceleration first exceeded $-a_1$. The reason comes from the fact that the threshold $-a_1$ might be exceeded within the stable zone of the tyre, then a reduction of brake pressure might lead to a waste in brake distance. If the wheel deceleration continues to increase and drops below a threshold $-a_2$ (i.e. $\dot{v}_R < -a_2 < -a_1$) then, at that point, the brake pressure is decreased. This will prevent the wheel from decelerating any further and could eventually result in the wheel gaining speed or accelerating. At the point where the wheel acceleration passes again $-a_1$, the brake pressure drop is stopped and held at a constant level. If the wheel actually starts accelerating and the wheel acceleration exceeds a relatively high threshold a_4 (i.e. $\dot{v}_R > a_4 \gg 0$), the brake pressure is

increased in order to prevent the wheel from over-accelerating. If the wheel acceleration drops smaller than a_4, but still bigger than a threshold (i.e. $0 < a_3 < \dot{v}_R < a_4$), the brake pressure is hold constant. When the wheel deceleration drops below a_3, the driver's braking action is again passed through to the brakes. If again the wheel deceleration passes $-a_1$, the brake pressure will be reduced immediately (the brake pressure holding phase no longer exists), the second cycle starts. Running through such cycles, the wheel will be prevented from locking, leading to an improved steering ability. Also, the brake force will be held close to its maximum, thus the braking distance is reduced.

1.4 Academic research on ABS

Since the introduction of the Bosch algorithm, in 1978, several scientific research publications have been devoted to the development of ABS algorithms. Among the proposed results, one can mainly distinguish between two completely different kinds of ABS designs: those based on logic switchings triggered by wheel acceleration thresholds and those based on wheel slip regulation. The wheel slip is generally defined as a percentage of the difference between the longitudinal wheel speed and the vehicle speed compared to the vehicle speed (see Section 1.5).

Approaches based on logic switchings triggered by wheel deceleration thresholds (see, e.g., [Leiber 1979], [Kuo 1992], [Kiencke 2000], [Bosch 2004] and the references therein) have quite interesting properties: they are very robust with respect to changes in the road conditions and are able to keep the wheel slip in a neighborhood of the optimal point, without using explicitly the value of the optimal setpoint. Most commercial ABS systems implemented on real cars use this control technique, for example the Bosch algorithm [Bosch 2004], presented in Section 1.3. However, a particularly unpleasant characteristic of these approaches is that they are often based on heuristic arguments, and thus tuning the thresholds involved in this kind of algorithms might be a difficult task. Besides, if the vehicle cannot detect the optimal value of the wheel slip, this approach fails to work. The reason is that these approaches cannot stabilize the system around an arbitrary reference that is not the optimal wheel slip.

Most ABS algorithms proposed in the scientific literature are based on wheel slip regulation (see, e.g., [Unsal 1999], [Johansen 2003], [Savaresi 2007], [Choi 2008], [Pasillas-Lépine 2012], and the references therein). They are often based on a clear mathematical background and they work even if there is no well-defined maximum point of the wheel slip for which the braking force is maximal. Nevertheless, these approaches are confronted with some drawbacks. Firstly, it is not always clear how one can estimate the wheel slip precisely. Secondly, the value of the optimal wheel slip is in general unknown and not easy to estimate in real-time.

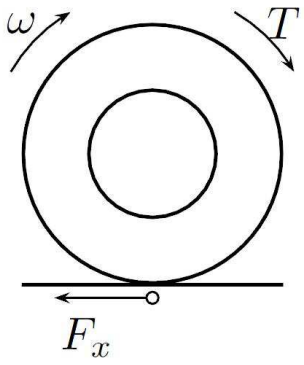

Figure 1.3: Single-wheel model

More recently, a quite different class of ABS control systems has been proposed by using the concept of extended braking stiffness (XBS) (see, e.g., [Gustafsson 1998], [Sugai 1999] and [Ono 2003]). In order to achieve the ABS control goal, these approaches aim to regulate the XBS in the neighborhood of its optimal value, which is always the same (zero). Their main difficulty comes from the fact that XBS must be estimated in real-time.

One can say that the XBS based-approaches take advantages of both the hybrid and continuous ABS since they doesn't use neither heuristic arguments nor the wheel slip or its optimal value. To our knowledge, the real-time XBS estimation methods that have been proposed in the literature are still quite complex or based on simplified hypothesis. Therefore, we present in Part I a simpler method to estimate XBS. Although these ABS algorithms have been validated in numerical simulations and (or) in test-rig experiments, their implementation in the context of new advanced actuators, like electric in-wheel motors, is still questionable. The analysis of [Gerard 2012] identifies that the main cause of failure of the five-phase hybrid control strategy proposed in [Pasillas-Lépine 2006] is the delays induced by the actuator. Motivated by this fact, Part II aims to provide a stable compensation of the actuator delay for ABS systems.

1.5 Single-wheel dynamics

In most research publications on the ABS, the single-wheel model is used for the preliminary design and testing. Despite its simplicity, all the basic phenomena related to ABS control appear in it [Gerard 2012]. In this section, we give a short description of a second order wheel dynamics that will be used in the two motivating examples of Chapters 2 et 3. We believe that this section can help the readers to better follow this thesis. More detailed descriptions of the system modelling for ABS

control or the tyre characteristics models will be presented later in Section 5.2.

A graphical representation of the torque balance for the single-wheel model is presented in Figure 1.3. The braking control torque applied to the wheel is denoted T_w, the angular velocity ω, and the tyre longitudinal force F_x. It is well known that the angular velocity of the wheel has the following dynamics

$$I\dot{\omega} = -RF_x + T_w, \tag{1.1}$$

where I denotes the moment of inertia of the wheel and R is the wheel's radius.

The tyre longitudinal force F_x depends on the road, tyre, and suspensions parameters. Most often, researchers consider that F_x is modelled by the relation

$$F_x = \mu(\lambda)F_z, \tag{1.2}$$

where F_z denotes the vertical load and $\mu(.)$ is called the *tyre characteristic*. In quasi-static condition, it can be simply assumed that F_z is constant. The friction between the wheel and the road is identified via the tyre characteristic $\mu(.)$. In the literature, the mathematical formulas of $\mu(.)$ are described as functions of the wheel slip whose coefficients depend on the road conditions. The wheel slip λ is defined as

$$\lambda = \frac{R\omega - v_x}{v_x}, \tag{1.3}$$

that is the difference between the wheel longitudinal velocity $R\omega$ and the vehicle speed v_x, normalized by the vehicle speed v_x. Figure 1.4 shows us the tyre characteristic $\mu(\lambda)$ for different road conditions.

In ABS control systems, two output variables are usually considered for regulation purposes: the wheel acceleration and the wheel slip. Thus, we define two state variables: x_1 is the wheel slip and $x_2 = R\frac{d\omega}{dt} - a_x(t)$ is the wheel acceleration offset (that is the difference between the acceleration of the wheel and that of the vehicle). Differentiating these state variable and using (1.1) as well as the definition of the wheel slip, we obtain the following dynamics

$$\begin{aligned} \frac{dx_1}{dt} &= \frac{1}{v_x(t)}\left(-a_x(t)x_1 + x_2\right) \\ \frac{dx_2}{dt} &= -\frac{a\mu'(x_1)}{v_x(t)}\left(-a_x(t)x_1 + x_2\right) + \frac{R}{I}\frac{dT_w}{dt} - \frac{da_x(t)}{dt}, \end{aligned} \tag{1.4}$$

where $a = \frac{R^2}{I}F_z$, v_x is the vehicle speed, $a_x(t) = dv_x/dt$ is the vehicle's longitudinal acceleration. The term $\mu'(.)$ is the derivative of the tyre characteristic $\mu(.)$ with respect to λ, and is called the *extended braking stiffness* or *XBS* [Ono 2003].

It is worth noting that in the context of an ABS-controlled braking manoeuvre, the

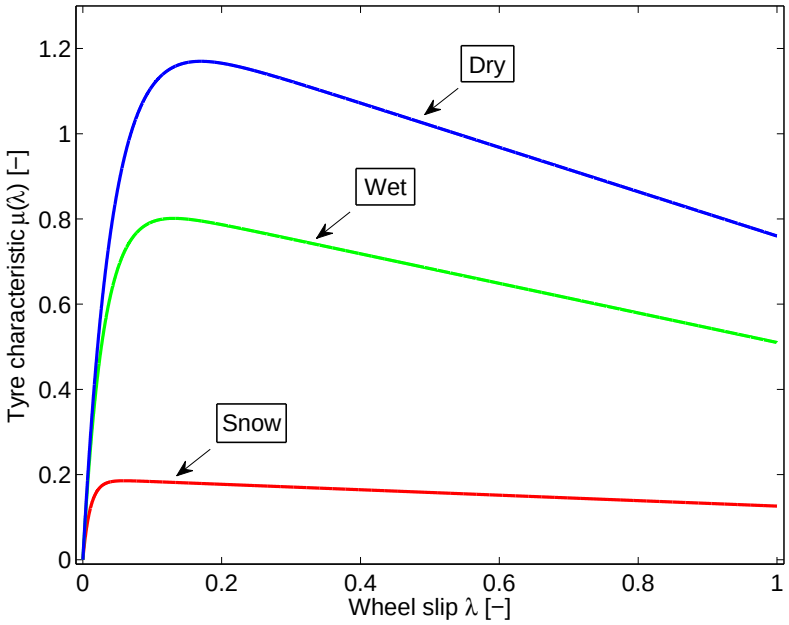

Figure 1.4: The tyre characteristic $\mu(\lambda)$ given by Burckhardt's model [Burckhardt 1993]

vehicle's acceleration $a_x(t)$ stays almost constant and close to the maximum value a_x^* allowed by the road's conditions [Pasillas-Lépine 2012]. Besides, the wheel slip λ remains relatively small. In such conditions, we can consider that $(-a_x x_1 + x_2) \simeq x_2$. This approximation is exact if the vehicle's speed $v_x(t)$ is constant, but it remains reasonable in the case of ABS manoeuvres [Gerard 2012]. We will return to discuss this assumption with more details in Section 5.2.2. Now, thanks to the previous approximation, a simpler dynamics is obtained

$$\begin{aligned} \frac{dx_1}{dt} &= \frac{1}{v_x(t)} x_2 \\ \frac{dx_2}{dt} &= -\frac{a}{v_x(t)} \mu'(x_1) x_2 + \frac{R}{I} \frac{dT_w}{dt}. \end{aligned} \tag{1.5}$$

The dynamics (1.5) plays a fundamental role in this thesis. It is used in the two illustrative examples of the general introduction, which motivated our research. Observing (1.5), it can be seen that the value of XBS is needed for the control design. Nevertheless, it cannot be computed due to the fact that the wheel slip λ cannot be measured and the parameters of the tyre characteristics $\mu(\lambda)$ are unknown. Therefore, in the motivating example of Chapter 2, the problem of observing XBS, i.e. $\mu'(\lambda)$, will be discussed. Moreover, the braking dynamics is often impacted by the delays coming from measurement filtering, tyre dynamics, and actuator limitations. It has

been shown that the delay is the main reason of the failure in implementing some theoretical ABS algorithms in test benches (see, e.g., [Solyom 2004], [Solyom 2003], [Kienhöfer 2008], and [Gerard 2012]). Thus, in the motivating example of Chapter 3, we will consider the problem of compensating the delays in the control input of (1.5).

Chapter 2

Switching observation of singular systems

The objective of this chapter is to introduce the observation problem for a class of singular systems. To that aim, we start by providing a simple example of singular switched observer design, associated to XBS observation, in the context of ABS. By choosing the control inputs that ensure the observability of the considered system, we can build a model-based observer and show that our observer is still valid in the singular case. The stability analysis of our observer is proved using tools for switched linear systems. This has motivated us to generalize this observer to a special class of singular nonlinear systems with a scalar output, which constitutes the main objective of Part I. Finally, we provide a review of existing related works and summarize our contributions.

2.1 A motivating example coming from ABS

2.1.1 Problem statement

As mentioned in the previous chapter, a certain knowledge on the tyre-road friction interface, such as the tyre characteristic or the XBS, is needed in the control design of ABS systems. Many different approaches for the identification of this interface have been proposed in the literature. Among them, an estimation of the XBS based on online least square methods for a wheel deceleration model has been presented in [Ono 2003]. In that work, two delicate assumptions are made when considering the model of the wheel acceleration. First, the XBS is considered as a constant. Second, it is assumed that the vehicle dynamics evolves considerably more slowly than the wheel dynamics. In other words, the wheel speed v_x is considered constant. We can write the wheel acceleration model used in [Ono 2003] in the following form

$$\begin{aligned} \frac{dz_1}{dt} &= -\frac{a}{v_x} z_1 z_2 + bu, \\ \frac{dz_2}{dt} &= 0 \end{aligned} \tag{2.1}$$

where $b = R/I$ and $u = dT_w/dt$ denotes the derivative of the control torque applied to the wheel. The state variables are defined as $z_1 = Rd\omega/dt$ and $z_2 = \mu'(\lambda)$. The reason for which we are interested in (2.1) is that it can be obtained directly from (1.5) shown in the previous section. If we replace z_1 and z_2 into the second equation of (1.5), we obtain the dynamics (2.1).

Now we consider the problem of estimating the unmeasured XBS in (2.1) provided that the wheel acceleration z_1 is measurable. In control theory, when the model of a physical system is well known and the measurements are not corrupted by a high level of noise, one can build a *state observer* to estimate the system's states by using measurements of the input and output of the real system. The model of the state observer is in fact obtained by copying the model of the real system. Besides, a correcting term should be added to the observer dynamics in order to stabilize it. The XBS is one of the state variables of (2.1), this raises the possibility of building a state observer to estimate the XBS.

2.1.2 The proposed method

A classical method for observing a nonlinear system is to build a high gain observer [Bornard 1991], [Gauthier 1992] and [Gauthier 1994]. If the nonlinear system is uniformly observable, which means that the observability does not depend on the control input, then it can be transformed into a special form called the *uniformly observable form* [Gauthier 1981]. A high-gain observer can be derived from this normal form and changed back to the original coordinates of the nonlinear system. Note that the uniform observability is the key point for the application of this method and, in fact, many other methods [Hammouri 2003]. A more detailed description of this last point will be presented later in Section 2.2.3.

Since (2.1) is not uniformly observable at $z_1 = 0$ (see Section 2.2.3), we cannot apply classical methods to observe it. Therefore, we propose to build directly the following model-based observer for (2.1)

$$\begin{aligned} \frac{d\widehat{z}_1}{dt} &= -\frac{a}{v_x} z_1 \widehat{z}_2 + bu + k_1(z_1)\frac{z_1}{v_x}(z_1 - \widehat{z}_1) \\ \frac{d\widehat{z}_2}{dt} &= k_2(z_1)\frac{z_1}{v_x}(z_1 - \widehat{z}_1), \end{aligned} \tag{2.2}$$

where $\widehat{z} = (\widehat{z}_1, \widehat{z}_2)^T$ is the observer state and $K = (k_1, k_2)^T$ is the observer gain. We define the error $e = z - \hat{z}$, and subtract (2.2) from (2.1) to obtain the following observer error dynamics

$$\frac{de}{dt} = \frac{z_1}{v_x} \begin{pmatrix} -k_1(z_1) & -a \\ -k_2(z_1) & 0 \end{pmatrix} e. \tag{2.3}$$

There are two important remarks in the observer dynamics (2.2). The first remark is that (2.2) is multiplied by the term z_1/v_x, except for the control input. The main reason is that with such an observer, the right hand side of the observer error dynamics (2.3) is also multiplied by z_1/v_x. It is important to highlight that if the right hand side of (2.3) is divided by z_1/v_x then (2.3) becomes linear. We will see later that the linearization of (2.3) can be done via a change of the time scale, which simplifies considerably the computation of the observer gains for which (2.3) is asymptotically stable. The second remark is that the observer gain K must be chosen depending on the sign of z_1. A possible choice is

$$k_i(z_1) = \begin{cases} k_i^+ & \text{if } z_1 > 0 \\ k_i^- & \text{if } z_1 < 0. \end{cases} \tag{2.4}$$

To understand the motivation behind the switching gain above, when the wheel acceleration z_1 is positive, let us suppose that there is a certain observer gain matrix K ensuring the asymptotically convergence of the observer (2.2). When z_1 changes its sign, the dynamics of (2.2) also changes. If the same gain matrix K is used, the observer (2.2) might be unstable. Therefore, the fact of choosing K depending on the sign of z_1 helps us to avoid this problem and the observer is thus convergent, independently on the sign of z_1.

We introduce the time scale

$$\tau(t) := \int_0^t \frac{|z_1(\sigma)|}{v_x} d\sigma. \tag{2.5}$$

In this new time scale, the system (2.3) can be written in the form of a *linear switched system* as follows

$$\frac{de}{d\tau} = \begin{cases} A_+ e = \begin{pmatrix} -k_1^+ & -a \\ -k_2^+ & 0 \end{pmatrix} e & \text{if } z_1 > 0 \\ \\ A_- e = \begin{pmatrix} k_1^- & a \\ k_2^- & 0 \end{pmatrix} e & \text{if } z_1 < 0. \end{cases} \tag{2.6}$$

Note that $dt/d\tau = |z_1|/v_x \geq 0$, independently of the value of z_1. This property ensures the conservation of the observer convergence, meaning that if the observer is asymptotically stable in the time scale τ, it is also asymptotically stable in the original time scale t. Such a time scale τ is called *regular* if the scalar function z_1/v_x is never zero. It is called *singular* if it may vanish.

When the time scale is singular, the observer error dynamics (2.3) is still valid in the original time scale t and equal to zero in this case. At that instant, we must

ensure that the control input u is different from zero in order to make the dynamics of the observer transversal to the subspace characterized by $z_1 = 0$. And the sign of the control input will decide the direction of the switch from A_+ and A_- or vice versa. Thanks to the fact that the control torque u in ABS systems is not equal to zero when the wheel acceleration z_1 is zero, the observer (2.2) is always valid to estimate the states of (2.1).

2.1.3 The key point

The remaining problem is to find the observer gain $K(z_1)$ that makes the system asymptotically stable. Usually, the stability analysis of an observer is done through that of the observer error. It can be seen that (2.6) belongs to the class of autonomous switched linear systems. In the literature, the stability analysis problems for switched systems are mostly solved by Lyapunov-like theorems [Lin 2009]. However, these Lyapunov-like theorems cannot be used to prove the asymptotic stability of our switching system (2.6) and only the uniform stability can be obtained [Balde 2009]. Indeed, one can easily find the conditions on the observer gain $K(z_1)$ such that each subsystem is asymptotically stable (i.e. the two matrices A_+ and A_- are 2×2 real Hurwitz matrices). Then, following [Balde 2009], define $\upsilon(.) := [0, \infty[\rightarrow \{+, -\}$ as a measurable switching function and describe (2.6) using $\upsilon(.)$ in the following form

$$\frac{de}{d\tau} = \upsilon(s)A_+e(\tau) + (1 - \upsilon(\tau))A_-e(\tau). \tag{2.7}$$

Next, define the function $\Gamma(A_+, A_-) := 1/2(tr(A_+)tr(A_-) - tr(A_+A_-))$ where $tr(X)$ denotes the trace of a matrix X. In Theorem 1 of [Balde 2009], the authors analyze the stability of (2.7) through $\Gamma(A_+, A_-)$. It is easy to check that for our switched system (2.7), we have $\Gamma(A_+, A_-) \leq -\sqrt{det(A_+)det(A_-)}$ where $det(X)$ denotes the determinant of a matrix X. Therefore, the switched system (2.7) is either unbounded or uniformly stable, but never uniformly asymptotically stable (see [Balde 2009, Theorem 1]).

Recently, some LaSalle-like results on the stability of switched linear systems have been proposed ([Hespanha 1999] and [Hespanha 2004]). The stability properties are proved via regularity assumptions on the set of switching signals. The authors show that if the switchings are not arbitrarily fast, i.e. slow switchings, it is then possible to maintain the asymptotic stability of linear switched systems. Under slow switchings, applying Theorem 4 of [Hespanha 2004], one can prove that (2.6) is uniformly globally exponentially stable if there exists a positive definite symmetric matrix P that satisfies, simultaneously, the two non-strict Lyapunov equations

$$A_+^T P + PA_+ = -Q \quad \text{and} \quad A_-^T P + PA_- = -Q, \tag{2.8}$$

where A_+ and A_- are defined in (2.6) and $Q = -C^T C$. Since the output of (2.2) is z_1 then $C = \begin{pmatrix} 1 & 0 \end{pmatrix}$.

One example of P is

$$P = \begin{pmatrix} \frac{1}{a} & 0 \\ 0 & 1 \end{pmatrix}, \tag{2.9}$$

with $k_1^+ = a/2$, $k_1^- = 1/2$ and $k_2^+ = k_2^- = -1$.

Due to the fact that (2.1) cannot be transformed in the uniformly observable form when $z_1 = 0$, the well-known method to construct a high gain observer cannot be applied. Nevertheless, we can design an observer like (2.2) to estimate the state variables of (2.1). The asymptotic stability of the observer is ensured by two conditions: the control input is different to zero when (2.1) is singular and the switchings between two subsystems of (2.6) are slow. Motivated by the construction of (2.2), in the next section, we devote our attention to the observer design for a more general class of singular nonlinear systems (that cannot be written in the uniformly observable form).

2.2 Observing a class of singular systems

2.2.1 Problem statement

Consider a class of nonlinear systems with scalar output of the form

$$\begin{aligned} \frac{dz}{dt} &= s(y)Az + Bu \\ y &= Cz, \end{aligned} \tag{2.10}$$

where $z(t) \in \mathbb{R}^n$ and $y(t) \in \mathbb{R}$ is the measurement. We assume that s is a strictly increasing real-valued function depending on the scalar output y and that $s(0) = 0$. We assume additionally that the pair (A, C) is observable, which means that the rank of the matrix $(C, CA, \ldots, CA^{n-1})^T$ is equal to n.

It is obvious to see that the dynamics (2.1) is a particular case of (2.10), since it can be written as follows

$$\begin{aligned} \frac{dz}{dt} &= \frac{z_1}{v_x} \begin{pmatrix} 0 & -a \\ 0 & 0 \end{pmatrix} z + \begin{pmatrix} b \\ 0 \end{pmatrix} u \\ y &= \begin{pmatrix} 1 & 0 \end{pmatrix} z, \end{aligned} \tag{2.11}$$

where $z = (z_1, z_2)^T$, $A = \begin{pmatrix} 0 & -a \\ 0 & 0 \end{pmatrix}$, $B = \begin{pmatrix} b \\ 0 \end{pmatrix}$, and $C = \begin{pmatrix} 1 & 0 \end{pmatrix}$. The function $s(y) = z_1/v_x = y/v_x$ and it is clear that $s(0) = 0$. Besides, the pair (A, C) is observable since the rank of $(C, CA)^T$ is equal to 2.

In a more complicated case where XBS isn't constant, the single-wheel model is

described by a third-order dynamics (see Section 5.3.2) as follows

$$\begin{aligned} \frac{dz}{dt} &= \frac{z_1}{v_x}\begin{pmatrix} 0 & -a & 0 \\ 0 & c & 1 \\ 0 & 0 & 0 \end{pmatrix} z + \begin{pmatrix} b \\ 0 \\ 0 \end{pmatrix} u \\ y &= \begin{pmatrix} 1 & 0 & 0 \end{pmatrix} z, \end{aligned} \tag{2.12}$$

where $z = (z_1, z_2, z_3)^T$. It is not difficult to check that this dynamics also belongs to (2.10). Motivated by the fact that the problem of observing (2.1) is solved in the previous section, we wonder whether a singular switched observer can still be built to observe (2.10).

2.2.2 The proposed method

We will follow the same procedure as in Section 2.1.2 to construct the observer for (2.10). First, we build the following model-based observer

$$\frac{d\hat{z}}{dt} = s(y)(A\hat{z} + K(s(y))(y - C\hat{z})) + Bu, \tag{2.13}$$

that yields an error $e = z - \hat{z}$ that satisfies

$$\frac{de}{dt} = s(y)(A - K(s(y))C)e. \tag{2.14}$$

Since the real-valued function $s(y)$ might be positive or negative, we define the new time scale τ as follows

$$\tau(t) := \int_0^t |s(y(\sigma))| d\sigma, \tag{2.15}$$

to ensure that $dt/d\tau \geq 0$, independently of the sign of $s(y)$. We recall that the time re-scaling τ is called regular if the scalar-valued function s is never zero and singular if it may vanish. When the time re-scaling is singular, the observer error dynamics becomes

$$\frac{de}{d\tau} = \begin{cases} A_+ e = (A - K^+ C)e & \text{if : } s(y) > 0 \\ A_- e = (-A + K^- C)e & \text{if : } s(y) < 0, \end{cases} \tag{2.16}$$

where

$$K(s(y)) = \begin{cases} K^+ & \text{if : } s(y) > 0 \\ K^- & \text{if : } s(y) < 0. \end{cases} \tag{2.17}$$

Despite of the fact that the time re-scaling is singular, the observer can still be constructed in the original time scale, its dynamics depends on the control input $u(t)$. If the control at that time instant is equal to zero, the observer will stay forever in the invariant subspace that is characterized by $y(t) = 0$. In order to avoid this problem, we assume that $u(t) \neq 0$ when $y(t) = 0$. Independently of the sign of the control input, the observer dynamics is thus always transversal to the subspace characterized by $y(t) = 0$.

In a nutshell, the general problem of observers synthesis for singular nonlinear systems studied in Part I can be summarized follows:

Objective of Part I: Given a singular nonlinear observer dynamics with scalar output as (2.10), show that it is always possible to find a set of observer gains for which the switching observer error (2.16) is uniformly exponentially stable.

2.2.3 Uniform observability

In this section, we will explain the reason for which (2.10) cannot be transformed into the uniformly observable form. But before doing that let's recall here some classical concepts. Consider a single-input single-output control-affine system of the form [Gauthier 1981]

$$\begin{aligned} \frac{dz}{dt} &= f(z) + g(z)u \\ y &= h(z), \end{aligned} \tag{2.18}$$

where $z \in \mathbb{R}^n$, $u \in \mathbb{R}$ and $y \in \mathbb{R}$. It is assumed that f and g are complete C^∞-smooth vector fields on $\mathbb{R}^n$, and that h is a C^∞ real-valued function. If the system (2.18) is uniformly observable, by an appropriate (local) change of coordinates $\xi = \phi(z)$, it can be transformed into the *uniformly observable form* [Gauthier 1981]

$$\begin{aligned} \frac{d\xi_1}{dt} &= \xi_2 + \overline{g}_1(\xi_1)u \\ &\vdots \\ \frac{d\xi_{n-1}}{dt} &= \xi_n + \overline{g}_{k-1}(\xi_1, \ldots, \xi_{n-1})u \\ \frac{d\xi_n}{dt} &= \overline{f}_n(\xi_1, \ldots, \xi_n) + \overline{g}_n(\xi_1, \ldots, \xi_n)u \\ y &= \xi_1. \end{aligned} \tag{2.19}$$

Here, the *uniform* adjective refers to the independence of the observability of (2.18) with respect to the control input u. Indeed, from the knowledge of u and $y = \xi_1$ we

can determine ξ_2, from the knowledge of u, y and ξ_2 we can determine ξ_3, and so on.

Following [Gauthier 1981] (see also, e.g., [Respondek 2002] and [Hammouri 2003]), the necessary and sufficient conditions for (2.18) to admit locally at any z the uniformly observable form (2.19) is that (a) dim span $\{dh, \dots, dL_f^{n-1}h\} = n$ and that (b) in the neighborhood of z

$$[D_j, g] \subset D_j, \tag{2.20}$$

for any $1 \leq j \leq n$, where $D_j = \ker\{dh, \dots, dL_f^{n-1}h\}$. The term $L_f h$ stands for the Lie derivative of the smooth function h with respect to the smooth vector field f, which is defined as

$$L_f h(z) = dh(z) \cdot f(z) = \sum_{i=1}^{n} \frac{\partial h}{\partial z_i} f(z), \tag{2.21}$$

and

$$L_f^k h = L_f(L_f^{k-1}h). \tag{2.22}$$

For the problem of observing a system of the form (2.18) that can be converted into the form (2.19), instead of building directly an observer based on (2.18), one builds the observer based on the uniformly observable form (2.19) and then transform back to the original coordinates by applying $z = \phi^{-1}(\xi)$. The interest of this approach is that the asymptotic convergence of the observer can be guaranteed if the observer gain is chosen sufficiently large. This method, however, is mainly applied when there is no noise in the dynamics nor on the observations. For more details of this method, we refer the reader to [Bornard 1991], [Gauthier 1992] and [Gauthier 1994].

It can be seen that the class of systems (2.10) is a special class of (2.18) with

$$f(z) = s(y)Az, \qquad g(z) = B \quad \text{and} \quad h(z) = Cz. \tag{2.23}$$

Besides, it is not difficult to see that the condition (a) is not satisfied when $y = 0$. Indeed, the fact that $y = 0$ implies $s(y) = 0$, then

$$\dim \text{span}\{dh, \dots, dL_f^{n-1}h\} = \dim \text{span}\{C, CAs(y), \dots, CA^{n-1}s(y)\} = 1 < n. \tag{2.24}$$

Thus, (2.10) is not uniformly locally observable at $y = 0$. We say that (2.10) is singular when $y = 0$. Due to this singularity, it is not possible to design the observer for (2.10) using the mentioned-above approach. This clarifies the motivation for our research: construct an observer for (2.10) that works even in the singular case.

2.3 State of the art: Nonlinear observers and XBS estimation

2.3.1 Linear observers

The knowledge of the system's state is necessary to solve several control problems such as stabilization, optimization, or decoupling problems. In many practical cases, however, not all the states of the system are accessible from direct measurements. In such situations, a reasonable approximation of the unmeasurable states is needed. A device that reconstructs an approximation of the system's state based on the measured input and output signals is called a state observer. The model of an observer is typically derived from that of the system. Besides, a correcting term is usually added into the observer dynamics in order to improve its convergence rate. As a consequence, the observer is able to reconstruct the system's state variables more rapidly than the dynamics of the system.

The problem of observing linear systems was firstly solved by [Luenberger 1964]. In Luenberger's observer, the correcting term is the product of a matrix gain and of the discrepancy between the true measured outputs and the value of the output computed from the observer. The convergence rate of the observer is tuned through this matrix gain. We would like to choose the observer gain as big as possible in order to make the observer error converge rapidly to zero. The observer, however, becomes sensitive to perturbations (measurement noise for example) in this case. Therefore, a good compromise between stability and precision should be taken into account in choosing the observer gain. The Kalman filter is a way to manage this compromise. The Kalman filter can be regarded as the Luenberger observer with a time-varying gain that is chosen with the aim of minimizing the observer error [Bernard 2002].

In a local context, linear observer theory can be used to construct a locally convergent observer for nonlinear systems. If the nonlinear system is known to operate in the neighborhood of some fixed state, one may linearize it around this operating condition and then design a Luenberger observer to estimate locally the system's state. In the case where the nonlinear system doesn't operate in the neighborhood of some fixed state, the system's state can still be estimated by a linear method that is the extended Kalman filter (EKF). The EKF is well known by its simplicity and its reasonable performance. The nonlinear system is linearized at the current operating point and the EKF is then built for this linearized system [Eykhoff 1974]. Unfortunately, due to the linearization, the EKF is convergent only when the initial estimate error is small enough and the process is correctly modeled. In the same spirit as the EKF, Zeitz proposed an extended Luengerber observer basing on a local linearization technique around the reconstructed state [Zeitz 1987].

2.3.2 Lyapunov-based observers and high-gain observers

The nonlinear observer design problem has received a considerable amount of attention in the literature. Nevertheless, there exists no solution to the nonlinear observer design problem in its full generality [Respondek 2004]. Depending on the properties of a particular nonlinear system, one can choose an appropriate way to design its observer.

Early results in the design of nonlinear observers are based on Lyapunov-based theorems ([Thau 1973] and [Kou 1975]). As in the linear case, the authors still construct the nonlinear observer by copying the nonlinear system and add a linear correcting term. Then, Lyapunov stability theory is used to prove the stability of the observer error dynamics. A more advanced framework was introduced by Tsinias, who pursues an observer analog of control Lyapunov functions and uses them for output feedback design ([Tsinias 1989] and [Tsinias 1993]). Although some sufficient conditions for the existence of an asymptotically stable observer have been provided, these approaches aren't constructive since they don't show a systematic technique for the construction of the observer. A solution for this un-constructive problem is Raghavan's observer that actually has the same observer structure as Thau's method, but provides a constructive iteration to get the observer gain [Raghavan 1994].

If a nonlinear system is observable independently of the control input (i.e. uniform observability), then one can use a change of coordinates to transform it into the uniformly observable form [Gauthier 1981]. An example of the uniformly observable form for a single-input single-output control-affine system is the form (2.19), presented in Section 2.2.3. This class of systems can be found in many practical cases. The observer design for these nonlinear uniformly observable systems is proposed by [Bornard 1991], [Gauthier 1992], and [Gauthier 1994] (see [Farza 2004] for a possible extension and a more recent account). The basic idea is to construct a *high-gain observer* for the uniformly observable form and then express it in the initial coordinates. The term *high-gain* means that the observer error can be made to decay at an arbitrary exponential rate. Of course, the high gain observer can only be used in the case where the output is not corrupted with a high level of noise, and when the model has been correctly identified.

2.3.3 Error linearization based observer

Another classical approach for observing nonlinear systems has been proposed in [Krener 1983] and [Bestle 1983]. Based on the fact that the observer design problem for linear systems is much easier than that for nonlinear systems, a natural question to ask is when a nonlinear system can be transformed into a linear system. Sufficient and necessary conditions for the existence of such a transformation are provided in [Krener 1983] in order to linearize uncontrolled nonlinear systems with a single out-

put. Then, the observer is easily constructed using the linear theory. Finally, the observer constructed in the new coordinates is transformed back to the original coordinates. It is important to note that the uniform observability of nonlinear systems isn't sufficient for the application of this approach. Indeed, some additional conditions are required for the existence of the linearization transformation. Therefore, this approach is less general than the method of high-gain observers for which the uniform observability is enough to build the observer. Some results of [Marino 1990] and [Krener 1985] have enlarged the applicative range of this observer design technique. In the former, the author provides necessary and sufficient conditions for transforming a single output nonlinear system with control inputs into a special adaptive observer form. While in the latter, a more general class of nonlinear system with multi-input and multi-output is considered.

More recently, the design of observers using this method has achieved a new progress. The transformation from nonlinear observed systems into a linear observed form is done not only via a change of state and output coordinates but using also an output dependent time re-scaling. Two independent researches of [Respondek 2001] and [Guay 2002] have provided different necessary and sufficient conditions that ensure the existence of an appropriate coordinate change and an output dependent time re-scaling. Note that the function of the output defining the time-scaling considered in these works is positive, the time re-scaling is then never zero (i.e regular time re-scaling). Inspired of this fact, in the first part of this thesis (see Chapters 2, 4 and 5), we extend the results obtained by [Respondek 2004] to the case of singular time re-scalings.

2.3.4 Recent techniques

In [Kazantzis 1998], the authors rely on the linear Luenberger observer theory to propose a nonlinear analogue to autonomous nonlinear systems with single output. The construction of the nonlinear observer is realized via the resolution of a system of singular first-order linear partial differential equations (PDEs). Using Lyapunov's auxiliary theorem [Lyapunov 1992], necessary and sufficient conditions for solvability are derived. The local analytic properties of the solution enable the development of methods based on series expansions.

Recently, several extensions of the Kazantzis-Kravaris observer have been proposed. In [Krener 2002a], the authors extend this method to any real analytic observable nonlinear system. The construction of the observer is based on the solution of a singular first-order nonlinear PDE. Besides, in [Krener 2002b] the authors provide a local observer for some nonlinear systems around a critical point where the linearization isn't observable or not detectable. Another interesting extension of the method of Kazantzis and Kravaris is given in [Andrieu 2006]. The authors state that sufficient conditions for the existence of the observer involve a partial differential

equation whose solution should be injective. The injectivity property of the solution can be obtained by choosing the dimension of the dynamical system defining the observer to be less than or equal to $2 + 2n$, where n is the dimension of the system. The authors show that an approximation of the solution of the PDE is sufficient for the implementation of the observer.

An attempt to remove the usual global Lipschitz restriction or high-gain feedback in the nonlinear observer design problem is introduced in [Arcak 2001]. In this approach, the observer error system is presented as the feedback interconnection of a linear system and a time-varying multivariable sector nonlinearity. The global convergence of the observer is achieved thanks to the satisfaction by the observer gain matrices of the circle criterion. In output-feedback design, the observer is combined with control laws that ensure input-to-state stability (ISS) with respect to the observer error. The robustness analysis of the observer with respect to unmodeled dynamics is achieved via a small-gain assignment in a jet engine compressor example. This method is then generalized to systems with multi-variable monotone nonlinearities that satisfy an analog of the scalar nondecreasing property [Fan 2003].

In [Besançon 1996], the authors notice that for some particular classes of non-uniformly observable systems (i.e. systems admiting *singular inputs*, for which some pairs of states cannot be distinguished), observers have been proposed irrespective of the inputs (see, e.g., [Hara 1976], [Funahashi 1979], [Walcott 1987], and [Raghavan 1994]). This phenomenon is related to a common property of these systems: for any pair of indistinguishable states for some input u, the error between the trajectories obtained from these states with input u tends to zero, and then a reduced observer can be constructed. Based on this observation, the authors present a more general class of nonlinear systems for which such an observer can be designed. The main idea of [Besançon 2007] is to transform a nonlinear system, by immersion under quite mild conditions, into a triangular structure that allows an observer design. The procedure for immersion into this form is constructive and the observer convergence is ensured by an appropriate excitation condition. Besides, in some observation applications, such as fault detection, or parameter estimation, the observer design of non-uniform observable systems can be achieved thanks to the selection of appropriate inputs [Besançon 2013]. The authors state that the input selection amounts to a control problem and propose a systematic way to resolve it by some appropriate optimization approaches.

When some parameters of the system are unknown, the problem of state observation is resolved by an *adaptive observer*. In [Besançon 2000], the author shows that most of all available adaptive observer designs for nonlinear systems are based on the same property, namely the possible representation of the system under a special form, called by the author the *nonlinear adaptive observer form*. This normal form (see also [Farza 2009]) indeed highlights the underlying properties for an adaptive observer to be designable, as well as additional properties that allow parameter es-

timation. As an example, the adaptive observer design for a class of state affine systems is shown. In the case of multiple-input multiple-output (MIMO) linear time-varying systems, one can use [Zhang 2002] to construct a global exponential adaptive observer. The proposed method is conceptually simple and computationally efficient. The author also provides a robustness analysis of the proposed adaptive observer in the presence of modeling and measurement noises.

2.3.5 Extended braking stiffness observation

In [Gustafsson 1997], the author proposes a scheme to identify different road surfaces thanks to the value of the so-called *slip slope*, which is the initial slope of the tyre characteristic curve $\mu(\lambda)$ at the wheel slip $\lambda = 0$. It is important to highlight that, in this approach, the slip slope is considered as constant. Its value is recursively computed by a Kalman filter. Besides, the author uses a change detection algorithm running in parallel with the Kalman filter in order to get reliable and accurate estimates of the slip slope and, at the same time, to be able to follow abrupt changes quickly in the road surface. An example of estimating the slip slope for different road surfaces has been shown. This approach, however, is confronted to two delicate points: first, it uses the wheel slip λ that is unmeasured; and second, it is designed to work only during normal driving and is kept inactive during braking.

The main idea in the estimation approach in [Umeno 2002] is the relationship between the tyre-road friction and the frequency characteristics of wheel speed vibration. That is, the strength of the resonance and its frequency band. The author states that the resonance characteristic of the wheel angular velocity depends on tyre-road friction: on an asphalt road, the torsional resonance of the tyre exhibits a large peak; while the presence of the peak is not clear on a low friction surface. Based on the tyre vibration model during normal driving and a mathematical formula of the road disturbance, a second order transfer function from the road disturbance to the angular wheel speed is obtained. The XBS and the resonance frequency are deduced from this transfer function, depending on its parameters. In order to estimate these parameters, the authors firstly change the second order transfer function back into a continuous time equation, then obtain a linear regression by applying the bilinear transformation and finally use the recursive least squares method. Experimental tests have been done on a test vehicle with ABS. Afterwards [Ono 2003], the authors consider the XBS as constant, like [Gustafsson 1997], but with the XBS defined for any wheel slip λ. Starting form the wheel deceleration model, the authors assume that the vehicle dynamics evolves more slowly than the wheel dynamics to achieve a differential equation of the wheel velocity in which the XBS is proportional to the break point frequency of this equation. Therefore, the problem of estimating the XBS can be solved by identifying this break point frequency. The authors apply the online least squares method [Ljung 1987] to the differential equation of the wheel ve-

locity to estimate the XBS. The performance of the estimated XBS is experimentally evaluated in the ABS braking control.

In [M'sirdi 2006], a sliding observer is proposed. The use of the sliding mode approach to construct the observer is motivated by its robustness with respect to the parameters and modeling errors. The observation scheme is composed of two steps. In the first step, the authors consider the nominal modeling of the vehicle with the wheel and vehicle dynamics. This model is then linearized in a small region near zero wheel slip, in which the XBS is constant. Next, the authors construct a second order sliding mode observer to estimate the wheel angular velocity, using only the wheel angular position measurements. In the second step, after proving that the observer is convergent in finite time by means of perturbation rejection, the authors use the recursive least square method to estimate XBS as well as the wheel effective radius. The effectiveness and robustness of this approach are verified on a real experimental vehicle. It is well known that the XBS is the derivative of the tyre characteristic $\mu(\lambda)$ with respect to the wheel slip λ at the operational point, so that one can estimate separately $\mu(\lambda)$ and λ, and then derive these estimate values with respect to the time and finally take the ratio of these derivatives in order to get the estimate XBS. The application of this approach is not easy due to the fact that the derivative of estimate signals normally amplifies noises. Recently, a new idea for estimating derivative noisy signals has been provided in [Villagra 2011] using algebraic algorithms [Mboup 2009]. This approach is tested in noisy simulations and in real experimentations, some very promising results have been obtained.

Fitting the static tyre characteristic (for example, the Burckhardt model) under the assumption that the wheel slip measurements are known, is the basic idea of the approaches proposed in [Tanelli 2009] and [de Castro 2010]. Two different linear parametrizations for the static model of the tyre characteristic are presented. From these linear paramaterizations, the XBS can be computed easily. The former is approximated using a linear combination of fixed exponentials. The fitting curve is analyzed and tested both in simulations and on data collected on an instrumented test vehicle. The latter is based on a neural network, the authors show on simulations a good performance, similar to the former method.

2.4 Main contributions of Part I

2.4.1 Switching observers for singular systems

As introduced in Section 2.2, our objective is to observe a class of singular systems with a scalar output. Such singular systems cannot be observed using the methods proposed in the literature. Therefore, we proposed a systematic technique to construct a time re-scaling based switching observer that can estimate the system's state

even in the singular case (see Sections 2.1.2 and 2.2.2). The switching nature of the observer comes from the fact that there are two different dynamics, for positive and negative values of the output-dependent function $s(y)$. In Chapter 4, a first positive result supporting the stability analysis of the observer error dynamics in the new time scale is obtained through the following theorem

Theorem. *Consider an observable pair (A, C). Define $Q = C^T C$. For any given pair of gains K^+ and K^-, define*

$$A_+ = A - K^+ C \quad \text{and} \quad A_- = -A + K^- C. \tag{2.25}$$

If K^+ is such that A_+ is Hurwitz, then there exists a unique K^- such that the two following Lyapunov equations

$$A_+^T P + P A_+ = -Q \quad \text{and} \quad A_-^T P + P A_- = -Q \tag{2.26}$$

admit a common solution P that is symmetric and positive definite.

Moreover, if (A, C) is in the observer normal form, then the components k_i^- of K^- are expressed in terms of the components k_i^+ of K^+ by

$$k_i^- = (-1)^i k_i^+ + \big(1 - (-1)^i\big) a_i,$$

where the constants a_i are the coefficients of the characteristic polynomial of A.

This theorem has two important consequences. First, it states that for the observer error dynamics that is an autonomous switched linear system of the form (2.16), it is always possible to find a pair of the observer gains such that there exists a positive definite symmetric matrix satisfying simultaneously the two non-strict Lyapunov equations, introduced in [Hespanha 2004]. Second, if the pair (A, C) is in observer normal form, then we can obtain explicit expressions that show the relationship between the components of the two observer gains.

The proof of this theorem relies on two points, presented as Claim 4.1 and Lemma 4.2, in Chapter 4. In Claim 4.1, we show that the equality of the spectra of two observable uncontrolled linear systems is equivalent to that of their outputs, provided that the two initial conditions are related via some special matrix. Moreover, if this matrix exists then it is unique. The proof of Claim 4.1 relies mainly on the Cayley-Hamilton theorem and the analytic properties of the system output. Lemma 4.2 is a consequence of Claim 4.1. It states that if the pair (A, C) is in the observable form, then the components of the observer gain K^- can be expressed in terms of the components of K^+.

Under the assumption that the time between any two consecutive switchings is no smaller than a dwell-time (or, in other words, slows switchings), it is easy to see that the result of the theorem allows all conditions of the LaSalle-like theorem

proposed by [Hespanha 2004] to be satisfied, the observer error dynamics is globally exponentially stable in the new time scale. Furthermore, we prove that the relation between the original time and the time re-scaling is bijective, then the asymptotic convergence of the observer is equivalent in the two time scales.

Corollary. *Consider the system (2.16) and assume that, in the new time-scale, there exists a dwell-time τ_D. If the gain matrices K^+ and K^- ensure the common solvability of the two coupled Lyapunov equations (2.26), then the origin of (2.16) is uniformly globally exponentially stable (in the new time-scale).*

2.4.2 XBS estimation based on a switching observer

In Chapter 5, we deal with the XBS estimation problem, for ABS systems. The knowledge of XBS is important for ABS control systems and in our research, because it can be used in order to increase the robustness of five-phase ABS hybrid algorithms. We would like to highlight that the solution of this problem has been our main source of motivation for considering the more general problem considered in Chapter 4. The design of the switching observer to estimate the XBS in this chapter is thus presented independently compared to the theoretical results obtained in Chapter 4.

The estimation of XBS is firstly considered in the case of constant road conditions in Section 5.3. The adjective *constant* should be understood in the sense that some of the coefficients of the tyre characteristic are known since their values depend on road conditions. We describe the tyre characteristic using the model proposed by [Burckhardt 1993] and assume that the value of c_2 of Burckhardt's model is known. A nice property of this formula is that one can establish a relation between its first two order derivatives. It is important to stress that the first order derivative of the tyre characteristic is the XBS. We take advantage of this property to form a three-dimensional XBS dynamics

$$\begin{aligned} \frac{dz_1}{dt} &= \frac{-a}{v_x(t)} z_1 z_2 + bu \\ \frac{dz_2}{dt} &= (cz_2 + z_3)\frac{z_1}{v_x(t)} \\ \frac{dz_3}{dt} &= 0, \end{aligned} \tag{2.27}$$

where the wheel acceleration offset and the XBS are the two state variables and the third state variable is an unknown constant, whose value depends on road conditions. The parameters a, b, and c are positive constants and u is the control input. For this

dynamics, we propose the following observer

$$\begin{aligned}
\frac{d\widehat{z}_1}{dt} &= \frac{-a}{v_x} z_1 \widehat{z}_2 + bu + \frac{k_1(z_1)}{v_x} z_1 (z_1 - \widehat{z}_1) \\
\frac{d\widehat{z}_2}{dt} &= (c\widehat{z}_2 + \widehat{z}_3)\frac{z_1}{v_x} + \frac{k_2(z_1)}{v_x} z_1 (z_1 - \widehat{z}_1) \\
\frac{d\widehat{z}_3}{dt} &= \frac{k_3(z_1)}{v_x} z_1 (z_1 - \widehat{z}_1),
\end{aligned} \tag{2.28}$$

where $\widehat{z}_i$ are the observer states and k_i, for $1 \leq i \leq 3$, are the observer gains.

Our main achievement is presented in the following theorem that gives conditions on the observer gains in order to ensure the global asymptotic stability of the switching observer error dynamics provided that the switchings are slow. The proof of the theorem is obtained with the help of Theorem 4 of [Hespanha 2004].

Corollary. *Assume that the three following conditions are satisfied*

(i) The gain $K^+ = \begin{pmatrix} k_1^+ & k_2^+ & k_3^+ \end{pmatrix}$ *satisfies*

$$k_1^+ > c,\ k_2^+ < -\frac{c}{a} k_1^+,\ \textit{and}\ -\frac{(ck_1^+ + ak_2^+)(c - k_1^+)}{a} < k_3^+ < 0. \tag{2.29}$$

(ii) The gain $K^- = \begin{pmatrix} k_1^- & k_2^- & k_3^- \end{pmatrix}$ *satisfies*

$$k_1^- < c,\ k_2^- < -\frac{c}{a} k_1^-,\ \textit{and}\ 0 < k_3^- < -\frac{(ck_1^- + ak_2^-)(c - k_1^-)}{a}. \tag{2.30}$$

(iii) The gains K^+, K^- *satisfy*

$$\frac{(c - k_1^-)}{ak_3^-} = \frac{(c - k_1^+)}{ak_3^+} > 0\ \textit{and}\ (ck_1^+ + ak_2^+) = (ck_1^- + ak_2^-) < 0. \tag{2.31}$$

Then, the origin of the error dynamics associated to systems (2.27) and (2.28) is uniformly globally exponentially stable, provided that the switching signal admits a strictly positive dwell-time.

We continue with the validation of the three-dimensional observer, which is constructed following the previous theorem, on data coming from the-tyre-in-the-loop experimental facility of TU Deflt, acquired in the context of ABS research [Gerard 2012]. We show in Figure 5.2 the comparison between the XBS estimated by the three-dimensional observer and the theoretical value obtained from the wheel slip and the derivative of the tyre characteristic.

Since the road conditions are generally unknown for practical ABS systems, we thus present in Section 5.4 a four-dimensional XBS dynamics. The main idea behind this modelling is the parametrization of Burckhardt's model by fixed exponentials,

which has been proposed in [Tanelli 2009] and [de Castro 2012]. In our work, we approximate Burckhardt's model by two fixed exponentials and a wheel slip linearly dependent term. The coefficients of the approximate model could be identified using least squares estimation, but their values depend on road conditions. Just like for the Burckhardt model, we can also formulate a relation between the first three order derivatives of the approximate tyre characteristic. Thanks to this relation and defining new state variables, we can formulate a four-dimensional XBS dynamics. This dynamics can be seen as a generalization of the previous three-dimensional one and it has a very important property: all its parameters are known and not dependent on road conditions. This explains the fact that the model-based observer of this dynamics will give the estimated values of XBS, independently on road conditions. The stability of the four-dimensional observer can be obtained following the same approach as for the mentioned above theorem. Numerical simulations are taken to test the effectiveness of the observer in a scenario of unknown changes of road conditions.

Chapter 3

Input-delay compensation for linearizable systems

As in Chapter 2, we start with a simple problem in ABS systems: the compensation of actuator delays, in the context of wheel acceleration control. We solve this problem by providing a control law that is based on the prediction of the system's state, which is safely implemented by an explicit integration via quadratures, of a stable delayed differential equation. Expanding our idea, the main objective of Part II is to solve the input delay compensation problem for a particular class of nonlinear systems in triangular form. A review of some recent results for time delay systems in the literature is then presented. Finally, we highlight our main contributions.

3.1 Brake actuator delay compensation

The concrete implementation of several theoretical ABS strategies has been confronted to some difficulties generated by several experimental phenomena, in particular the delays (see, e.g., [Solyom 2004], [Solyom 2003], [Kienhöfer 2008], [Gerard 2012], and [Miller 2013]). Measurement filtering, tyre dynamics, and actuator limitations have been identified to be the main sources of these delays [Gerard 2012]. Besides, since current ABS algorithms are deeply associated to the hydraulic nature of today's actuators [Bosch 2004], then adapting these algorithms to other actuators, like those of in-wheel motor based electric vehicles (with a quicker response time) or heavy-duty trucks (with a slower response) has focused some attention in recent years. In this section, we will consider the compensation of the delays induced by actuator limitations in ABS systems.

We recall here the wheel acceleration model (2.1) already shown in Section 2.1.1, but we take into account a constant time delay $h > 0$ in the braking torque $u(t)$. That is

$$\begin{aligned} \frac{dz_1}{dt} &= -\frac{a}{v_x} z_1(t) z_2(t) + b u(t-h) \\ \frac{dz_2}{dt} &= 0. \end{aligned} \tag{3.1}$$

As in [Gerard 2012], we define the control objective to be the tracking of the wheel

acceleration $z_1(t)$ towards a given reference z_1^*. And we suppose that in (3.1) the value z_2 of XBS is known. If we assume z_2 to be both known and constant, for a given speed, this system can be written

$$\dot{x}(t) = cx(t) + bu(t-h), \tag{3.2}$$

where $c = (-a\mu'(\lambda))/v_x$ and $\mu'(\lambda)$ is the XBS. Observe that (3.2) might be either stable or unstable, depending on whether the tyre is in its stable or unstable domain.

Without the delay h, the tracking problem for (3.2) is a trivial task. One can easily define the control input as follows

$$u(t) = \frac{1}{b}\big(-cx(t) - \alpha(x(t) - x^*(t)) + \dot{x}^*(t)\big), \tag{3.3}$$

where the control gain α is a positive constant.

In the presence of h, the control problem becomes more delicate since the control input u must compensate the delay h in order to ensure the tracking of $x(t)$. To compensate the effects of the delay, the control u must use the future values of the state x as well as the reference x^* at the time instant $t+h$, which is not always available. For example, the reference trajectory might be unknown in advance since it might be computed in real time. Therefore, instead of making the wheel acceleration $x(t)$ track the reference $x^*(t)$, we should make it converge towards $x^*(t-h)$. Moreover, for the future values of x, we have no other choice than to estimate them. We introduce $x^P(t,h)$, called the *state prediction*, as the estimate state of $x(t+h)$ computed at the time instant t. We apply to (3.2) the following control law

$$u(t) = \frac{1}{b}\big(-cx^P(t,h) - \alpha e(t) + \dot{x}^*(t)\big), \tag{3.4}$$

where the tracking error $e(t)$ is defined as

$$e(t) := x(t) - x^*(t-h), \tag{3.5}$$

thus we obtain the closed-loop system

$$\dot{e}(t) = -\alpha e(t-h) + c\big(x(t) - x^P(t-h,h)\big). \tag{3.6}$$

If the state prediction x^P is estimated perfectly, which means $x^P(t,h) = x(t+h)$ and as a consequence $x^P(t-h,h) = x(t)$, we obtain an ideal error dynamics

$$\dot{e}(t) = -\alpha e(t-h), \tag{3.7}$$

which is exponentially stable if the control gain α satisfies the condition $0 < \alpha < \pi/2h$.

Until now, we haven't discussed yet how we can estimate $x^P(t,h)$. Fortunately, we know that if $x^P(t,h)$ is perfectly estimated, we might obtain an exponentially stable error dynamics (3.7) that we call the *target error dynamic*. Since (3.7) is stable, then if we integrate it we can get the future values of the tracking error at the time instant t. So, we come up with the following idea: the state prediction $x^P(t,h)$ is computed indirectly via the future values of the tracking error that are computed before. Nevertheless, the actual error dynamics (3.6) is usually different from the target error dynamics (3.7). Therefore, an integral term should be added to the prediction of the tracking error in order to compensate the mismatch between the target and the actual error dynamics. At every time instant t, we define the *error prediction* as

$$e^P(t,s) := e(t) - \alpha \int_t^{t+s} e(\tau - h)d\tau - \beta \int_{-\infty}^{t+s} p(\tau - h)d\tau, \tag{3.8}$$

for $s \in [0,h]$. We denote $p(t)$ as the *prediction bias* that is the difference between the error prediction $e^P(t-h,h)$ at the time instant $t-h$ and the real error $e(t)$

$$p(t) := e^P(t-h,h) - e(t). \tag{3.9}$$

Now, with the definition of the tracking error (3.5), we can easily estimate the prediction state $x^P(t,s)$ at every time instant t via the error prediction $e^P(t,s)$ by taking

$$x^P(t,s) := x^*(t+s-h) + e^P(t,s), \quad \forall\, s \in [0,h]. \tag{3.10}$$

From (3.5), (3.9) and (3.10), we obtain

$$\begin{aligned} x^P(t-h,h) &= x^*(t-h) + e^P(t,h) + x(t) - x(t) \\ &= -e(t) + e^P(t,s) + x(t) \\ &= p(t) + x(t). \end{aligned} \tag{3.11}$$

We replace (3.11) into (3.6), the error dynamics then becomes

$$\dot{e}(t) = -\alpha e(t-h) - cp(t). \tag{3.12}$$

By differentiating (3.9) and using (3.8) and (3.12), we obtain the dynamics of the prediction bias

$$\begin{aligned} \dot{p}(t) &= \dot{e}^P(t-h,h) - \dot{e}(t) \\ &= -\beta p(t-h) + \dot{e}(t-h) - \dot{e}(t) - \alpha e(t-h) + \alpha e(t-2h) \\ &= -\beta p(t-h) + c\big(p(t) - p(t-h)\big). \end{aligned} \tag{3.13}$$

It can be proved via a Lyapunov-Krasovkĭi approach that the dynamics (3.13) is globally exponentially stable for appropriate values of the gain β. Besides, the two equations (3.12) and (3.13) are cascaded, then it may also be shown that (3.12) is input-state-stable from the input $p(t)$.

3.2 Input delay compensation for nonlinear systems

As a first step towards the generalization of the ideas presented in the previous section, we consider now the case of a second order system

$$\begin{aligned} \dot{x}_1(t) &= f_1\big(x_1(t)\big) + x_2(t) \\ \dot{x}_2(t) &= f_2\big(x(t)\big) + u(t-h), \end{aligned} \tag{3.14}$$

where $x(t) := [x_1(t)\, x_2(t)]^\top \in \mathbb{R}^2$ and $y(t) = x_1(t)$ is the output. The control objective is again the output tracking problem, that is $y(t) = x_1(t) \to y^*(t-h) = x_1^*(t-h)$ as $t \to \infty$. We apply the same approach to compensate the input delay. Following the classical backstepping procedure, one can consider that $x_2(t)$ is a virtual control input to the $\dot{x}_1$-equation. Therefore, in order to achieve the control objective, this virtual control input must converge towards the following term

$$x_2^*(t) := -f_1(x_1^P(t,h)) - \alpha_1 e_1(t) + \dot{x}_1^*(t), \tag{3.15}$$

where $x_1^P(t,h)$ denotes the prediction of $x_1(t+h)$ computed at the time instant t and the error $e_1(t)$ is defined as

$$e_1(t) := x_1(t) - x_1^*(t-h). \tag{3.16}$$

If we define

$$e_2(t) := x_2(t) - x_2^*(t-h), \tag{3.17}$$

the control $u(t-h)$ must ensure that

$$\lim_{t\to\infty} e_2(t) = 0. \tag{3.18}$$

To that end, we define the control input as

$$u(t) := -f_2(x_1^P(t,h), x_2^P(t,h)) - \alpha_2 e_2(t) + \dot{x}_2^*(t), \tag{3.19}$$

where $x_2^P(t,h)$ denotes the prediction of $x_2(t+h)$ computed at the time instant t.

As before, it is obvious that if the prediction of $x(t+h)$ is perfect, the reference

error dynamics can be written in a cascaded form

$$\begin{aligned} \dot{e}_1(t) &= -\alpha_1 e_1(t-h) + e_2(t) \\ \dot{e}_2(t) &= -\alpha_2 e_2(t-h), \end{aligned} \tag{3.20}$$

The computation of the state prediction $x^P(t,h)$ is then based on (3.20). The remaining task is to find the control gains α_1 and α_2 such that the control objective is fulfilled.

We have been able, in Chapter 6, to generalize these ideas for a class of nonlinear systems with a constant input delay that can be transformed into a triangular form

$$\begin{aligned} \dot{x}_1(t) &= f_1\big(x_1(t)\big) + x_2(t) \\ \dot{x}_2(t) &= f_2\big(x_1(t), x_2(t)\big) + x_3(t) \\ &\vdots \\ \dot{x}_{n-1}(t) &= f_{n-1}\big(x_1(t), \ldots, x_{n-1}(t)\big) + x_n(t) \\ \dot{x}_n(t) &= f_n\big(x(t)\big) + u(t-h), \end{aligned} \tag{3.21}$$

where $x(t) := [x_1(t) \cdots x_n(t)]^\top \in \mathbb{R}^n$ and $y(t) = x_1(t)$ is the system's output, for which we have a reference $y^*(t)$.

Objective of Part II: Given a class of nonlinear systems with a constant input delay that can be linearized into a triangular form (3.21), find the control law to compensate the input delay and to solve the output tracking problem.

3.3 Existing methods for input delay compensation

3.3.1 Linear systems

One of the first attempts to control processes affected by input delays goes back to the work of Otto J. M. Smith [Smith 1959]. He stated that the response of a process with delays should be the same as that for the same process without delay, but delayed by a time equal to that of the delay. Based on this principle, he proposed a time delay compensator, named the *Smith predictor* that consists of a classical controller (for example a PID controller) and the *nominal model* of the process with time delay, in the frequency domain. The nominal model is composed of a transfer function of the process without time delay followed by a time delay term. There are two feedback loops in the Smith predictor: a positive loop feeds the output of the nominal model and a negative loop feeds the output of the transfer function of the process without time delay. Besides, there is a third negative feedback loop through

the process with time delay and its effect is canceled out by the positive feedback loop of the Smith predictor. As a consequence, it can be seen that total feedback is based on the output of the transfer function of the process without time delay. In other words, the total feedback is based on a *prediction* of the output measured from the process with time delay. Since its apparition, the Smith predictor has become the most popular algorithm to compensate time delays used in the industry. Nevertheless, due to the fact that the Smith predictor always retains the poles of the process, it cannot be applied to unstable linear time-delay systems [Wang 1998].

Another popular approach used to deal with the input delay for general (stable or unstable) linear systems is the *Finite Spectrum Assignment (FSA)* method, sometimes called *Artstein model reduction* in the time domain (see [Manitius 1979] and [Artstein 1982]; or [Richard 2003] for a more recent account). The main idea behind the FSA approach is to generate the prediction of the state variable over one delay interval. Then, a feedback of the predicted state is applied, thereby compensating the effect of the time delay. This results in a closed-loop with a finite number of eigenvalues, which can be assigned arbitrarily. This also explains why this approach can be applied to unstable linear systems. Recently, in [Wang 1998], the authors extend the FSA for linear time delay systems in the frequency domain. From another point of view - the Artstein model reduction, the prediction of the state variable over one delay interval can be considered as a change of the state variable that reduces linear systems with delayed control to systems without delays in the control input.

In practice, the application of the FSA approach might be a difficult task since it involves the implementation of the integral term, which needs to be calculated on-line. It is shown by [Engelborghs 2001] and [Van Assche 1999] that the numerical implementation of the integral term might be unstable, at least when the original system is unstable. To deal with this problem, some interesting results have been provided. In [Mazenc 2011a], the authors present a different way to predict the state variable over one delay interval. The stability of this operator is guaranteed by replacing the state matrix (that might be unstable) by a stable matrix. Besides, one can approximate the integral term by a sum of point-wise delays by using a quadrature rule [Manitius 1979]. Such approximations, however, might be unstable due to the high-frequency mechanisms [Watanabe 1981]. A safe way to implement the integral term is explored in [Mondié 2003]. The authors consider the use of a low pass filter, which is able to eliminate high-frequency mechanisms, and show using a simple example how to verify the safe implementation of the FSA approach.

3.3.2 Nonlinear systems

In the literature, the compensation of input delays for nonlinear systems is frequently attached to two control design tools, called *backstepping* and *forwarding*.

In the forwarding approach, feedforward nonlinear systems with input delays are

considered. The word *forward* refers to the absence of feedback in the structure of the system. If feedforward systems are described by equations having a specific triangular structure, called the *feedforward form*, one can use the result presented in [Mazenc 2004]. The key ingredients of this result are, on the one hand, several modifications of the feedforward form by changes of coordinates, input and time scale and, on the other hand, bounded feedbacks. In [Krstic 2009] and [Krstic 2010], the authors propose a nonlinear version of the Smith Predictor and its various predictor-based modifications for linear plants (for example the FSA approach) to compensate input delays of arbitrary length in feedforward nonlinear systems. The authors show that global stabilization is maintained but requires the online solution of a nonlinear integral equation. In other words, the predictor state, which is used in the nominal control law to compensate for the input delay, isn't obtainable explicitly. Nevertheless, for a class of *strict-feedforward* systems, the author gives an explicit formula for the predictor state.

For the backstepping approach, nonlinear systems in the feedback form are considered. In [Mazenc 2006], the authors carry out the design of globally uniformly asymptotically stabilizing feedbacks for a family of nonlinear systems in feedback form with a delay in the input that can be arbitrarily large. The main idea is the construction of a Lyapunov-Krasovkĭi functional. A continuously differentiable control law, which depends on the value of the delay is constructed. Nevertheless, some limitations in the considered family of nonlinear systems in feedback form and in the mentioned above control law are stated in [Mazenc 2011b]. To overcome these limitations, the authors consider a new family of systems with input delays and explore an appropriate Lyapunov-Krasovkĭi functional. The control design is then illustrated in a second order example of the pendulum. It is shown in [Karafyllis 2006] that finite-time global stabilization for nonlinear triangular systems with delays can be achieved by time-varying locally Lipschitz distributed delay feedback.

For a general nonlinear input-delayed systems, in [Georges 2007] the authors extend the finite spectrum assignment approach available for linear input-delayed systems to the prediction of the state variable. A nonlinear feedback control based on the state prediction is then proposed to stabilize nonlinear systems with input time delays. As in the linear case, the computation of the nonlinear feedback control is difficult due to the integral term, which cannot be explicitly computed. To avoid this difficulty, the authors approximate the control by using both a state prediction approximation and the *dynamic inversion* of a fixed point problem. The effectiveness of this approach has been demonstrated on illustrative examples.

3.4 Main contributions of Part II

To compensate input delays, most of the available methods use a prediction of the future of the system's state that is based on the integration of the delayed system. The numerical implementation of such predictions is, however, difficult due to the integral terms, which might not be explicitly computable or might lead to an unstable system ([Engelborghs 2001] and [Mondié 2003]), at least when the dynamical system is unstable. We thus look for a simple alternative way of estimating the future values of the system's state that can be implemented in practice and leads to a stable behaviour of the feedback system.

Observing the available methods in the literature, one might come up with a simple but probably abusive conclusion: a prediction of the future of the system's state based on the integration of a stable and linear system is likely to lead to a stable numerical scheme; while the integration of an unstable and/or nonlinear system might be confronted with a more delicate numerical implementation. Nevertheless, if the control objective is to ensure the tracking of the system's output towards a given reference, we can consider the reference model for the error dynamics as a part of the control design. In other words, to estimate the future values of the system's state, instead of directly integrating the system's dynamics that might be unstable and/or nonlinear, we follow a two-steps procedure. In the first step, we integrate the reference error dynamics, which can be chosen to be linear and stable, in order to obtain the error prediction. In the second step, we compute the state prediction using the obtained error prediction. Such a prediction scheme is straightforward and stable. We describe the details of our prediction scheme in Section 6.2. It is worth mentioning that, at each instant t, we compute the error prediction for each instant in the interval $[t, t+h]$, using the past values of all error in the interval $[t-h, t]$. Furthermore, in order to damp the perturbation coming from the mismatch between the ideal and actual error dynamics, we add an integral of the prediction bias into the error prediction. After obtaining the state prediction, one can build a simple control law that compensates the input delays and achieves the tracking of the system's output.

In the spirit of our simple prediction scheme, we consider in Section 6.3 the output tracking problem of a particular class of systems with input delays in triangular form, or in other words the class of restricted-feedback linearizable systems as presented in (3.21). We are interested in this system class because conditions for the existence of a global transformation into this triangular form are available (see, e.g., [Dayawansa 1985] and [Respondek 1986]; or [Respondek 2002] for a more recent reference). We follow an inversion procedure (a backstepping procedure) to find the input that tracks the desired output. Of course, such an inversion scheme is realizable thanks to the future values of the system's state that are estimated by our simple prediction scheme. Our main result is the following theorem.

Notation. For a square matrix β we use β_m and β_M to denote, respectively, its smallest and biggest eigenvalues.

Theorem. *Consider the restricted-feedback linearizable system (3.21) and assume that, for each $1 \leq i \leq n$, there exists γ_i such that*

$$|f_i(z) - f_i(y)| \leq \gamma_i |z - y|, \qquad \forall\ z,\, y \in \mathbb{R}^i. \tag{3.22}$$

At each instant t, for $s \in [0, h]$, construct the error prediction starting with

$$e_n^P(t,s) = e_n(t) - \alpha_n \int_t^{t+s} e_n(\tau - h)d\tau - \beta_n \int_{-\infty}^{t+s} p_n(\tau - h)d\tau \tag{3.23}$$

and, from $i = n-1$ down to 1, with

$$\begin{aligned} e_i^P(t,s) = e_i(t) - \alpha_i \int_t^{t+s} e_i(\tau - h)d\tau - \beta_i \int_{-\infty}^{t+s} p_i(\tau - h)d\tau \int_t^{t+s} \\ + \int_t^{t+s} e_{i+1}^P(\tau - h, h)d\tau, \end{aligned} \tag{3.24}$$

where

$$e_i(t) = x_i(t) - x_i^*(t-h), \qquad \forall\, i \in \{1, \ldots, n\}. \tag{3.25}$$

and

$$p_i(t) = e_i^P(t-h, h) - e_i(t). \tag{3.26}$$

Construct the state prediction, starting with

$$x_1^*(t) = y^*(t) \quad \textit{and} \quad x_1^P(t,h) = x_1^*(t) + e_1^P(t,h), \tag{3.27}$$

and, from $i = 2$ up to n, with

$$x_i^P(t,h) = x_i^*(t) + e_i^P(t,h), \tag{3.28}$$

where

$$x_i^*(t) = -f_{i-1}(x_1^P(t,h), \ldots, x_{i-1}^P(t,h)) - \alpha_{i-1}e_{i-1}(t) + \dot{x}_{i-1}^*(t), \tag{3.29}$$

and consider the controller

$$u(t) = -f_n(x^P(t,h)) - \alpha_n e_n(t) + \dot{x}_n^*(t). \tag{3.30}$$

Then, given any $h^* > 0$, if the matrices associated to the control gains

$$\alpha = diag\{\alpha_1 \cdots \alpha_n\} \quad \textit{and} \quad \beta = diag\{\beta_1 \cdots \beta_n\}$$

satisfy

$$\alpha_m \geq 4 + \alpha_M(\alpha_M + 2)h^* \tag{3.31}$$
$$\beta_m \geq 4\gamma + \beta_M(\beta_M + 2\gamma)h^*, \tag{3.32}$$

the origin of the closed-loop system is uniformly globally exponentially stable for each $h \in [0, h^*]$.

It is worth mentioning that the closed-loop system dynamics is composed of two closed-loop subsystems: that of the error prediction and that of the bias prediction. Since the closed-loop system dynamics has a cascaded structure, the proof of the previous theorem relies on the classical procedure to establish the stability of cascaded systems of ordinary differential equations. In Section 6.4, we illustrate the effectiveness of the theorem using a pendulum equation that is nonlinear and might be unstable.

Part I

Switching observation of singular systems

Chapter 4

Switching observer for systems with linearizable error dynamics via singular time-scaling

---

The content of this chapter is strongly based on :

T.-B. Hoang, W. Pasillas-Lépine, and W. Respondek. A switching observer for systems with linearizable error dynamics via singular time-scaling. Submitted to *International Symposium on Mathematical Theory of Networks and Systems*, Groningen (The Netherlands), 2014.

The altenative proofs included in the Appendices are not rigorous; these drafts are only included in order to show that several approaches are possible for proving Theorem 4.1. The statements and the proofs of the results presented in Section 4.3 have been obtained by Witold Respondek. They are included in this thesis only for the purpose of completeness.

Abstract: In this paper, we propose a new observer design for nonlinear systems that can be linearized using a change of coordinates and a singular time re-scaling. Our observer is a switched system and the observer error dynamics are described, after time re-scaling, by a switched linear system that is uniformly exponentially stable. We also give necessary and sufficient conditions for linearizability via a change of coordinates and a singular time re-scaling. Our methods are illustrated on an example coming from the ABS literature.

4.1 Introduction

The aim of an observer is to reconstruct, from the past values of the measured outputs, the states of a system for which a measure is not available [Bernard 2002]. For linear systems, the classical works of Kalman [Kalman 1960] and Luenberger [Luenberger 1964] propose two well known approaches to solve the observation problem. The Luenberger observer has been extended to the case of nonlinear systems that can be linearized using a change of coordinates (see, e.g., [Krener 1983], [Krener 1985] and [Marino 1990]) and to the class of uniformly observable systems

(see, e.g., [Bornard 1991], [Gauthier 1992] and [Gauthier 1994]). More recent techniques (see, e.g., [Kazantzis 1998], [Krener 2002a], and [Andrieu 2006]) have proposed still more flexibility in the observer design avoiding, for example, the necessity of considering high gains to counter nonlinear terms. Nevertheless, for systems that are not uniformly observable, the observation problem remains difficult because for them the observability properties depend on the control inputs that are applied to the system (see, e.g., [Besançon 2013] and [Dufour 2010]).

The aim of our paper is to propose an observer for a particular class of non-uniformly observable systems that are affine, with respect to the unmeasured states, up to a multiplication by a function of the output. Our work is strongly inspired by the time-rescaling approach proposed in [Guay 2002] and [Respondek 2004], for the construction of observers for systems that cannot be linearized using a coordinate change only (see also [Moya 2002]). The change of time scale considered in those works is regular and therefore the proposed observers can be constructed for uniformly observable systems only. In our approach, we handle the case of singular time-rescalings (and thus we deal with a class of of non-uniformly observable systems) and we solve the observer problem by transforming the observer error dynamics into a switched linear system, for which several stability analysis methods are available. In particular, the Lasalle-like approach of [Hespanha 2004] can be used directly to prove the stability of the constructed observer.

To summarize, the novelty of our approach is two-fold. Firstly, we construct an observer for a class of non-uniformly observable systems (clearly, the convergence of the observer is assured for a certain family of distinguishing inputs only). Secondly, although the original system is continuous (smooth actually), we propose for it a switching asymptotically convergent observer.

In the second section we present a new observer design for the class of systems linearizable via a singular time-rescaling. We also state Theorem 4.1 that shows how to tune the observer gains. Section 3 of the paper analyzes the conditions that a nonlinear system must satisfy in order to be transformable into an affine system, with respect to the unmeasured states, up to a multiplication by a function of the output vanishing at the zero value of the output. Section 4 illustrates these ideas in the case of a simple estimation problem associated to ABS systems. The Appendix contains mathematical proofs.

4.2 Switchings and singular observer design

In this paper, we consider systems of the following form

$$\dot{x} = f(x) + g(x)u, \quad y = h(x), \tag{4.1}$$

where $x(t) \in \mathbb{R}^n$ and $y(t) \in \mathbb{R}$ is the measurement, and both f and g are C^∞-vector fields on $\mathbb{R}^n$. Among such systems, we have a particular interest for those that can be transformed, using a C^∞-diffeomorphism $z = \Phi(x)$, into the following affine (with respect to the unmeasured states) form

$$\dot{z} = s(y)\big(Az + d(y)\big) + b(y)u, \quad y = Cz, \tag{4.2}$$

where the pair (A, C) is observable and the vector fields b and d depend on the output only. Conditions for the existence of such a transformation are given in Section 4.3.

Our interest for this class of systems comes from the possibility of building the observer

$$\frac{d\hat{z}}{dt} = s(y)\big(A\hat{z} + d(y) + K(s(y))(y - C\hat{z})\big) + b(y)u, \tag{4.3}$$

using a gain $K(\cdot)$ that depends on the system's output only. Defining the error $e = z - \hat{z}$, we obtain the observer error dynamics

$$\frac{de}{dt} = s(y)(A - K(s(y))C)e. \tag{4.4}$$

In the case of a non-vanishing function s (which we call the *regular* case), the analysis of the asymptotic stability of (4.4) has already been considered in [Respondek 2004]. In fact, if s is strictly positive, the observer gain $K(s(y))$ can be taken as a constant matrix K such that $A - KC$ is Hurwitz, which renders the error dynamics

$$\frac{de}{d\tau} = (A - KC)e$$

asymptotically stable with respect to the new time-scale τ given by $\frac{d\tau}{dt} = s(y(t))$.

In this paper, our aim is to construct an observer that works even in the case when the function s might vanish (which we call the *singular* case). But when the function $s(y(t))$ changes its sign, we are confronted with three problems. Firstly, on time-intervals when $s(y(t))$ is negative, we have to assure an (exponential) divergence of the error with respect to τ (and not its convergence). Secondly, we have to be sure that the time instances t_i at which $s(y(t_i)) = 0$ do not accumulate. Thirdly, system (4.2) is not uniformly observable. Indeed, it is easy to see that the control $u(t) \equiv 0$ renders indistinguishable any two states $z_0 \neq \tilde{z}_0$ such that $Cz_0 = C\tilde{z}_0 = 0$ (see Proposition 4.1 below).

The first problem will be solved by allowing the gain K to depend on $s(y)$ (actually on the sign of $s(y)$) whereas the second by ensuring the existence of a dwell time. Finally, the third problem by avoiding controls that make the system unobservable. In order to handle these three problems, the key step in our approach is to consider as a new time-scale

$$\tau(t) = \int_0^t |s(y(\nu))| d\nu. \tag{4.5}$$

This choice ensures that $d\tau/dt \geq 0$, independently of the values of $s(y)$. Throughout the function $s(y)$ is supposed strictly increasing and such that $s(y) = 0$ if and only if $y = 0$ and that $s'(0) \neq 0$.

We will assume that at any time instant t_i such that $y(t_i) = 0$, the control $u(t)$ law has been designed to achieve $dy(t_i)/dt \neq 0$ (or equivalently that the limits $u(t_i^-)$ and $u(t_i^+)$ of $u(t)$ at t_i from the left and from the right, respectively, are nonzero). This choice of u is to cross the observability singularity $\{Cz = 0\}$ with a nonzero velocity and thus to render the system observable even at that singular locus (compare Proposition 4.1 below). A consequence of our assumptions is that the function w such that $\tau(t) = w(t)$ is globally invertible. We denote w^{-1} its inverse. Even if the dynamics (4.2) might be indefinite in the new time-scale τ when $y(t) = 0$, one can still define its output by taking $y(\tau) = y(w^{-1}(\tau))$.

In the new time-scale, if the observer gains are defined as

$$K(s(y(\tau))) = \begin{cases} K^+ & \text{if : } s(y(\tau)) > 0 \\ K^- & \text{if : } s(y(\tau)) < 0, \end{cases} \tag{4.6}$$

then the observer error dynamics (4.4) become

$$\frac{de}{d\tau} = \begin{cases} (A - K^+C)e & \text{if : } s(y(\tau)) > 0 \\ (-A + K^-C)e & \text{if : } s(y(\tau)) < 0. \end{cases} \tag{4.7}$$

This last system can be written in the form of a switched system

$$\frac{de}{d\tau} = A_{\sigma(\tau)} e, \tag{4.8}$$

by defining the switching signal $\rho(t) = \text{sign}\big(y(t)\big)$ in the original time-scale, and transforming it into the new time as $\sigma(\tau) = \rho \circ w^{-1}(\tau)$.

Now, our aim is clear: we have to ensure the asymptotic stability of (4.7). In fact, we have transformed the analysis of the asymptotic stability of the origin of (4.4) into the stability analysis of (4.8), which is an autonomous switched linear system and numerous stability results are available (see, e.g., [Liberzon 2003]) for that class of systems. Most of them are based on a classical Lyapunov-functions-based approach but in addition to them, LaSalle-like results have been proposed more recently [Hespanha 2004]. In the latter, the stability properties of a switched linear system are proved via regularity assumptions on the set of switching signals.

Following [Hespanha 2004], inside the set of arbitrary pairs (e, σ), denote by $\mathcal{S}_{NC}$

the set of those that satisfy (4.8) and that are such that e is piecewise differentiable and σ piecewise constant. Define, moreover, the set $\mathcal{S}[\tau_D] \subset \mathcal{S}_{NC}$, with $\tau_D > 0$, of pairs for which any two consecutive discontinuities of σ are separated by no less than τ_D. The constant τ_D is called the *dwell-time*. The origin of a switched system of the form (4.8) is said to be *uniformly exponentially stable* if there exists constants a_0 and λ_0 such that, for each $\tau \geq 0$, we have $\|e(\tau)\| \leq a_0 \exp(-\lambda_0 \tau)\|e(0)\|$. In this definition, the word *uniform* refers to the fact that a_0 and λ_0 do not depend on the switching signal [Angeli 1999].

Under a dwell-time condition, as a particular case of Theorem 4 of [Hespanha 2004], one can prove that the switched linear system is uniformly exponentially stable if there exists a symmetric positive definite matrix that satisfies simultaneously the two non-strict Lyapunov equations below (4.10). The main result of this section, Theorem 4.1, shows that for our system (4.7) it is always possible to find a pair of gains K^+ and K^- such that this LaSalle-like condition is satisfied. The proof of Theorem 4.1 is detailed in the Appendix.

Recall that for any observable pair (A, C), there exist linear coordinates in which

$$A = \begin{pmatrix} a_1 & 1 & 0 & \dots & 0 \\ \vdots & 0 & 1 & \ddots & \vdots \\ \vdots & \vdots & \ddots & \ddots & 0 \\ \vdots & 0 & \dots & 0 & 1 \\ a_n & 0 & \dots & \dots & 0 \end{pmatrix}$$

and

$$C = \begin{pmatrix} 1 & 0 & \dots & 0 \end{pmatrix}.$$

In these coordinates, the system is in *observer normal form*.

Theorem 4.1. *Consider an observable pair (A, C). Define $Q = C^T C$. For any given pair of gains K^+ and K^-, define*

$$A_+ = A - K^+ C \quad \text{and} \quad A_- = -A + K^- C. \tag{4.9}$$

If K^+ is such that A_+ is Hurwitz, then there exists a unique K^- such that the two following Lyapunov equations

$$A_+^T P + P A_+ = -Q \quad \text{and} \quad A_-^T P + P A_- = -Q \tag{4.10}$$

admit a common solution P that is symmetric and positive definite.

Moreover, if (A, C) is in observer normal form, then the components k_i^- of K^-

are expressed in terms of the components k_i^+ of K^+ by

$$k_i^- = (-1)^i k_i^+ + \big(1 - (-1)^i\big) a_i,$$

where the constants a_i are the coefficients of the characteristic polynomial of A.

The following Theorem 4.2, which is the second main result of the paper and whose proof relies heavily on Theorem 4.1 and [Hespanha 2004, Theorem 4]), shows that our observer converges under suitable conditions.

Firstly, in order to guarantee the system's observability, it is assumed that the pair (A, C) is observable and that the function $Cb(y)$ does not vanish at $y = 0$ (the relative degree of the system is 1). These assumptions are natural consequences of the following result summarizing observability properties of system (4.2).

Proposition 4.1. *(i) System (4.2) is observable if and only if the pair (A, C) is observable and the system has relative degree one at any z such that $Cz = 0$.*

(ii) System (4.2) is never uniformly observable. In fact, the control $u(t) \equiv 0$ renders indistinguishable any two states $z_0 \neq \tilde{z}_0$ such that $Cz_0 = C\tilde{z}_0 = 0$.

(iii) If the pair (A, C) is observable and the system has relative degree one at any z such that $Cz = 0$, then any control $u(t)$ for which there exists ε_u such that u is continuous on $[0, \varepsilon_u[$ and $u(t) \neq 0$ for any $t \in [0, \varepsilon_u[$ distinguishes all states $z \in \mathbb{R}^n$.

Secondly, in order to avoid control signals for which the observer does not converge, we have to guarantee the system's observability when crossing the singularity $\{y = 0\} = \{Cz = 0\}$, see Proposition 4.1. We thus impose some restrictions on the controllers that are used to govern the system. In order to describe these restrictions, some notations are necessary. Fix an open subset Ω_0 that contains the origin and fix a compact set Ω that contains Ω_0. Fix $\varepsilon > 0$. Denote by Σ the intersection of Ω with the closed set $\{z \in \mathbb{R}^n : |Cz| \leq \varepsilon\}$. By construction, the set Σ is compact. Define a_0, d_0, and s_0 as the maxima of the functions $|CAz|$, $|Cd(y)|$, and $|s(y)|$, respectively, on Σ. Define b_0 as the minimum of $Cb(y)$ on Σ. Introduce the constant $\alpha = s_0(a_0 + d_0)/b_0$. And, finally, fix $\beta > \alpha$.

We say that a controller is *admissible* if it generates a control signal $u(\cdot)$ that satisfies together with its state trajectory $x(\cdot)$ the following properties:

(i) The control signal $u(t)$ is a piecewise continuous function of time such that $|u(t)| < \beta$, for $t \geq 0$;

(ii) On any given time interval $[a, b]$ such that the output satisfies $|y(t)| < \varepsilon$, for $t \in [a, b]$, the sign of $u(t)$ is constant and $|u(t)| > \alpha$.

(iii) If $x(0) \in \Omega_0$ then $x(t) \in \Omega$, for each $t \geq 0$;

These assumptions, on the system's observability and on the class of admissible controllers, lead to the following result.

Theorem 4.2. *Assume that the function $Cb(y)$ does not vanish at $y = 0$ and that the controller used to govern the system is admissible. If $x_0 \in \Omega_0$, then the switching signals $\rho(t)$ and $\sigma(\tau)$ generated by the controller admit a strictly positive dwell-time in the original and in the new time-scale, respectively.*

If, additionally, the pair (A, C) is observable and the gain matrices K^+ and K^- satisfy the conditions of Theorem 4.1 for the common solvability of the two coupled Lyapunov equations (4.10), then the origin of the observer's error dynamics (4.4) is asymptotically stable in the original time-scale associated to t and uniformly exponentially stable in the time-scale associated to τ.

4.3 Conditions for singular linearizability

In this section we answer the question of when there exists a diffeomorphism $z = \Phi(x)$ bringing system (4.1) into (4.2) such that the pair (A, C) is observable and $s(0) = 0$ but $s'(0) \neq 0$.

Denote by $C^\infty(X_0)$ the ring of $\mathbb{R}$-valued C^∞-functions defined locally in a neighborhood X_0 of $x_0 \in \mathbb{R}^n$. For a function $\varphi \in C^\infty(X_0)$, denote by $Z(\varphi)$ the set of zeros of φ, that is,

$$Z(\varphi) = \{x \in X_0 \,:\, \varphi(x) = 0\}.$$

We will need the following technical result.

Lemma 4.1. *Consider $\varphi \in C^\infty(X_0)$ and $\psi \in C^\infty(X_0)$ such that $d\psi(x_0) \neq 0$. The following conditions are equivalent:*

(i) $\varphi = \alpha\psi$, for some $\alpha \in C^\infty(X_0)$;

(ii) $Z(\varphi) \subset Z(\psi)$;

(iii) The function $\alpha = \frac{\varphi}{\psi} \in C^\infty(X_0 \setminus Z(\psi))$ can be prolonged to a smooth function $\hat{\alpha} \in C^\infty(X_0)$, that is, there exists a function $\hat{\alpha} \in C^\infty(X_0)$ such that $\hat{\alpha}(x) = \alpha(x)$, for any $x \in X_0 \setminus Z(\psi)$;

(iv) If X_0' is a compact containing x_0 in its interior, then there exists $M \in \mathbb{R}$ such that $|\frac{\varphi}{\psi}(x)| < M$, for any $x \in X_0' \setminus Z(\psi)$.

Our characterization of systems of the form (4.1) equivalent to (4.2) will be given in three steps. In the first step, using Proposition 4.1 below, we will construct a new vector field $\hat{f}$ in which we get rid of the singularities of the vector field f (using a singular time re-scaling). In the second step, we will construct a vector field $\hat{g}$ using the observability of the pair $(\hat{f}, h)$ (notice that the latter is observable although the original pair (f, h) is not, see Proposition 4.1(ii). In the third step, to the couple of vector fields $(\hat{f}, \hat{g})$ we attach, via a regular time re-scaling, a couple $(\bar{f}, \bar{g})$. The required time re-scaling is computable in terms of solutions of an ordinary differential equation on the output space (see Remark 2 following Theorem 4.3). Our necessary

and sufficient conditions are given in terms of the couple $(\bar{f}, \bar{g})$. Those conditions, as well as the construction of $(\bar{f}, \bar{g})$ follow from the main result of [Respondek 2004].

We will work around a fixed initial condition $x_0 \in \mathbb{R}^n$ and will assume that the diffeomorphism Φ satisfies $\Phi(x_0) = 0$.

Proposition 4.2. *If there exists a local diffeomorphism Φ transforming (4.1) into (4.2), then any among the equivalent conditions of Lemma 4.1 holds for all pairs $(\varphi, \psi) = (f_i, h)$, with $1 \leq i \leq n$, where f_i is the i-th component of f and h is the output function.*

If all pairs (f_i, h) of (4.1) satisfy the equivalent conditions of Lemma 4.1, then, due to condition (iii), each $\frac{f_i}{h} = \alpha$ can be extended to a C^∞-function $\hat{\alpha}$, which we will denote $\hat{f}_i$. Define the C^∞-vector field

$$\hat{f} = \hat{f}_1 \frac{\partial}{\partial x_1} + \cdots + \hat{f}_n \frac{\partial}{\partial x_n}.$$

A necessary condition for (4.1) to be transformed via $z = \Phi(x)$ into into (4.2) is that the pair $(\hat{f}, h)$ satisfies the following local observability rank condition (see, e.g., [Isidori 1995] and [Nijmeijer 1990])

$$\dim \operatorname{span} \{dh, dL_{\hat{f}}h, \ldots, dL_{\hat{f}}^{n-1}h\}(x_0) = n.$$

In that case, following [Krener 1983] (see also [Krener 1985]) define a vector field $\hat{g}$ (a "dummy" input) by

$$L_{\hat{g}} L_{\hat{f}}^j h = \begin{cases} 0 & \text{if } 0 \leq j \leq n-2 \\ 1 & \text{if } j = n-1. \end{cases} \tag{4.11}$$

For $j \geq 2$ we put $l_j = \frac{j(j-1)}{2} + 1$. In order to avoid the trivial case, we will assume throughout $n \geq 2$. We have the following results.

Theorem 4.3. System (4.1) *is, locally around x_0, equivalent under a diffeomorphism $z = \Phi(x)$ to the system (4.2), where $s(0) = 0$ and $s'(0) \neq 0$, if and only if in a neighborhood of x_0 all pairs $(\varphi, \psi) = (f_i, h)$, where f_i is the i-th component of f and h is the output function, fulfill the equivalent conditions of Lemma 4.1 and the vector fields $\hat{f}$ and $\hat{g}$ satisfy*

(i) the pair $(\hat{f}, h)$ satisfies at x_0 the local observability rank condition;

(ii) $dL_{\hat{g}} L_{\hat{f}}^n h = l_n \lambda dL_{\hat{f}} h \mod \operatorname{span}\{dh\}$, for some smooth function λ;

(iii) $\left[ad_{\bar{f}}^i \bar{g}, ad_{\bar{f}}^j \bar{g}\right] = 0$, *for $0 \leq i < j \leq n-1$, where $\bar{f} = \frac{1}{\bar{s}}\hat{f}$, $\bar{g} = \bar{s}^{n-1}\hat{g}$, and $\bar{s} = \exp\theta$, with θ being a solution of*

$$L_{ad_{\hat{f}}^j \hat{g}} \theta = \begin{cases} 0 & \text{if } 0 \leq j \leq n-2 \\ (-1)^{n-1}\lambda & \text{if } j = n-1. \end{cases}$$

(iv) $\left[g, ad_{\bar{f}}^{j}\bar{g}\right] = 0$, *for* $0 \leq j \leq n-2$.

Moreover, $d(0) = 0$ *if and only if* $\hat{f}(x_0) = 0$.

Remark 4.1. *The time re-scaling* $s(y)$ *is actually a product of two transformations* $s(y) = y\bar{s}(y)$. *Indeed, the dynamics to be linearized are obtained by, firstly dividing* f *by* $h = y$ *which gives* $\hat{f}$ *(a singular re-scaling) and then by dividing* $\hat{f}$ *by* $\bar{s} = \exp\theta$ *(a regular re-scaling).*

Remark 4.2. *The regular time re-scaling* $\bar{s} = \exp\theta$ *is defined by the ordinary differential equation*

$$\frac{d\theta(y)}{dy} = \lambda(y)$$

on the output space $\mathbb{R}$. *Hence it follows that*

$$s(y) = y\bar{s}(y) = y\exp(\int_0^y \lambda(v)dv).$$

4.4 Simulations on a simple example

In this section, we illustrate Theorems 4.1 and 4.2 with the design of an extended braking stiffness (XBS) observer, a problem that has its origins in the anti-lock brake systems literature (see, e.g., [Hoàng 2013] and the references therein).

During a straight-line ABS braking manoeuvre, the dynamics of the wheel can be described [Hoàng 2013] using the model

$$\begin{aligned} \frac{dz_1}{dt} &= \frac{-a}{v_x(t)}z_1z_2 + bu \\ \frac{dz_2}{dt} &= (cz_2 + z_3)\frac{z_1}{v_x(t)} \qquad \text{and} \qquad y = z_1, \\ \frac{dz_3}{dt} &= 0 \end{aligned} \tag{4.12}$$

where a, b, and c are known constants [1] The longitudinal speed of the vehicle (which is strictly positive during braking manoeuvres) is denoted v_x and the control u is the time-derivative of the brake pressure. The state z_1 is the wheel acceleration offset (the difference between the acceleration of the wheel and that of the vehicle), which is the only measurable variable. The state z_2 is the XBS, which is the derivative of the tyre characteristics (described by Burckhardt's model [Burckhardt 1993]). The

1. We consider here that the road conditions are known. The problem of unknown road conditions has been considered recently in [Hoàng 2014a], and leads to a four-dimensional model of the form (4.2) for which Theorem 4.1 can be applied (like for the simpler three-dimensional model considered here).

state z_3 is a constant that depends on the parameters of Burckhardt's model. The reader is referred to [Hoàng 2013] for a more detailed description of this model.

In its initial form, system (4.12) does not belong to the class of autonomous systems considered in the previous sections. Nevertheless, if we consider the regular time re-scaling $\frac{dt'}{dt} = \frac{1}{v_x(t)}$ and the new control $w(t) = u(t)v_x(t)$, then system (4.12) with respect to the new time t' is of the form (4.2). In order to keep a coherent notation with previous sections, in what follows, despite of the abuse of notation this new time scale is again denoted by t and the new control by u.

Our system is already in the form (4.2), so we can find new coordinates $\bar{z}$ in which (after a singular time re-scaling) the system is in the observer normal form: $\bar{z}_1 = z_1$, $\bar{z}_2 = z_2 + \frac{c}{a}z_1$, and $\bar{z}_3 = -\frac{z_3}{a}$. In these coordinates, we have $s(y) = -az_1$ and the following observer error dynamics

$$\frac{de}{ds} = \begin{cases} A_+ e = \begin{pmatrix} -\frac{c}{a} - k_1^+ & 1 & 0 \\ -k_2^+ & 0 & 1 \\ -k_3^+ & 0 & 0 \end{pmatrix} e & \text{if } s(y) > 0 \\ A_- e = \begin{pmatrix} \frac{c}{a} + k_1^- & -1 & 0 \\ k_2^- & 0 & -1 \\ k_3^- & 0 & 0 \end{pmatrix} e & \text{if } s(y) < 0. \end{cases} \tag{4.13}$$

If we want A_+ to be Hurwitz, the gain K^+ must satisfy

$$\begin{aligned} & k_1^+ > -\frac{c}{a} \\ & k_2^+ > 0 \\ & 0 < k_3^+ < (\frac{c}{a} + k_1^+)k_2^+. \end{aligned} \tag{4.14}$$

Since the coordinates are those of the observer normal form, Theorem 4.1 gives directly the value of K^- that must be used in the observer

$$\begin{aligned} k_1^- &= -k_1^+ - 2\frac{c}{a} \\ k_2^- &= k_2^+ \\ k_3^- &= -k_3^+. \end{aligned} \tag{4.15}$$

If we want, for example, the characteristic polynomial of A_+ to have a triple pole r, for the following numerical values

$$\begin{aligned} a &= 187.5\ (N.kg^{-1}),\ b = -4.4\ (N.m.bar^{-1}kg^{-1}), \\ c &= 24,\ v_x = 17.8\ (m/s),\ \text{and } r = 0.1, \end{aligned}$$

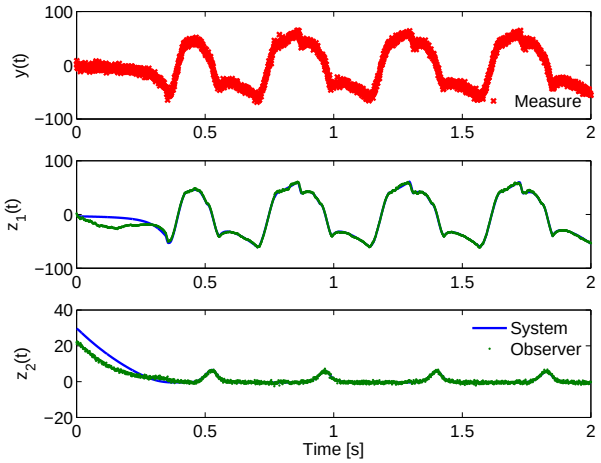

Figure 4.1: Simulation of a five-phase hybrid ABS algorithm [Hoàng 2013] with a closed-loop wheel acceleration control based on our singular observer.

we obtain, for example solving the Lyapunov equations of Theorem 4.1 with Matlab, the following matrices P_+ and P_-:

$$P_+ = P_- = \begin{pmatrix} 1.875 & 0 & -62.5 \\ 0 & 62.5 & 0 \\ -62.5 & 0 & 18750 \end{pmatrix},$$

whose equality is guaranteed by Theorem 4.1.

In order to apply Theorem 4.2, one must consider a control law that satisfies its conditions. A possible choice is the hybrid five-phase ABS described in [Pasillas-Lépine 2006], which satisfies all the required conditions to be admissible. With this control law, our switching observer (4.13) is thus uniformly exponentially stable in the new time-scale and asymptotically stable in the original time. The aim of our simulation is to verify this property. The simulation results are shown on Figures 4.1 and 4.2. At the time instants where the road conditions change (here $t = 0$), the observer errors are different from 0. Nevertheless, they converge asymptotically to 0 in the original time scale once the perturbation is over.

4.5 Proofs of main results

In order to prove Theorem 4.1, we will introduce and prove two claims and a lemma. We will need, moreover, an additional concept. Define $y_+(t, x_0^+)$ and

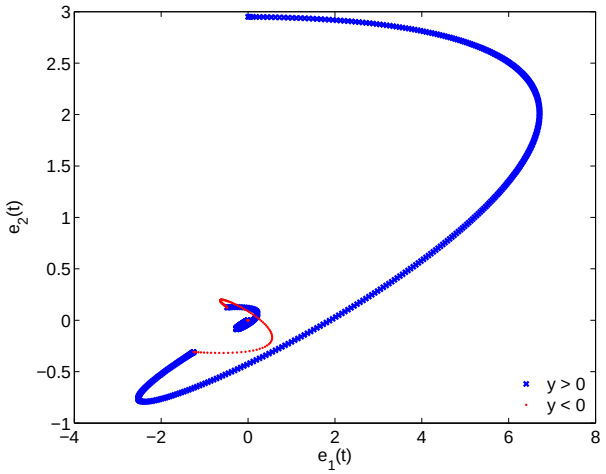

Figure 4.2: Phase-plane evolution of the previous simulation, obtained by a projection of the three-dimensional error on the (e_1, e_2) plane.

$y_-(t, x_0^-)$, as the solutions of systems

$$\left\{ \begin{array}{rcl} \dfrac{dx}{dt} & = & A_+ x \\ y & = & Cx \end{array} \right. \quad \text{and} \quad \left\{ \begin{array}{rcl} \dfrac{dx}{dt} & = & A_- x \\ y & = & Cx, \end{array} \right. \tag{4.16}$$

respectively, that start with the initial condition $x^\pm(0) = x_0^\pm$.

Claim 4.1. *Assume that the pairs (A_+, C) and (A_-, C) are both observable. The two following conditions are equivalent:*

(i) There exists a matrix S such that, for any initial condition x_0, the outputs of the two systems satisfy $y_-(t, Sx_0) = y_+(t, x_0)$.

(ii) The spectra of A_+ and A_- are equal.

Moreover, (iii) if S exists then it is unique.

Démonstration. Step 1: (i) implies (iii). The outputs of the system are analytic because the exponential function is analytic

$$y_\pm(t, x_0^\pm) = Ce^{tA_\pm} x_0^\pm. \tag{4.17}$$

The two outputs are equal if its derivatives of order k, for $k \geq 0$, coincide

$$y_+^{(k)}(0, x_0^+) = y_-^{(k)}(0, x_0^-). \tag{4.18}$$

If S exists, for any fixed x_0^+ such that $x_0^- = Sx_0^+$, we have

$$CA_+^k x_0^+ = CA_-^k Sx_0^+, \quad \text{for } 0 \leq k \leq n-1. \tag{4.19}$$

Since this is true for $\forall x_0^+$ and $x_0^- = Sx_0^+$, from the equation (4.19), we obtain

$$CA_+^k = CA_-^k S, \quad \text{for } 0 \leq k \leq n-1. \tag{4.20}$$

Since (A, C) is observable, then (A_+, C) and (A_-, C) are observable because they are obtained from (A, C) by an output injection. Define

$$M_+ = \begin{pmatrix} C \\ CA_+ \\ \vdots \\ CA_+^{n-1} \end{pmatrix} \quad \text{and} \quad M_- = \begin{pmatrix} C \\ CA_- \\ \vdots \\ CA_-^{n-1} \end{pmatrix}, \tag{4.21}$$

where rank (M_+) = rank (M_-) = n. Therefore, if the matrix S existes then it is unique

$$\begin{aligned} M_+ &= M_- S \\ \Rightarrow S &= M_-^{-1} M_+. \end{aligned} \tag{4.22}$$

Step 2: (i) implies (ii). The characteristic polynomial of A_+ is defined as

$$p(\lambda) = \lambda^n + p_{n-1}^+ \lambda_+^{n-1} + \ldots + p_1^+ \lambda + p_0^+, \tag{4.23}$$

where p_k^+, for $0 \leq k \leq n-1$, are its coefficients. Substituting the matrix A_+ for λ, the Cayley-Hamilton theorem states that $p(A) = 0$. Thus,

$$A_+^n = -p_{n-1}^+ A_+^{n-1} - \ldots - p_1^+ A_+ - p_0^+. \tag{4.24}$$

Multiplying this equation by C in the left, we obtain

$$CA_+^n = -p_{n-1}^+ CA_+^{n-1} - \ldots - p_1^+ CA_+ - p_0^+ C. \tag{4.25}$$

Similarly, the same computations are taken for A_- and we obtain

$$CA_-^n S = -p_0^- CS - p_1^- CA_- S - \ldots - p_{n-1}^- CA_-^{n-1} S, \tag{4.26}$$

where p_k^-, with $0 \leq k \leq n-1$, are the coefficients of the characteristic polynomial of A_-.

Since $CA_+^k = CA_-^k S$, for $0 \leq k \leq n-1$, therefore we obtain the following condition

$$p_k^+ = p_k^-. \tag{4.27}$$

This implies that the spectra of A_+ and A_- are equal.

Step 3: (ii) implies (i). Suppose that there exists a matrix S such that $x_0^+ = Sx_0^-$.

The two outputs are expressed as (4.17). Since they are analytic functions, in order to prove that they are equal, we will show that their derivatives of order k coincide, for any $k \geq 0$.

Indeed, it is trivial that the output derivatives of order k coincide, for any $0 \leq k \leq n-1$. We will check whether or not the outputs derivative of order $k = n$ coincide. Since (A_+, C) is observable, the vector CA_+^n can be expressed as a linear combination of the vectors that compose the basis $\{C, CA_+, \ldots, CA_+^{n-1}\}$. In other words,

$$CA_+^n = -\alpha_{n-1}^+ CA_+^{n-1} - \ldots - \alpha_1^+ CA_+ - \alpha_0^+ C. \tag{4.28}$$

If we apply the Cayley-Hamilton theorem, we obtain the expression of CA_+^n as in (4.25). Compare these two equations, we obtain $\alpha_k^+ = p_k^+$, for $0 \leq k \leq n-1$.

Repeating the same computations, we obtain (4.26) and $\alpha_k^- = p_k^-$, for $0 \leq k \leq n-1$.

Since the spectra of A_+ and A_- are equal, the characteristic polynomials of A_+ and A_- coincide. Thus, $p_k^+ = p_k^-$, for $0 \leq k \leq n-1$. Therefore,

$$CA_+^n = CA_-^n S. \tag{4.29}$$

This implies that the output derivatives of order k coincide, for $0 \leq k \leq n$.

Now, we suppose that the output derivatives of order k coincide, for $0 \leq k \leq n+i$ and a fixed $i \geq 0$. We will show that $CA_+^{n+i+1} = CA_-^{n+i+1} S$. Indeed, the vector CA_+^n is expressed as in (4.25). Multiplying this equation by A_+^{i+1} on the right, we obtain

$$CA_+^{n+i+1} = -p_{n-1}^+ CA_+^{n+i} - \ldots - p_0^+ CA_+^{i+1}. \tag{4.30}$$

Similarly, the vector CA_-^n can be expressed as

$$CA_-^n = -p_{n-1}^+ CA_-^{n-1} - \ldots - p_1^+ CA_- - p_0^+ C. \tag{4.31}$$

Multiplying this equation by $A_-^{i+1} S$ on the right, we obtain

$$CA_-^{n+i+1} S = -p_{n-1}^+ CA_-^{n+i} S - \ldots - p_0^+ CA_-^{i+1} S. \tag{4.32}$$

Since the output derivatives of order k coincide, for $0 \leq k \leq n+i$, thus

$$CA_+^{n+i+1} = CA_-^{n+i+1} S.$$

Therefore, we know that the output derivatives of order k coincide, for any $k \geq 0$, which means that

$$y_-(t, Sx_0) = y_+(t, x_0). \tag{4.33}$$

■

Claim 4.2. *Assume that the pair (A, C) is observable. Then, for any observer gain vector K^+, there exists a unique gain K^- such that the spectra of A_+ and A_- are equal.*

Lemma 4.2. *Assume that the pair (A, C) is observable. We have:*

(i) For any observer gain vector K^+, there exists a unique gain K^- and a unique matrix S such that $y_-(t, Sx_0) = y_+(t, x_0)$.

(ii) If, moreover, the coordinates x are such that the pair (A, C) is in observer form then

$$S = diag\big((-1)^0, (-1)^1, (-1)^2, \cdots, (-1)^{n-2}, (-1)^{n-1}\big) \tag{4.34}$$

and

$$k_i^- = (-1)^i k_i^+ + \big(1 - (-1)^i\big) a_i. \tag{4.35}$$

Démonstration. Step 1: proof of (i). The point (i) is obtained directly, by applying first Claim 4.2 (which is a standard fact of control theory), and then Claim 4.1.

Step 2: proof of (ii) Define the gain matrices

$$K^+ = \begin{pmatrix} k_1^+ & \dots & k_n^+ \end{pmatrix}^T \text{ and } K^- = \begin{pmatrix} k_1^- & \dots & k_n^- \end{pmatrix}^T. \tag{4.36}$$

Since (A, C) is in observer normal form, the matrices $A_\pm$ have the following form

$$\begin{aligned} A_+ &= \begin{pmatrix} a_1 - k_1^+ & 1 & 0 & \dots & 0 \\ \vdots & 0 & 1 & \ddots & \vdots \\ \vdots & \vdots & \ddots & \ddots & 0 \\ \vdots & 0 & \dots & 0 & 1 \\ a_n - k_n^+ & 0 & \dots & \dots & 0 \end{pmatrix} \\ \text{and } \ A_- &= \begin{pmatrix} -a_1 + k_1^- & -1 & 0 & \dots & 0 \\ \vdots & 0 & -1 & \ddots & \vdots \\ \vdots & \vdots & \ddots & \ddots & 0 \\ \vdots & 0 & \dots & 0 & -1 \\ -a_n + k_n^- & 0 & \dots & \dots & 0 \end{pmatrix}. \end{aligned} \tag{4.37}$$

The characteristic polynomial of the matrix A_+ is

$$det(Is - A_+) = (k_n^+ - a_n) + (k_{n-1}^+ - a_{n-1})s \quad + \ldots + (k_1^+ - a_1)s^{n-1} + s^n. \tag{4.38}$$

and the characteristic polynomial of the matrix A_- is

$$det(Is - A_-) = (-1)^n(k_n^- - a_n) + \ldots \quad + (-1)^1(k_1^- - a_1)s^{n-1} + s^n. \tag{4.39}$$

Since, by Claim 4.2, the spectra of A_+ and A_- are equal (which means that the characteristic polynomials of A_+ and A_- coincide), we obtain that (4.38) and (4.39) coincide. Therefore,

$$k_i^- = (-1)^i k_i^+ + (1 - (-1)^i) a_i. \tag{4.40}$$

Now, it remains to compute the matrix S. Define

$$S = \begin{pmatrix} s_{11} & s_{12} & \dots & s_{1n} \\ \vdots & \vdots & \vdots & \vdots \\ s_{n1} & s_{n2} & \dots & s_{nn} \end{pmatrix}. \tag{4.41}$$

We cannot use directly the equation (4.22) to compute the matrix S, because the computations of the matrices M^+ and M^- are difficult. We know, however, that each equation from (4.20) will help us to identify each line of the matrix S. We denote e_j, for $1 \leq j \leq n$, as the lines of the identity matrix of order n.

– Indeed, from $C = CS$, we obtain

$$\begin{pmatrix} s_{11} & \dots & s_{1n} \end{pmatrix} = e_1. \tag{4.42}$$

– From $CA_+ = CA_-S$, we obtain

$$-(k_1^+ - a_1)C + e_2 = (k_1^- - a_1)CS - e_2 S. \tag{4.43}$$

Because of (4.40), for $i = 1$ and $C = CS$, thus

$$\begin{pmatrix} s_{21} & \dots & s_{2n} \end{pmatrix} = -e_2. \tag{4.44}$$

– From $CA_+^2 = CA_-^2 S$, we obtain

$$\begin{array}{rl} & -(k_1^+ - a_1)CA_+ - (k_2^+ - a_2)C + e_3 \\ = & (k_1^- - a_1)CA_-S - (k_2^- - a_2)CS + e_3 S. \end{array} \tag{4.45}$$

Because of equation (4.40), for $1 \leq i \leq 2$ and $CA_+^k = CA_-^k S$, for $0 \leq k \leq 1$, thus

$$\begin{pmatrix} s_{31} & \dots & s_{3n} \end{pmatrix} = e_3. \tag{4.46}$$

– By continuing this computation with each equation of (4.20), up to the last equation

$$CA_+^{n-1} = CA_-^{n-1} S.$$

We obtain

$$\begin{aligned} & -(k_1^+ - a_1)CA_+^{n-2} - \ldots - (k_{n-2}^+ - a_{n-2})CA_+ \\ & -(k_{n-1}^+ - a_{n-1})C + e_n \\ = \; & (-1)^0(k_1^- - a_1)CA_-^{n-2}S + \ldots + \\ & (-1)^{n-2}(k_{n-1}^- - a_{n-1})CS + (-1)^{n-1}e_nS. \end{aligned} \tag{4.47}$$

As a consequence of equation (4.40) and $CA_+^k = CA_-^kS$, for $0 \leq k \leq n-2$, thus

$$\begin{pmatrix} s_{n1} & \ldots & s_{nn} \end{pmatrix} = (-1)^{n-1}e_n. \tag{4.48}$$

At the end, the matrix S is obtained as

$$S = \begin{pmatrix} 1 & 0 & 0 & \ldots & 0 & 0 \\ 0 & -1 & 0 & \ldots & 0 & 0 \\ 0 & 0 & 1 & \ldots & 0 & 0 \\ \vdots & \vdots & \vdots & \vdots & \vdots & \vdots \\ 0 & 0 & 0 & \ldots & (-1)^{n-2} & 0 \\ 0 & 0 & 0 & \ldots & 0 & (-1)^{n-1} \end{pmatrix},$$

or

$$S = \operatorname{diag}\big((-1)^0, (-1)^1, \cdots, (-1)^{n-2}, (-1)^{n-1}\big). \tag{4.49}$$

■

Démonstration. Step 1. Since (A, C) is observable, the pairs (A_+, C) and (A_-, C) are also observable. Moreover, by Claim 4.1, the matrices A_+ and A_- are Hurwitz. When the matrices A_+ and A_- are Hurwitz, it is well known that each equation $A_\pm^T P_\pm + P_\pm A_\pm = -Q$ always has a unique solution, which is symmetric positive definite when (A, C) is observable, even if the matrix Q is just positive semi-definite. One possible way to describe P_+ is the following

$$P_+ = \int_0^\infty (e^{tA_+})^T C^T C e^{tA_+} dt. \tag{4.50}$$

Thus,

$$\begin{aligned} x_0^+ P_+ x_0^+ &= \int_0^\infty (Ce^{tA_+}x_0^+)^T (Ce^{tA_+}x_0^+) ds \\ &= \int_0^\infty (y_+(t, x_0^+))^T y_+(t, x_0^+) dt \\ &= \int_0^\infty ||y_+(t, x_0^+)||^2 dt, \end{aligned} \tag{4.51}$$

where the output $y_+(t, x_0^+) = Ce^{tA_+}x_0^+$.
Similarly, we also have

$$P_- = \int_0^\infty (e^{tA_-})^T C^T C e^{tA_-} dt. \tag{4.52}$$

Then,

$$(Sx_0^+)^T P_-(Sx_0^+) = \int_0^\infty ||y_-(t, x_0^+)||^2 dt, \tag{4.53}$$

where the output $y_-(t, Sx_0^+) = Ce^{tA_-}Sx_0^+$.

By Lemma 4.2, we know that, for any observer gain vector K^+, there exist a unique gain vector K^- and a unique matrix S such that $y_-(t, Sx_0^+) = y_+(t, x_0^+)$. We then obtain

$$(x_0^+)^T S^T P_- S x_0^+ = (x_0^+)^T P_+ x_0^+, \quad \forall x_0^+. \tag{4.54}$$

Therefore,

$$S^T P_- S = P_+. \tag{4.55}$$

If (A, C) is in observer normal form, by Lemma 4.2, the matrix S is given by (4.49). Thus,

$$\begin{aligned} & S^T P_- S = P_+ \\ \Leftrightarrow \quad & p_{ij}^+ = \begin{cases} p_{ij}^- & \text{if : } ((i+j) \bmod 2 = 0) \\ -p_{ij}^- & \text{if : } ((i+j) \bmod 2 \neq 0), \end{cases} \end{aligned} \tag{4.56}$$

where p_{ij}^+, p_{ij}^- are respectively the elements of the i-th line and j-th column of the matrices P_+, P_-.

Step 2. In the observer normal form, the matrix A_+ is described by (4.37). Observing A_+, we have the following relation

$$A_+ e_i = e_{i-1}, \quad \text{for } 2 \leq i \leq n, \tag{4.57}$$

where e_i, with $1 \leq i \leq n$, are the columns of the identity matrix of order n.

Now, multiply the Lyapunov equation $A_+^T P_+ + P_+ A_+ = -Q$ by e_i^T on the left hand side, and e_j on the right hand side, for $2 \leq i, j \leq n$, we then obtain

$$e_i^T (A_+^T P_+ + P_+ A_+) e_j = -e_i^T Q e_j. \tag{4.58}$$

Using the relation (4.57), we obtain

$$\begin{aligned} & e_{i-1}^T P_+ e_j + e_i^T P_+ e_{j-1} = -e_i^T Q e_j \\ \Leftrightarrow \quad & p^+_{(i-1)j} + p^+_{i(j-1)} = -q_{ij} \\ \Leftrightarrow \quad & p^+_{(i-1)j} + p^+_{i(j-1)} = 0, \quad \text{for } 2 \leq i, j \leq n, \end{aligned} \tag{4.59}$$

because $q_{ij} = 0$, for $2 \leq i, j \leq n$. This condition implies that the sum of the two adjacent elements on the antidiagonal and on the other parallel lines with the anti-diagonal are always equal to 0. Therefore, all the elements on the anti-diagonal and on the other parallel lines with the anti-diagonal are equal in absolute value. If the number of elements on the anti-diagonal and on the other parallel lines with the anti-diagonal is even, then we have $p^+_{ij} = -p^+_{ji}$. However, since the matrix P_+ is symmetric, then $p^+_{ij} = -p^+_{ji} = 0$. If the number of elements on the anti-diagonal and on the other parallel lines with the anti-diagonal is odd, then $p^+_{ij} = p^+_{ji}$. Finally, we obtain

$$p^+_{ij} = \begin{cases} p^+_{ji} = p^+_{ii} & \text{if : } ((i+j) \bmod 2 = 0) \\ & \quad \& \ (|i-j| \bmod 4 = 0), \\ p^+_{ji} = -p^+_{ii} & \text{if : } ((i+j) \bmod 2 = 0) \\ & \quad \& \ (|i-j| \bmod 4 = 2), \\ -p^+_{ji} = 0 & \text{if : } ((i+j) \bmod 2 \neq 0). \end{cases} \tag{4.60}$$

Similarly, the matrix A_- has a following property

$$A_- e_i = -e_{i-1}, \quad \text{for } 2 \leq i \leq n. \tag{4.61}$$

With the similar computations and the arguments, we obtain

$$p^-_{ij} = \begin{cases} p^-_{ji} = p^-_{ii} & \text{if : } ((i+j) \bmod 2 = 0) \\ & \quad \& \ (|i-j| \bmod 4 = 0), \\ p^-_{ji} = -p^-_{ii} & \text{if : } ((i+j) \bmod 2 = 0) \\ & \quad \& \ (|i-j| \bmod 4 = 2), \\ -p^-_{ji} = 0 & \text{if : } ((i+j) \bmod 2 \neq 0). \end{cases} \tag{4.62}$$

Combine (4.56), (4.60) and (4.62), we obtain

$$p_{ij}^{+} = \begin{cases} p_{ij}^{-} = p_{ii} & \text{if : } ((i+j) \bmod 2 = 0) \\ & \quad \& \ (|i-j| \bmod 4 = 0), \\ p_{ij}^{-} = -p_{ii} & \text{if : } ((i+j) \bmod 2 = 0) \\ & \quad \& \ (|i-j| \bmod 4 = 2), \\ p_{ij}^{-} = 0 & \text{if : } ((i+j) \bmod 2 \neq 0). \end{cases} \tag{4.63}$$

or,

$$P_{+} = P_{-} = \begin{pmatrix} p_{11} & 0 & -p_{22} & 0 & \dots \\ 0 & p_{22} & 0 & \dots & \dots \\ -p_{22} & 0 & \ddots & \dots & \dots \\ 0 & \dots & \dots & \ddots & \dots \\ \vdots & \vdots & \vdots & \vdots & p_{nn} \end{pmatrix}. \tag{4.64}$$

■

Appendix A - Alternative proof of Lemma 4.2

This section is devoted to providing an alternative proof of Lemma 4.2 that has already been proved in Section 4.2. The main difference between this alternative proof and the previous one is the way how the matrix S is computed. Instead of using the analytic property of the outputs, we employ the Laplace transformation to compute it.

The outputs of the systems are given by

$$y_{\pm}(t, x_0^{\pm}) = Ce^{tA_{\pm}}x_0^{\pm}. \tag{4.65}$$

Since the pair (A, C) is in observer form, then the matrix $C = \begin{pmatrix} 1 & 0 & \dots & 0 \end{pmatrix}$. This leads to the fact that the matrices $Ce^{tA_{\pm}}$ are zero every where except for the first row. Thus, we can obtain an explicit expression of the matrices $Ce^{tA_{\pm}}$ if we can compute the first row of the matrices $e^{tA_{\pm}}$.

It is well known that the exponential matrix can be computed thanks to the inverse Laplace transformation [Moler 2003]

$$e^{tA_{\pm}} = \mathcal{L}^{-1}\{(sI - A_{\pm})^{-1}\}. \tag{4.66}$$

Besides, the matrix $(Is - A^{\pm})^{-1}$ is computed as below

$$\begin{aligned}(Is - A_{\pm})^{-1} &= \frac{1}{det(Is - A_{\pm})}[com(Is - A_{\pm})]^t \\ &= \frac{1}{det(Is - A_{\pm})} \begin{pmatrix} C_{11}^{\pm} & C_{12}^{\pm} & \dots & C_{1n}^{\pm} \\ \vdots & \vdots & \vdots & \vdots \\ C_{n1}^{\pm} & C_{n2}^{\pm} & \dots & C_{nn}^{\pm} \end{pmatrix}^t ,\end{aligned} \tag{4.67}$$

where $C_{ij}^{\pm}$, for $1 \leq i, j \leq n$ are the matrix of cofactors.

Let's compute the exponential matrix e^{tA_+}. We recall below the matrix $(Is - A_+)$

$$(Is - A_+) = \begin{pmatrix} s + (k_1^+ - a_1) & -1 & 0 & 0 & \dots & 0 \\ (k_2^+ - a_2) & s & -1 & 0 & \dots & 0 \\ \vdots & \vdots & \vdots & \vdots & \vdots & \vdots \\ (k_{n-2}^+ - a_{n-2}) & 0 & 0 & \dots & -1 & 0 \\ (k_{n-1}^+ - a_{n-1}) & 0 & 0 & \dots & s & -1 \\ (k_n^+ - a_n) & 0 & 0 & \dots & 0 & s \end{pmatrix}. \tag{4.68}$$

The determinant of $(Is - A_+)$ was calculated in Section 4.2

$$det(Is - A_+) = (k_n^+ - a_n) + (k_{n-1}^+ - a_{n-1})s + \ldots + (k_1^+ - a_1)s^{n-1} + s^n. \tag{4.69}$$

As explained earlier, since we only care about the first row of e^{tA_+} then we don't need to compute every matrix of cofactors C^+ij but the first column of $[com(Is - A_+)]$

$$[com(Is - A_+)]^t = \begin{pmatrix} s^{n-1} & C_{12}^+ & \dots & C_{1n}^+ \\ s^{n-2} & C_{22}^+ & \dots & C_{2n}^+ \\ \vdots & \vdots & \vdots & \vdots \\ s & C_{(n-1)2}^+ & \dots & C_{(n-1)n}^+ \\ 1 & C_{n2}^+ & \dots & C_{nn}^+ \end{pmatrix}^t . \tag{4.70}$$

Finally, the exponential matrix e^{tA_+} has the form

$$e^{tA_+} = \mathcal{L}^{-1} \left\{ \frac{1}{det(Is - A_+)} \begin{pmatrix} s^{n-1} & C_{12}^+ & \dots & C_{1n}^+ \\ s^{n-2} & C_{22}^+ & \dots & C_{2n}^+ \\ \vdots & \vdots & \vdots & \vdots \\ s & C_{(n-1)2}^+ & \dots & C_{(n-1)n}^+ \\ 1 & C_{n2}^+ & \dots & C_{nn}^+ \end{pmatrix}^t \right\}, \tag{4.71}$$

where $det(Is - A_+)$ is described in (4.69). The validation of (4.71) is assured since the matrix K^+ is chosen such that A_+ is Hurwitz and then $det(Is - A_+)$ is different

to 0.

The exponential matrix e^{tA_-} can be computed in the similar way

$$e^{tA_-} = \mathcal{L}^{-1}\left\{\frac{1}{det(Is - A_-)}\begin{pmatrix} s^{n-1} & C_{12}^- & \dots & C_{1n}^- \\ s^{n-3} & C_{32}^- & \dots & C_{3n}^- \\ \vdots & \vdots & \vdots & \vdots \\ (-1)^{n-2}s & C_{(n-1)2}^- & \dots & C_{(n-1)n}^- \\ (-1)^{n-1} & C_{n2}^- & \dots & C_{nn}^- \end{pmatrix}^t\right\} \tag{4.72}$$

where $det(Is - A_-)$ is also different to 0 since $det(Is - A_-) = det(Is - A_+)$.

Replace (4.71) and (4.72) into (4.65), we get the following expression of the two outputs

$$\begin{aligned} y^+(t, x_0^+) &= Ce^{tA_+}x_0^+ \\ &= C\mathcal{L}^{-1}\{(sI - A_+)^{-1}\}x_0^+ \\ &= \begin{pmatrix}1 & 0 & \dots & 0\end{pmatrix}\mathcal{L}^{-1}\left\{\frac{1}{det(Is - A_+)}\begin{pmatrix} s^{n-1} & C_{12}^+ & \dots & C_{1n}^+ \\ s^{n-2} & C_{22}^+ & \dots & C_{2n}^+ \\ \vdots & \vdots & \vdots & \vdots \\ s & C_{(n-1)2}^+ & \dots & C_{(n-1)n}^+ \\ 1 & C_{n2}^+ & \dots & C_{nn}^+ \end{pmatrix}^t\right\} x_0^+, \end{aligned} \tag{4.73}$$

and

$$\begin{aligned} y^-(t, x_0^-) &= Ce^{tA_-}x_0^- \\ &= C\mathcal{L}^{-1}\{(sI - A_-)^{-1}\}x_0^- \\ &= \begin{pmatrix}1 & 0 & \dots & 0\end{pmatrix}\mathcal{L}^{-1}\left\{\frac{1}{det(Is - A_-)}\begin{pmatrix} s^{n-1} & C_{12}^- & \dots & C_{1n}^- \\ -s^{n-2} & C_{22}^- & \dots & C_{2n}^- \\ s^{n-3} & C_{32}^- & \dots & C_{3n}^- \\ \vdots & \vdots & \vdots & \vdots \\ (-1)^{n-2}s & C_{(n-1)2}^- & \dots & C_{(n-1)n}^- \\ (-1)^{n-1} & C_{n2}^- & \dots & C_{nn}^- \end{pmatrix}^t\right\} x_0^-. \end{aligned} \tag{4.74}$$

Observing (4.73), (4.74) and knowing that $det(Is - A_-) = det(Is - A_+)$, we conclude that the two outputs are identical (or, in other words $y^+(t, x_0^+) = y^-(t, x_0^-)$) if the initial conditions are given by

$$x_0^- = Sx_0^+, \tag{4.75}$$

where

$$S = \begin{pmatrix} 1 & 0 & 0 & \dots & 0 & 0 \\ 0 & -1 & 0 & \dots & 0 & 0 \\ 0 & 0 & 1 & \dots & 0 & 0 \\ \vdots & \vdots & \vdots & \vdots & \vdots & \vdots \\ 0 & 0 & 0 & \dots & (-1)^{n-2} & 0 \\ 0 & 0 & 0 & \dots & 0 & (-1)^{n-1} \end{pmatrix}, \tag{4.76}$$

or

$$S = \operatorname{diag}\big((-1)^0, (-1)^1, \cdots, (-1)^{n-2}, (-1)^{n-1}\big). \tag{4.77}$$

Appendix B - Alternative proof of Theorem 4.1

In this section, we continue to employ the Laplace transformation to give an alternative proof of Theorem 4.1. The key point is to show that the Laplace transformation of the matrices P_+ and P_-, which are the unique solution of the two Lyapunov equations

$$A_\pm^T P_\pm + P_\pm A_\pm = -Q, \tag{4.78}$$

respectively, are equal.

As said in Section 4.2, the two matrices P_+ and P_- can be written as the following

$$P_\pm = \int_0^\infty (e^{tA_\pm})^T C^T C e^{tA_\pm} dt. \tag{4.79}$$

Since the inverse Laplace transformation is linear, then basing on (4.71) we have

$$\begin{aligned} Ce^{tA_+} &= C\mathcal{L}^{-1}\{(sI - A_+)^{-1}\} \\ &= \begin{pmatrix} 1 & 0 & \dots & 0 \end{pmatrix} \mathcal{L}^{-1} \left\{ \frac{1}{det(Is - A_+)} \begin{pmatrix} s^{n-1} & C_{12}^+ & \dots & C_{1n}^+ \\ s^{n-2} & C_{22}^+ & \dots & C_{2n}^+ \\ \vdots & \vdots & \vdots & \vdots \\ s & C_{(n-1)2}^+ & \dots & C_{(n-1)n}^+ \\ 1 & C_{n2}^+ & \dots & C_{nn}^+ \end{pmatrix}^t \right\} \\ &= \mathcal{L}^{-1} \left\{ \frac{1}{det(Is - A_+)} \begin{pmatrix} s^{n-1} & s^{n-2} & \dots & s & 1 \end{pmatrix} \right\}. \end{aligned} \tag{4.80}$$

Thus, the matrix P_+ can be represented

$$\begin{aligned} P_+ &= \int_0^\infty (e^{tA_+})^t C^t C e^{tA_+} dt \\ &= \lim_{t\to\infty} I_+(t), \end{aligned} \tag{4.81}$$

where

$$I_+(t) = \int_0^t \mathcal{L}^{-1}\left\{ \frac{1}{det(Is - A_+)} \begin{pmatrix} s^{n-1} \\ \vdots \\ s \\ 1 \end{pmatrix} \right\} \mathcal{L}^{-1}\left\{ \frac{1}{det(Is - A_+)} \begin{pmatrix} s^{n-1} & \dots & s & 1 \end{pmatrix} \right\} dt. \tag{4.82}$$

Now we apply the Final Value Theorem property of the Laplace transformation

$$\lim_{t\to\infty} I_+(t) = \lim_{s\to 0} sI_+(s), \tag{4.83}$$

where $I_+(s)$ is the Laplace transformation of $I_+(t)$. Then, (4.81) becomes

$$P_+ = \lim_{s\to 0} sI_+(s). \tag{4.84}$$

Since $I_+(t)$ is an integral then we apply the Laplace transformation of an integral and we obtain

$$I_+(s) = \frac{\mathcal{L}\left\{ \mathcal{L}^{-1}\left\{ \frac{1}{det(Is-A_+)} \begin{pmatrix} s^{n-1} \\ \vdots \\ s \\ 1 \end{pmatrix} \right\} \mathcal{L}^{-1}\left\{ \frac{1}{det(Is-A_+)} \begin{pmatrix} s^{n-1} & \dots & s & 1 \end{pmatrix} \right\} \right\}}{s}, \tag{4.85}$$

or,

$$sI_+(s) = \mathcal{L}\left\{ \mathcal{L}^{-1}\left\{ \frac{1}{det(Is - A_+)} \begin{pmatrix} s^{n-1} \\ \vdots \\ s \\ 1 \end{pmatrix} \right\} \mathcal{L}^{-1}\left\{ \frac{1}{det(Is - A_+)} \begin{pmatrix} s^{n-1} & \dots & s & 1 \end{pmatrix} \right\} \right\}. \tag{4.86}$$

From (4.84) and (4.86), the matrix P_+ is now written as

$$P_+ = \lim_{s\to 0} \mathcal{L}\left\{\mathcal{L}^{-1}\left\{\frac{1}{det(Is - A_+)}\begin{pmatrix} s^{n-1} \\ \vdots \\ s \\ 1 \end{pmatrix}\right\}\mathcal{L}^{-1}\left\{\frac{1}{det(Is - A_+)}\begin{pmatrix} s^{n-1} & \dots & s & 1 \end{pmatrix}\right\}\right\}. \tag{4.87}$$

Observing (4.87), we note that there is the Laplace transformation of a multiplication of two function. For two given functions $f(t)$ and $g(t)$, the Laplace transformation of the product $f(t)g(t)$ is

$$\mathcal{L}\{f(t)g(t)\} = \frac{1}{2\pi i}\int_{\gamma-i\infty}^{\gamma+i\infty} F(\sigma)G(s-\sigma)d\sigma, \tag{4.88}$$

where $\gamma = Re(\sigma)$ is chosen such that the integral is convergent. This implies that γ should lie entirely within the region of convergence of $F(\sigma)$, or in other words, γ should be bigger than the real part of any singularity of $F(\sigma)$. In our case, $\gamma > 0$ because that all the zeros $F(\sigma)$ are equal to zero and all its poles has negative real part since A_+ is Hurwitz.

Applying (4.88), the matrix P_+ is now computed as the following

$$P_+ = \lim_{s\to 0}\left(\frac{1}{2\pi i}\int_{\gamma-i\infty}^{\gamma+i\infty}\left[\frac{1}{det(I\sigma - A_+)}\begin{pmatrix} \sigma^{n-1} \\ \vdots \\ \sigma \\ 1 \end{pmatrix}\right]\times \left[\frac{1}{det(I(s-\sigma) - A_+)}\begin{pmatrix}(s-\sigma)^{n-1} & \dots & (s-\sigma) & 1\end{pmatrix}\right]d\sigma\right). \tag{4.89}$$

Next, it can be noticed that we can put the limit inside the integral

$$P_+ = \frac{1}{2\pi i}\int_{\gamma-i\infty}^{\gamma+i\infty}\frac{1}{[det(I\sigma - A_+)][det(-I\sigma - A_+)]}\begin{pmatrix} \sigma^{n-1} \\ \vdots \\ \sigma \\ 1 \end{pmatrix}\begin{pmatrix}(-\sigma)^{n-1} & \dots & (-\sigma) & 1\end{pmatrix}d\sigma \tag{4.90}$$

$$
\begin{aligned}
P_+ = & \frac{1}{2\pi i}\int_{\gamma-i\infty}^{\gamma+i\infty} \frac{1}{[det(I\sigma - A_+)][det(-I\sigma - A_+)]} \times \\
& \begin{pmatrix}
\sigma^{n-1}(-\sigma)^{n-1} & \sigma^{n-1}(-\sigma)^{n-2} & \sigma^{n-1}(-\sigma)^{n-3} & \dots & \sigma^{n-1}(-\sigma) & \sigma^{n-1} \\
\sigma^{n-2}(-\sigma)^{n-1} & \sigma^{n-2}(-\sigma)^{n-2} & \dots & \dots & \sigma^{n-2}(-\sigma) & \sigma^{n-2} \\
\sigma^{n-3}(-\sigma)^{n-1} & \sigma^{n-3}(-\sigma)^{n-2} & \dots & \dots & \sigma^{n-3}(-\sigma) & \sigma^{n-3} \\
\vdots & \vdots & \vdots & \vdots & \vdots & \vdots \\
\sigma(-\sigma)^{n-1} & \sigma(-\sigma)^{n-2} & \dots & \dots & \sigma(-\sigma) & \sigma \\
-(\sigma)^{n-1} & (-\sigma)^{n-2} & \dots & \dots & (-\sigma) & 1
\end{pmatrix} d\sigma \\
= & \frac{1}{2\pi i}\int_{\gamma-i\infty}^{\gamma+i\infty} \frac{1}{[det(I\sigma - A_+)][det(-I\sigma - A_+)]} \times \\
& \begin{pmatrix}
(-1)^{n-1}\sigma^{2n-2} & (-1)^{n-2}\sigma^{2n-3} & (-1)^{n-3}\sigma^{2n-4} & \dots & (-1)\sigma^{n} & \sigma^{n-1} \\
(-1)^{n-1}\sigma^{2n-3} & (-1)^{n-2}\sigma^{2n-4} & \dots & \dots & (-1)\sigma^{n-1} & \sigma^{n-2} \\
(-1)^{n-1}\sigma^{2n-4} & (-1)^{n-2}\sigma^{2n-5} & \dots & \dots & (-1)\sigma^{n-2} & \sigma^{n-3} \\
\vdots & \vdots & \vdots & \vdots & \vdots & \vdots \\
(-1)^{n-1}\sigma^{n} & (-1)^{n-2}\sigma^{n-1} & \dots & \dots & (-1)\sigma^{2} & \sigma \\
(-1)^{n-1}\sigma^{n-1} & (-1)^{n-2}\sigma^{n-2} & \dots & \dots & (-1)\sigma & 1
\end{pmatrix} d\sigma
\end{aligned}
\tag{4.91}
$$

Observing this matrix and noting that P_+ is symmetric, we conclude

$$
p_{ij}^+ = \begin{cases}
p_{ji}^+ = p_{ii}^+ & \text{if : } ((i+j) \bmod 2 = 0) \,\&\, (|i-j| \bmod 4 = 0), \\
p_{ji}^+ = -p_{ii}^+ & \text{if : } ((i+j) \bmod 2 = 0) \,\&\, (|i-j| \bmod 4 = 2), \\
-p_{ji}^+ = 0 & \text{if : } ((i+j) \bmod 2 \neq 0),
\end{cases}
\tag{4.92}
$$

where p_{ij}^+, for $1 \leq i, j \leq n$, are the elements of the $i-$th line and $j-$th column P_+.

Repeat the same steps for the computation of P_-, we have

$$
\begin{aligned}
P_- = \lim_{s\to 0} \Bigg(& \frac{1}{2\pi i}\int_{\gamma-i\infty}^{\gamma+i\infty} \left[\frac{1}{det(I\sigma - A_-)} \begin{pmatrix} \sigma^{n-1} \\ -\sigma^{n-2} \\ \vdots \\ (-1)^{n-2}\sigma \\ (-1)^{n-1} \end{pmatrix} \right] \times \left[\frac{1}{det(I(s-\sigma) - A_-)} \times \right. \\
& \left. \begin{pmatrix} (s-\sigma)^{n-1} & -(s-\sigma)^{n-2} & \dots & (-1)^{n-2}(s-\sigma) & (-1)^{n-1} \end{pmatrix} \right] d\sigma \Bigg)
\end{aligned}
\tag{4.93}
$$

Thus,

$$P_- = \frac{1}{2\pi i}\int_{\gamma-i\infty}^{\gamma+i\infty} \frac{1}{[det(I\sigma - A_-)][det(-I\sigma - A_-)]} \begin{pmatrix} \sigma^{n-1} \\ -\sigma^{n-2} \\ \vdots \\ (-1)^{n-2}\sigma \\ (-1)^{n-1} \end{pmatrix} \times$$
$$\begin{pmatrix} (-\sigma)^{n-1} & -(-\sigma)^{n-2} & \dots & (-1)^{n-2}(-\sigma) & (-1)^{n-1} \end{pmatrix} d\sigma$$
$$= \frac{1}{2\pi i}\int_{\gamma-i\infty}^{\gamma+i\infty} \frac{d\sigma}{[det(I\sigma - A_-)][det(-I\sigma - A_-)]} \times$$
$$\begin{pmatrix} (-1)^{n-1}\sigma^{2n-2} & (-1)^{n-1}\sigma^{2n-3} & \sigma^{n-1}\sigma^{2n-4} & \dots & (-1)^{n-1}\sigma^{n} & (-1)^{n-1}\sigma^{n-1} \\ (-1)^{n-2}\sigma^{2n-3} & (-1)^{n-2}\sigma^{2n-4} & (-1)^{n-2}\sigma^{2n-5} & \dots & (-1)^{n-2}\sigma^{n-1} & (-1)^{n-2}\sigma^{n-2} \\ (-1)^{n-3}\sigma^{2n-4} & \dots & \dots & \dots & (-1)^{n-3}\sigma^{n-2} & (-1)^{n-3}\sigma^{n-3} \\ \vdots & \vdots & \vdots & \vdots & \vdots & \\ (-1)\sigma^{n} & (-1)\sigma^{n-1} & \dots & \dots & (-1)\sigma^{2} & (-1)\sigma \\ \sigma^{n-1} & \sigma^{n-2} & \dots & \dots & \sigma & 1 \end{pmatrix}. \tag{4.94}$$

Observing this matrix and noting that P_- is symmetric, we conclude

$$p_{ij}^- = \begin{cases} p_{ji}^- = p_{ii}^- & \text{if : } ((i+j) \bmod 2 = 0) \,\&\, (|i-j| \bmod 4 = 0), \\ p_{ji}^- = -p_{ii}^- & \text{if : } ((i+j) \bmod 2 = 0) \,\&\, (|i-j| \bmod 4 = 2), \\ -p_{ji}^- = 0 & \text{if : } ((i+j) \bmod 2 \neq 0), \end{cases} \tag{4.95}$$

where p_{ij}^-, for $1 \leq i, j \leq n$, are the elements of the $i-$th line and $j-$th column of P_-.

Comparing the elements p_{ii}^+ and p_{ii}^- of (4.92) and (4.95), we notice that they are equal

$$p_{ii}^+ = p_{ii}^- = p_{ii}. \tag{4.96}$$

Finally, from (4.92), (4.95), and (4.96), it can be seen clearly that the two symmetric positive definite matrices P^+, P^- are equal

$$P^+ = P^- = \begin{pmatrix} p_{11} & 0 & -p_{22} & 0 & \dots \\ 0 & p_{22} & 0 & \dots & \dots \\ -p_{22} & 0 & \ddots & \dots & \dots \\ 0 & \dots & \dots & \ddots & \dots \\ \vdots & \vdots & \vdots & \vdots & p_{nn} \end{pmatrix}. \tag{4.97}$$

Chapter 5

Application for ABS: Extended braking stiffness estimation

The content of this chapter is strongly based on :

T.B. Hoang, W. Pasillas-Lépine, A. De Bernardinis, M. Netto. Extended braking stiffness estimation based on a switched observer. Accepted for publication in *IEEE Transactions on Control Systems Technology.*

In the accepted version of the paper, Appendices A and B were deleted because of the length restrictions imposed on Brief papers.

Abstract: In the context of hybrid anti-lock brake systems (ABS), a closed-loop wheel-acceleration controller based on the observation of the extended braking stiffness (XBS) is provided. Its objective is to improve the system's robustness with respect to changes in the environment (as changes in road conditions, brake properties, etc.). The observer design is based on Burckhardt's tyre model, which provides a wheel acceleration dynamics that is linear up to time-scaling. The XBS is one of the state variables of this model. The paper's main result is an observer that estimates this unmeasured variable. When the road conditions are known, a three-dimensional observer solves the problem. But, for unknown road conditions, a more complex four-dimensional observer must be used instead. In both cases, the observer's convergence is analyzed using tools for switched linear systems that ensure uniform exponential stability (provided that a dwell-time condition is satisfied). Both experiments and simulations confirm the convergence properties predicted by the theoretical analysis.

5.1 Introduction

The anti-lock brake system (ABS) is now a standard equipment on most new passenger cars, in order to prevent wheel lock-up and limit the risk of skidding. With this system, the car maintains its steerability and reduces its braking distance, even in the case of an emergency braking. Historically, the first commercial ABS systems were designed using logic-based switching controllers [Morse 1995], in which the mode changes were determined by the evolution of the wheel's angular acceleration (see, e.g., [Leiber 1979], [Kuo 1992], [Kiencke 2000], [Bosch 2004]). The main force of these controllers is that they avoid the use of the (unmeasured) wheel slip

and of its (unknown) optimal value. They are therefore quite robust with respect to changes in tyre parameters and road conditions. Their main drawback is, however, that they were derived from purely heuristic arguments and are, as a consequence, difficult to tune. Despite of this, the ABS controllers present on today's commercial vehicles mainly belong to this category. More recently, mainly in an academic context, several wheel slip controllers have been proposed in the literature (see, e.g., [Unsal 1999], [Johansen 2003], [Savaresi 2007], [Choi 2008], [Pasillas-Lépine 2012]). The main interest of these controllers is that they apply a brake torque that converges to a specific value, which avoids the typical limit cycles generated by logic-switched algorithms. This leads to shorter braking distances, at least on standard road conditions. Unfortunately, these approaches assume (implicitly) that the wheel slip is measured (or estimated) and that its optimal value is known, two requirements that are often difficult to meet. Even if such algorithms might not be robust enough to be implemented on commercial ABS, they are still useful for some specific applications [Van Zanten 2002], like the electronic stability program (ESP).

In addition to hybrid and continuous approaches for ABS, which both have their pros and cons [Shida 2010], one can find a different research line (see, e.g., [Gustafsson 1998], [Sugai 1999], and [Ono 2003]) based on the concept of extended braking stiffness (XBS). The XBS is the slope $\mu'(\lambda)$ of the tyre characteristic $\mu(\lambda)$. For additional details, the reader is referred to Section 5.2. In standard conditions, there exists an (unknown) value of the wheel slip λ^* for which the curve μ reaches its maximum. That is, such that $\mu'(\lambda^*) = 0$. The main theoretical interest of XBS for braking strategies is hence clear: unlike wheel slip, that has an unknown optimal target value λ^*, the optimal value of XBS is always the same (zero). An intuitive approach for ABS control is thus to regulate the value of XBS around zero. But, actually, the XBS appears also in other contexts related to braking systems. A first example is wheel acceleration control. In this context, the XBS can be seen as a disturbance that must be compensated in order to increase either the controller's bandwidth or its delay margin (see, e.g., [Corno 2012, Gerard 2012, Hoàng 2012]). A second (related) example is wheel slip control. Indeed, since the wheel acceleration is closely related to the derivative of the wheel slip (see Section 5.2.2), the XBS appears also naturally in this domain [Pasillas-Lépine 2012]. One should stress, however, that the XBS cannot be measured directly using standard sensors. In order to use it in a control algorithm one must therefore address first its real-time estimation, which is the main objective of this paper. Because of the diversity of control problems in which the XBS appears, it would have been difficult to treat all of them here. The choice of the authors was thus to emphasize the contributions associated to the estimation problem, and to consider the control issues only for illustration purposes.

The simplest approach to estimate XBS is probably to consider this variable as a constant parameter, which allows the use of online least squares methods [Ono 2003]. Other approaches analyze the tyre/carcass resonance in the frequency

domain [Sugai 1999] or use algebraic methods [Villagra 2011]. Solutions based on wheel slip measurements are also available [Tanelli 2009]. Nevertheless, to the author's knowledge, the idea of exploiting the nonlinear XBS dynamics in a model-based observer has not been considered before in the literature, at least in the case of the longitudinal stiffness. The proposed approach is based on a new model for the wheel acceleration dynamics. In this model, the extended braking stiffness enters as one of the state variables. When the road conditions are known, this model is three-dimensional. Otherwise a fourth order dynamics is obtained. In both cases an observer can be constructed using a copy of the system's dynamics and adding a nonlinear correction term that is proportional to the observation error. After a suitable time-rescaling, the observer error is reduced to a linear switched system that can be analyzed using standard methods [Hespanha 2004]. When the observer switches admit a strictly positive dwell-time, the observer's convergence is global, uniform, and exponential. Compared to previous works, the authors believe that the main interest of this method comes from its simplicity and from the fact that the parameters of the tyre model are not needed by the proposed algorithm.

In order to illustrate on a concrete example the interest of this observer, the case of a simple academic ABS strategy [Pasillas-Lépine 2006] is considered. In their standard form, this kind of algorithms might fail to cycle correctly [Ait-Hammouda 2008] when there are significant changes in the environment (as changes in road conditions, brake properties, etc.). In a recent work [Gerard 2012], it has been shown that adding closed-loop wheel acceleration control during the phases for which the brake pressure is modified can compensate this lack of robustness. But, in order to reach the bandwidth required by this kind of controllers, an XBS estimate is necessary. The combination of such control laws with the proposed XBS observer has been tested both on simulations (with unknown and changing road conditions) and experimentally (with known and constant road conditions, imposed by the test-rig characteristics).

This paper is organized as follows. First, the system's dynamics is described in Section 5.2. Then, the main contributions of the paper (the design and the stability analysis of two switched observers) are presented in Sections 5.3 and 5.4, with the corresponding experimental and simulation results. An academic five-phase hybrid ABS and a closed-loop wheel-acceleration control law are briefly described in Section 5.5, in order to exhibit a potential application for these observers. Finally, concluding remarks and perspectives for future research are presented in Section 5.6.

5.2 System modelling

The basic dynamics of the wheel, which is central to this study, can be analyzed using a single-wheel model (see, e.g., [Olson 2003] and [Ono 2003]). The main reason

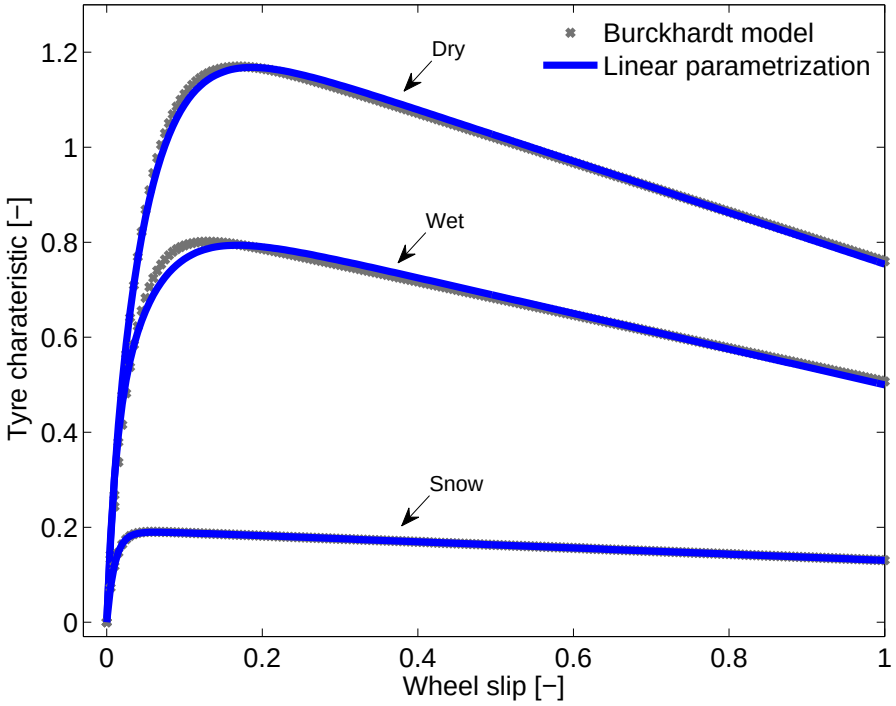

Figure 5.1: Comparison of the tyre characteristic $\mu(\lambda)$ given by Burckhardt's model (5.5) and its approximation (5.18), on different road conditions. For clarity, only the positive wheel slip part of the curve is shown (instead of the negative part, which corresponds to braking). The parameters of the tyre models are given in Section 5.4.1.

for using this model is that, despite of its simplicity, all the basic phenomena related to ABS control appear in it [Gerard 2012].

5.2.1 Wheel dynamics

The angular velocity ω of the wheel has the following dynamics:

$$I\frac{d\omega}{dt} = -RF_x + T_w, \tag{5.1}$$

where I denotes the inertia of the wheel, R its radius, F_x the longitudinal tyre force, and T_w the torque applied to the wheel. The torque $T_w = T_e - T_b$ is composed of the engine torque T_e and the brake torque T_b. It is assumed that during ABS braking the clutch is open and thus the engine torque is neglected. In other words, $T_b = \gamma_b P_b$, where $P_b > 0$ denotes the brake pressure and $\gamma_b > 0$ the brake efficiency.

The longitudinal tyre force F_x is often modelled by the relation

$$F_x = \mu(\lambda) F_z, \tag{5.2}$$

where F_z denotes the vertical load and

$$\lambda = \frac{R\omega - v_x}{v_x} \tag{5.3}$$

denotes the *wheel slip* [Kiencke 2000]. The longitudinal speed of the vehicle v_x, which is considered as an external variable of the model, is assumed to be strictly positive. In a braking manoeuvre, this implies $\lambda < 0$ and $F_x < 0$. The *tyre characteristic* $\mu(\cdot)$ is a function that is both smooth and odd. It satisfies $\mu(0) = 0$ and $\mu'(0) > 0$ (see Figure 5.1), where $\mu'(\lambda)$ denotes the derivative of μ with respect to λ. Several mathematical descriptions are available in order to describe this curve. Two of them are considered in Sections 5.3.1 and 5.4.1.

5.2.2 Wheel acceleration dynamics

The state variables of the model are

$$x_1 = \lambda \quad \text{and} \quad x_2 = R\frac{d\omega}{dt} - a_x(t),$$

where $a_x(t) = dv_x(t)/dt$ denotes the vehicle's longitudinal acceleration. The state x_1 is the wheel slip. The state x_2 is the *wheel acceleration offset*, that is, the difference between the acceleration of the wheel and that of the vehicle. These variables evolve with the following dynamics

$$\begin{aligned} \frac{dx_1}{dt} &= \frac{1}{v_x(t)}\left(-a_x(t)x_1 + x_2\right) \\ \frac{dx_2}{dt} &= -\frac{a\mu'(x_1)}{v_x(t)}\left(-a_x(t)x_1 + x_2\right) + \frac{R}{I}\frac{dT_w}{dt} - \frac{da_x(t)}{dt}, \end{aligned}$$

where $a = (R^2/I)F_z$ and the *extended braking stiffness* $\mu'(.)$ is defined as the derivative of the tyre characteristic $\mu(.)$ with respect to λ.

During an ABS-controlled braking manoeuvre, the vehicle's acceleration $a_x(t)$ stays almost constant and close to the maximal value a_x^* allowed by the road conditions [Gerard 2012]. Moreover, the wheel slip λ remains relatively small. In such conditions, the control and observer designs can be simplified by considering that $(-a_x x_1 + x_2) \simeq x_2$. This approximation is exact only at constant speed, but it remains reasonable in the case of ABS manoeuvres [Gerard 2012]. Its validity is checked *a posteriori* in Sections 5.3 and 5.4, by simulating the proposed observers on

the original (non-simplified) model. This approximation leads to a simpler dynamics

$$\begin{aligned} \frac{dx_1}{dt} &= \frac{1}{v_x(t)} x_2 \\ \frac{dx_2}{dt} &= -\frac{a}{v_x(t)} \mu'(x_1) x_2 + bu, \end{aligned} \tag{5.4}$$

where the control variable $u = dP_b(t)/dt$ is the derivative of the brake pressure and $b = -R\gamma_b/I$. Indeed, we have $T_w = -\gamma_b P_b$ (see Section 5.2.1), and thus $(R/I)dT_w/dt = b\, dP_b/dt$.

5.3 Observer design (known road conditions)

5.3.1 Tyre characteristic

In the literature, one can find several mathematical formulas that have been used to describe the tyre characteristic $\mu(\lambda)$, such as trigonometric functions in [Pacejka 2005], second order rational fractions in [Kiencke 2000] and [Pasillas-Lépine 2006], and exponentials in [Burckhardt 1993]. This section is based on Burckhardt's model introduced in [Burckhardt 1993]

$$\mu(\lambda) = c_1(1 - e^{-c_2\lambda}) - c_3\lambda, \tag{5.5}$$

where the coefficients c_i are constants depending on the road conditions, the tyre model, the tyre pressure, etc. Therefore, for the sake of robustness, the ABS algorithms should be able to handle the uncertainty associated with these coefficients. A typical tyre characteristic associated to this model is illustrated in Figure 5.1.

5.3.2 Extended braking stiffness dynamics

Burckhardt's tyre model is particularly interesting when it comes to estimate the value of the extended braking stiffness, which cannot be measured directly. Indeed, a simple mathematical formula for $\mu'(\lambda)$ can be obtained by differentiating (5.5), with respect to λ. From this formula and from the second order derivative of (5.5), one can establish a relation between these variables:

$$\mu''(\lambda) + c_2\mu'(\lambda) + c_2c_3 = 0. \tag{5.6}$$

Now, defining the wheel acceleration offset $z_1 = x_2$, the extended braking stiffness $z_2 = \mu'(x_1)$, the unknown product of parameters $z_3 = -c_2c_3$ as new vari-

ables, and combining equations (5.4) and (5.6) gives

$$\begin{aligned}\frac{dz_1}{dt} &= \frac{-a}{v_x(t)} z_1 z_2 + bu \\ \frac{dz_2}{dt} &= (cz_2 + z_3)\frac{z_1}{v_x(t)} \\ \frac{dz_3}{dt} &= 0,\end{aligned} \tag{5.7}$$

where $c = -c_2$ is a constant that depends on road conditions. This model can be seen as a generalization of the model proposed in [Ono 2003] and as a particular case of (5.4), associated to Burckhardt's tyre model. Somehow, considering the unknown constant z_3 as a new state variable (and not as a parameter) is not optimal. Indeed, the adaptive observer approach [Besançon 2000] could have been a more standard way to handle this problem. Nevertheless, that approach has not been followed here because (for the authors) it is not obvious how to combine it with the switchings introduced in the next section. While, using a representation of the form (5.7), the approach of [Hoàng 2014b] is directly applicable.

On the one hand, an interesting quality of this model is that the wheel slip (which cannot be measured) does not appear explicitly in it as a state variable. One might argue that this is not that interesting, since the velocity (which cannot be measured neither) appears instead in the system's dynamics. Nevertheless, at least at high speeds, it is much easier to estimate the vehicle's velocity than to estimate wheel slip [Daiss 1995]. On the other hand, the main drawback of our model (5.7) is that it is assumed that the value of c is known, which is true only for a fixed type of road conditions (the more complex case of unknown road conditions is considered later, in Section 5.4.

5.3.3 Observer Design

Since, unlike the wheel acceleration offset z_1, the extended braking stiffness z_2 is not directly measurable, it must be estimated using an observer. To that aim, one can start with a copy of the original system and add some terms proportional to the observation error, in order to ensure the convergence of the trajectories between both systems. As it is shown later, multiplying these terms by z_1 simplifies considerably

the analysis. At the end, one obtains

$$\begin{aligned}\frac{d\widehat{z}_1}{dt} &= \frac{-a}{v_x} z_1 \widehat{z}_2 + bu + \frac{k_1(z_1)}{v_x} z_1(z_1 - \widehat{z}_1) \\ \frac{d\widehat{z}_2}{dt} &= (c\widehat{z}_2 + \widehat{z}_3)\frac{z_1}{v_x} + \frac{k_2(z_1)}{v_x} z_1(z_1 - \widehat{z}_1) \\ \frac{d\widehat{z}_3}{dt} &= \frac{k_3(z_1)}{v_x} z_1(z_1 - \widehat{z}_1),\end{aligned} \tag{5.8}$$

where $\widehat{z}_i$ are the observer states.

In (5.8), the observer gains $k_i(z_1)$, for $1 \leq i \leq 3$, must depend on the value of z_1 in order to ensure the observer's stability independently of the sign of z_1. The simplest choice might be

$$k_i(z_1) = \begin{cases} k_i^+ & \text{if } z_1 > 0 \\ k_i^- & \text{if } z_1 < 0. \end{cases} \tag{5.9}$$

Even if the gains $k_i(z_1)$ are discontinuous, it must be stressed that the observer gains $k_i(z_1)z_i$ are continuous, which ensures the existence and uniqueness of solutions for (5.8) when $z_1(t)$ is considered as an external input.

Let us consider the observer errors $e_i := z_i - \widehat{z}_i$, for $1 \leq i \leq 3$. Subtracting equation (5.8) from equation (5.7) leads to

$$\frac{de}{dt} = \frac{z_1}{v_x} \begin{pmatrix} -k_1(z_1) & -a & 0 \\ -k_2(z_1) & c & 1 \\ -k_3(z_1) & 0 & 0 \end{pmatrix} e. \tag{5.10}$$

Notice that if the right hand side of (5.10) is divided by z_1/v_x then the observer error dynamics is transformed into a linear system. This leads to the idea of changing the time-scaling. Indeed, let

$$s(t) := \int_0^t \frac{|z_1(\tau)|}{v_x(\tau)} d\tau, \tag{5.11}$$

which ensures that $dt/ds > 0$, independently of the values of z_1. Since, for any function $\varphi : \mathbb{R} \to \mathbb{R}^n$, one has

$$\frac{d\varphi}{ds} = \frac{d\varphi}{dt}\frac{dt}{ds} = \frac{d\varphi}{dt}\frac{v_x}{|z_1(t)|}. \tag{5.12}$$

This implies

$$\frac{de}{ds} = \begin{cases} A_+ e = \begin{pmatrix} -k_1^+ & -a & 0 \\ -k_2^+ & c & 1 \\ -k_3^+ & 0 & 0 \end{pmatrix} e & \text{if } z_1 > 0 \\ A_- e = \begin{pmatrix} k_1^- & a & 0 \\ k_2^- & -c & -1 \\ k_3^- & 0 & 0 \end{pmatrix} e & \text{if } z_1 < 0, \end{cases} \tag{5.13}$$

which can be written using a more compact notation in the form

$$\frac{de(s)}{ds} = A_{\sigma(s)} e(s), \tag{5.14}$$

where σ denotes a piecewise constant signal that selects, at each instant, a matrix from the pair $\{A_+, A_-\}$.

5.3.4 Stability Conditions

It results from the previous section that the analysis of the asymptotic convergence of the observer (5.8) can be derived from the stability analysis of the error equation (5.14), which is an autonomous switched linear system. It appears that numerous stability results are available for that class of systems [Liberzon 2003]. Most of them are based on classical Lyapunov-functions. But some LaSalle-like results are also available [Hespanha 2004], for which the stability properties of the switched system are proved via regularity assumptions on the set of switching signals.

Define the switching signal $\sigma(t) = \text{sign}(z_1(t))$, and assume that the solutions of (5.14) are such that e and σ are piecewise differentiable and piecewise constant, respectively. Following [Liberzon 1999], define moreover the set $\mathcal{S}[\tau_D]$, with $\tau_D > 0$, of switchings for which any two consecutive discontinuities of σ are separated by no less than τ_D. The constant τ_D is called the *dwell-time*. The origin of a switched system of the form (5.14) is said to be *uniformly exponentially stable* if there exists constants c_0 and λ_0 such that, for each $t \geq 0$, we have $\|e(t)\| \leq c_0 \exp(-\lambda_0 t)\|e(0)\|$. In this definition, the word *uniform* refers to the fact that c_0 and λ_0 do not depend on the switching signal [Angeli 1999].

Under a dwell-time condition, as a particular case of Theorem 4 of [Hespanha 2004], one can prove that a switched linear system is uniformly exponentially stable if there exists a symmetric positive definite matrix that satisfies simultaneously two non-strict Lyapunov equations (more details on this point are given in Appendix A). The aim of Theorem 5.1 below is to show that, for the switched system (5.14), it is always possible to find a pair of gains K^+ and K^- such that this

LaSalle-like condition is satisfied. To ensure the stability of (5.14), a first natural condition is to impose the matrices A_+ and A_- to be Hurwitz. The corresponding conditions on the observer gains can be derived using Routh's criterion, which gives

$$k_1^+ > c, \quad k_2^+ < -\frac{c}{a}k_1^+, \quad \text{and} \quad -\frac{(ck_1^+ + ak_2^+)(c-k_1^+)}{a} < k_3^+ < 0; \tag{5.15}$$

and

$$k_1^- < c, \quad k_2^- < -\frac{c}{a}k_1^-, \quad \text{and} \quad 0 < k_3^- < -\frac{(ck_1^- + ak_2^-)(c-k_1^-)}{a}. \tag{5.16}$$

From these conditions, with the help of Theorem 4 of [Hespanha 2004], one can obtain the following result (proved in Appendix A, at the end of the paper).

Theorem 5.1. *Assume that the three following conditions are satisfied*
(i) The gain $K^+ = \begin{pmatrix} k_1^+ & k_2^+ & k_3^+ \end{pmatrix}$ *satisfies (5.15).*
(ii) The gain $K^- = \begin{pmatrix} k_1^- & k_2^- & k_3^- \end{pmatrix}$ *satisfies (5.16).*
(iii) The gains K^+ *and* K^- *satisfy*

$$\frac{(c-k_1^-)}{ak_3^-} = \frac{(c-k_1^+)}{ak_3^+} > 0 \quad \textit{and} \quad (ck_1^+ + ak_2^+) = (ck_1^- + ak_2^-) < 0. \tag{5.17}$$

Then, the system (5.14) is uniformly exponentially stable, provided that the switching signal σ *admits a strictly positive dwell-time.*

This result gives at least a certain degree of freedom: we can chose any K^+ that stabilizes the system. Once this choice has been made, it imposes however an almost unique choice for K^- (in order to assign the same spectrum to A_+ and A_-). We do not know, in general, if this constraint can be avoided, but this issue is discussed in [Hoàng 2014b].

5.3.5 Experimental results

The observer design proposed in this section has been validated on data coming from the tyre-in-the-loop experimental facility of TU Delft, acquired in the context of ABS research [Gerard 2012]. The test-rig consists in a large steel drum on the top of which the tyre is rolling. The tyre is mounted on a wheel that is attached to a rotating axle, which has a rigidly constrained height. The axle is supported by two bearings on both sides of the wheel. The bearing housings are connected to a fixed frame by means of piezo-electric force transducers. A hydraulic disk brake is mounted on one side of the axle. The pressure in the calliper is locally controlled by an analog electronic circuit connected to a servo-valve, in order to match the reference pressure. An illustration of this test-rig can be seen on Section 9.4 of [Pacejka 2005]. The setup

has been used for several years, at TU Delft, for tyre modelling and identification (see [Pacejka 2005, Section 9.4] and [Zegelaar 1998, Appendix A], and the references therein).

In order to satisfy the conditions imposed by Theorem 5.1, for positive z_1's, the following observer gains are chosen

$$\begin{aligned} k_1^+ &= c + (\beta_1 + 2\beta_2) \\ k_2^+ &= -(\beta_2^2 + 2\beta_1\beta_2 + ck_1^+)/a \\ k_3^+ &= -\beta_1\beta_2^2/a. \end{aligned}$$

And, for negative z_1's,

$$\begin{aligned} k_1^- &= c - (\beta_1 + 2\beta_2) \\ k_2^- &= -(\beta_2^2 + 2\beta_1\beta_2 + ck_1^-)/a \\ k_3^- &= \beta_1\beta_2^2/a, \end{aligned}$$

where β_1 and β_2 are positive constants that assign the spectrum of the error dynamics. More precisely, the error dynamics (5.13) will always have two real eigenvalues $-\beta_1$ (with multiplicity 1) and $-\beta_2$ (with multiplicity 2), independently of the sign of z_1. The interest of assigning the same spectrum to A_+ and A_- is explained in [Hoàng 2014b].

The experimental results are shown in Figure 5.2, where it can be seen that the states of the system and of the observer remain close to each other. In this figure, the observer's variable $\hat{z}_1$ is compared to the measure of z_1, while the variable $\hat{z}_2$ is compared to an estimation $\mu'(x_1)$ of the XBS obtained directly from the measure of wheel slip. One can observe in this figure a surprising phenomenon: the noise of the observed variable $\hat{z}_2$ is bigger when the wheel acceleration is positive. A possible explanation for these oscillations might be that the norm of K^+ is bigger than that of K^-, a constraint imposed by Theorem 5.1.

This phenomenon reduces the accuracy of the estimation, which is nevertheless good enough to detect whether the tyre is in its stable or unstable region. The proposed observer has however another weak point: it only works correctly when the parameter c_2 of Burckhardt's model is known, at least approximatively. The knowledge of this parameter is closely related to the knowledge of road conditions, a problem that is considered in the next section.

5.4 Observer design (unknown road conditions)

In contrast to the simpler approach of Section 5.3, it is now assumed that the observer does not have any information on the road conditions (and thus on the

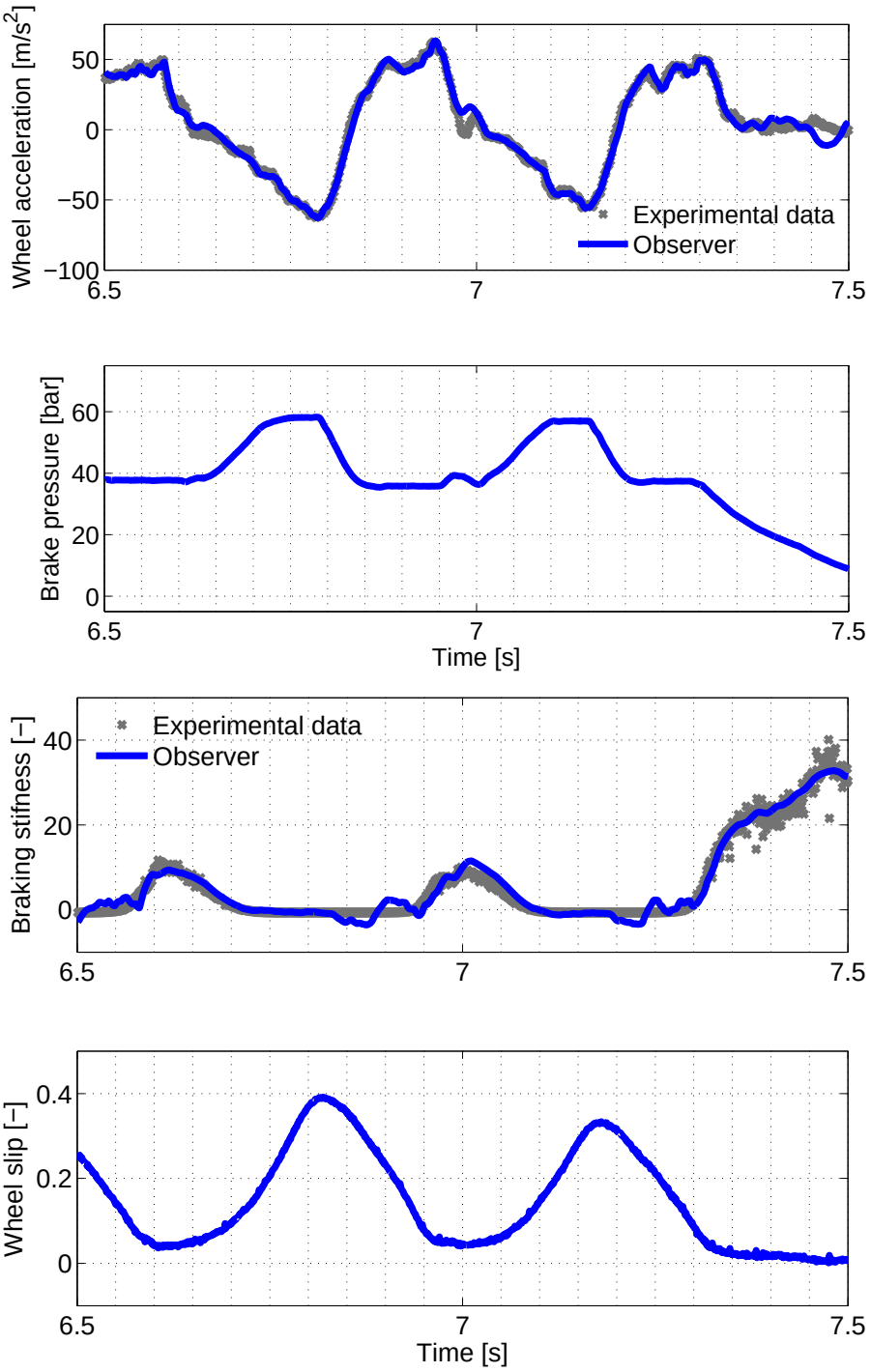

Figure 5.2: Comparison between experimental measurements and the estimated states given by the observer (5.8), during an ABS test [Pasillas-Lépine 2006]. The parameters of the test-rig tyre characteristics are: $c_1 = -1.24$, $c_2 = -34$, and $c_3 = 0.65$. The system parameters are: $I = 1.2kg.m^2$, $R = 0.3m$, $F_z = 2500N$, and $\gamma_b = 17.5N.m/bar$. The speed of the drum is $65\,km/h$. The XBS estimated by the observer is compared to the theoretical value obtained from the wheel slip and the derivative of the tyre characteristic.

	Burckhardt's model			Approximate model		
	c_1	c_2	c_3	θ_0	θ_1	θ_2
Dry road	1.28	24	0.52	-0.53	25.22	7.2
Wet road	0.86	34	0.35	-0.36	8.86	24
Snow	0.28	50	0.05	-0.05	0.24	14

Table 5.1: Tyre model parameters

parameters of Burckhardt's model). This new context imposes the use a more complex four-dimensional observer, which can be considered as a generalization of the previous three-dimensional observer (5.8).

5.4.1 Tyre characteristic

The main difficulty with Burckhardt's model (5.5) is that its parametrization is nonlinear. Recently, in [Tanelli 2009], an alternative parametrization of this model by exponentials has been proposed (see also [de Castro 2012]). This kind of approximations can be traced back up to the work of Prony [Prony 1795] (see [Hildebrand 1974] for a modern treatment). In this section, Burckhardt's model is approximated with a similar parametrization

$$\mu(\lambda) = \theta_0\lambda + \theta_1\frac{e^{d_1\lambda}-1}{d_1} + \theta_2\frac{e^{d_2\lambda}-1}{d_2}, \tag{5.18}$$

defined for $\lambda \leq 0$. The constants d_1 and d_2 must be chosen in such a way that $-c_2 \in [d_1, d_2]$. Since, for negative wheel slip, the parameter c_2 varies in the range $[-50, -24]$, one can take $d_1 = 22$ and $d_2 = 52$. The parameters of Burckhardt's model are shown in Table 5.1. For different road conditions, the coefficients θ_i can be identified using the Least Squares method (see Table 5.1). In Figure 5.1, the tyre characteristics given by Burckhardt's model (5.5) is compared to its approximation (5.18).

5.4.2 Extended braking stiffness dynamics

Computing the first, second and third derivatives of the approximate model (5.18), with respect to λ, one can see that these derivatives satisfy the following relation

$$\mu'''(\lambda) = \alpha_0 + \alpha_1\mu'(\lambda) + \alpha_2\mu''(\lambda), \tag{5.19}$$

where $\alpha_0 = d_1d_2\theta_0$, $\alpha_1 = -d_1d_2$, $\alpha_2 = (d_1 + d_2)$. Therefore, following the ideas of Section 5.3, we take as state variables $z_1 = x_2$, $z_2 = \mu'(\lambda)$, $z_3 = \mu''(\lambda)$, and $z_4 = \alpha_0$.

Now, combining equations (5.4) and (5.19) gives

$$\begin{aligned}
\frac{dz_1}{dt} &= \frac{-a}{v_x(t)} z_1 z_2 + bu(t) \\
\frac{dz_2}{dt} &= \frac{z_1}{v_x(t)} z_3 \\
\frac{dz_3}{dt} &= \frac{z_1}{v_x(t)} (\alpha_1 z_2 + \alpha_2 z_3 + z_4) \\
\frac{dz_4}{dt} &= 0,
\end{aligned} \tag{5.20}$$

where a and b are defined in Section 5.2.

The most important property of this model is that the parameters α_1 and α_2 do not depend on the road conditions. This leads to the possibility of observing the extended braking stiffness, using neither the wheel slip nor the parameters that describe the tyre characteristic. It should be stressed, however, that this model is only valid for *constant* road conditions. In the case of a change in the road conditions (see, e.g., Figure 5.3), the validity of the model fails temporarily, which might induce a brief divergence between the system and the observer states.

5.4.3 Observer design

For system (5.20), an observer with an error dynamics that is linearizable by a time-scaling can be constructed following the same approach as in Section 5.3. This leads to a switching error dynamics (5.13), with

$$A_+ = \begin{pmatrix} -k_1^+ & -a & 0 & 0 \\ -k_2^+ & 0 & 1 & 0 \\ -k_3^+ & \alpha_1 & \alpha_2 & 1 \\ -k_4^+ & 0 & 0 & 0 \end{pmatrix} \quad \text{and} \quad A_- = \begin{pmatrix} k_1^- & a & 0 & 0 \\ k_2^- & 0 & -1 & 0 \\ k_3^- & -\alpha_1 & -\alpha_2 & -1 \\ k_4^- & 0 & 0 & 0 \end{pmatrix}. \tag{5.21}$$

Conditions for the stability of (5.14), in the case of these new matrices A_+ and A_-, can be derived following the same approach as for Theorem 5.1 (see Appendix B).

5.4.4 Simulation results

In test-rigs like those of TU Delft, changes of road conditions are not possible. Nevertheless, numerical simulations can still be used to assess the performance of the proposed observer. This has been done considering the (non-simplified) model of Section 5.2 and using the observer's output to implement the control law of Section 5.5. In order to ensure the observer's stability, for positive z_1's, the following observer gains are chosen: $k_1^+ = \alpha_2 + 2(\beta_1 + \beta_2)$, $k_2^+ = (-\alpha_1 - k_1^+ \alpha_2 - (\beta_1^2 + \beta_2^2 + 4\beta_1\beta_2))/a$,

$k_3^+ = (-k_1^+\alpha_1 + ak_2^+\alpha_2 - 2\beta_1\beta_2(\beta_1+\beta_2))/a$, and $k_4^+ = -\beta_1^2\beta_2^2/a$. And, for negative z_1's, $k_1^- = \alpha_2 - 2(\beta_1+\beta_2)$, $k_2^- = (-\alpha_1 - k_1^-\alpha_2 - (\beta_1^2+\beta_2^2+4\beta_1\beta_2))/a$, $k_3^- = (-k_1^-\alpha_1 + ak_2^-\alpha_2 + 2\beta_1\beta_2(\beta_1+\beta_2))/a$, and $k_4^- = -\beta_1^2\beta_2^2/a$, where β_1 and β_2 are positive constants that assign the spectrum of the error dynamics, which has two double real eigenvalues $-\beta_1$ and $-\beta_2$.

Figure 5.3 shows the obtained simulation results. The details of the braking scenario are given in the figure's caption. The observer estimates accurately the values of the XBS, for different road conditions. During transitions, (which last $25\,ms$), the estimated XBS values change abruptly. The observer cannot give good estimations during these transitions. Nevertheless, as soon as they are over, the observer error decreases in a relatively short period of time that, of course, depends on the choice of β_1 and β_2.

5.5 Control design

A five-phase hybrid ABS algorithm [Pasillas-Lépine 2006] is described in Figure 5.4. Each of the algorithm's phases defines either a constant or quickly changed brake pressure $P_b(t)$ that is applied to the brake. The switches between each phase are triggered when the value of the wheel acceleration offset x_2 crosses some predefined threshold. The main interest of such hybrid approaches is that they do not use any information on the unmeasured variable x_1. Nevertheless, they are able to keep the wheel slip in a small neighborhood of its optimal value λ^*, for which the longitudinal tyre force is maximal (with the aim of minimizing the braking distance), without using explicitly the value of the optimal setpoint. The reader can find in [Pasillas-Lépine 2006] more details about this five-phase hybrid ABS algorithm.

When the algorithm of Figure 5.4 is tested on an experimental setup [Gerard 2012], it might fail to cycle correctly as soon as there are considerable changes in the environment. The main reason behind this lack of robustness is that, during the different phases, the wheel acceleration is controlled in open-loop, with a brake pressure increase that is independent of the wheel's acceleration. This shortcoming can be overcome [Gerard 2012] by controlling the wheel acceleration x_2 in closed-loop (around a predefined trajectory x_2^*), during the phases for which the brake torque changes quickly.

In order to do this, define $\tau := t - t_0$, where t_0 is the instant at which a given phase begins. Consider the time T needed by the reference trajectory x_2^* to go from the previous threshold ε_i to the next one ε_j. Ideally, the duration T should be as small as possible but, due to the physical limitations of the brake actuator, there exists a lower bound on the achievable T's. If $\dot{P}_b^M$ is defined as the maximum brake pressure derivative that the actuator can deliver (in absolute value), then the choice of the reference trajectory x_2^* must guarantee that $|\dot{P}| \leq \dot{P}_b^M$. Furthermore, in order

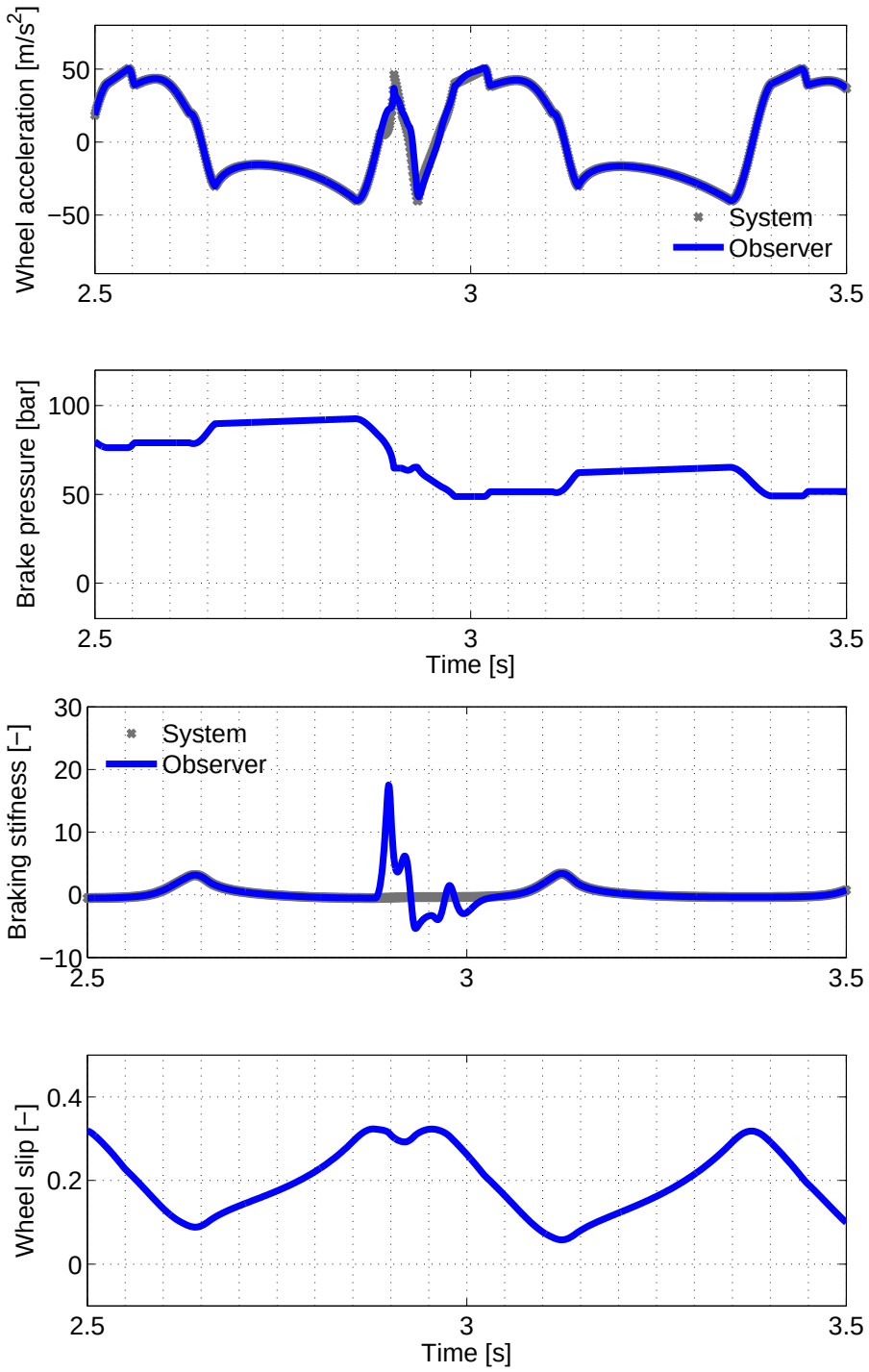

Figure 5.3: Simulation of a braking ABS scenario with changes of the road conditions: The car runs on dry asphalt during three seconds and on wet asphalt afterwards. In this figure, it can be seen that the XBS observer is highly perturbed by the swift road transition but that, once the transition is over, it converges again in a fraction of a second towards the appropriate state.

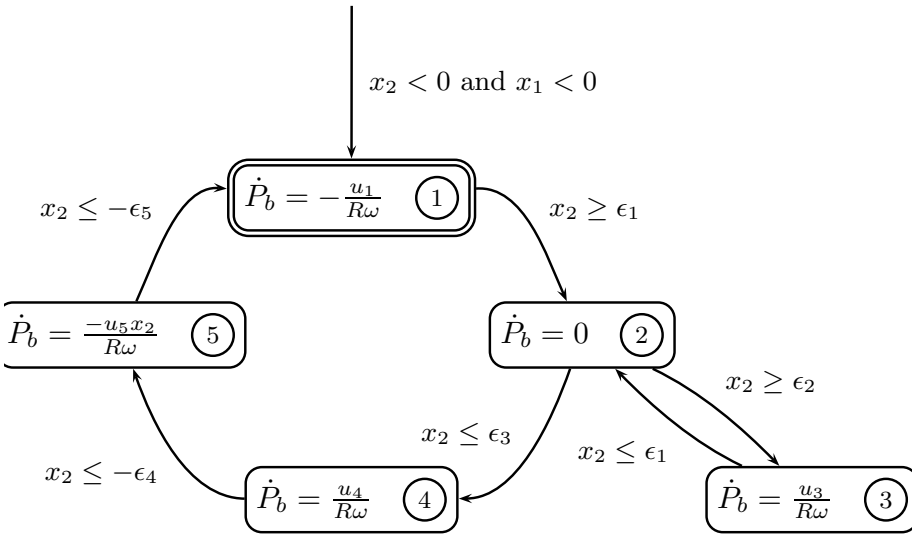

Figure 5.4: The academic five-phase hybrid ABS strategy proposed in [Pasillas-Lépine 2006]. The wheel acceleration thresholds ε_i and the brake pressure increase and decrease rates u_i must be tuned in order to obtain an asymptotically stable limit cycle (see, e.g., [Ait-Hammouda 2008] and [Pasillas-Lépine 2006]).

to minimize the system's sensitivity to actuator delays, it is natural to require a zero derivative for x_2^* at the beginning and at the end of each phase [Gerard 2012]. A possible choice for a reference trajectory x_2^* that goes from ε_i to ε_j is therefore

$$x_2^*(\tau) = a_0 + a_1\tau + a_2\tau^2 + a_3\tau^3, \tag{5.22}$$

where $a_0 = \varepsilon_i$, $a_1 = 0$, $a_2 = -3(\varepsilon_i - \varepsilon_j)/T^2$, and $a_3 = 2(\varepsilon_i - \varepsilon_j)/T^3$. By imposing, additionally, the constraint $T \geq (3/2b)|\varepsilon_i - \varepsilon_j|/\dot{P}_b^M$, one can ensure that the reference trajectory respects the brake actuator's limitations described above.

Now, define the tracking error $\xi = x_2 - x_2^*$ and the control law

$$u(t) = \frac{1}{b}\left(\frac{a}{v_x}\hat{\mu}'(t)x_2 + \frac{dx_2^*(t)}{dt} - \alpha\xi(t)\right), \tag{5.23}$$

where $\alpha > 0$ is the control gain and $\hat{\mu}'(t)$ is an estimation of the extended braking stiffness $\mu'(x_1(t))$. In the absence of estimation error, the tracking error converges exponentially to zero, provided that the control gain α is taken big enough. Observe, however, that the gain α is limited by the delay margin of the system [Hoàng 2012]. In this approach, the choice of controlling only the variable x_2 might be surprising. But it appears that the stability of all other variables actually comes from the fact that they are bounded functions of the wheel slip x_1, which remains bounded both for

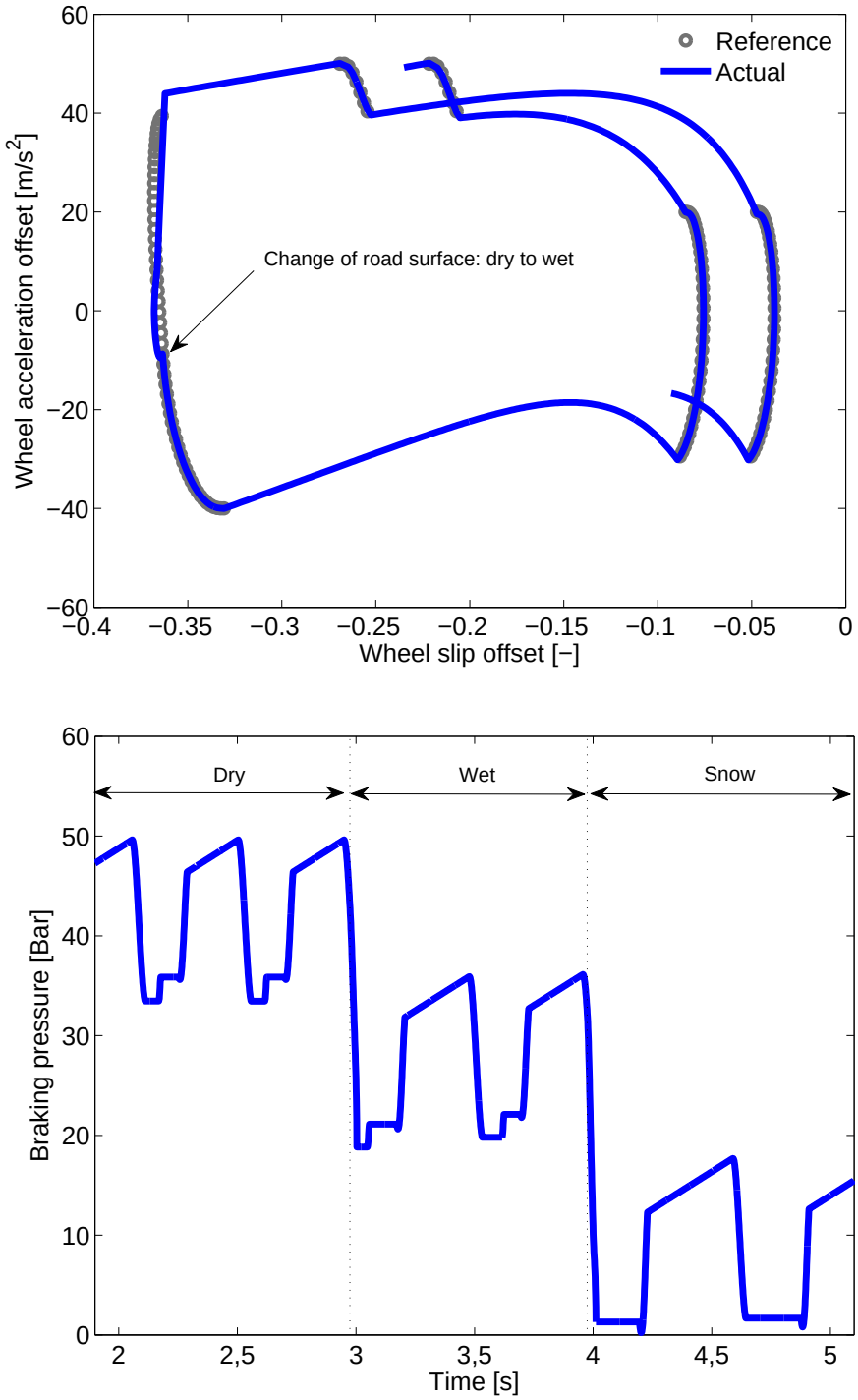

Figure 5.5: The wheel acceleration tracking (during phases 1, 3, and 4) is achieved using the observer of Section 5.4 and the control design of Section 5.5. The car runs on dry asphalt during three seconds, then on wet asphalt for one second, and finally on snow until the end of the simulation. When the road conditions change, the brake pressure is reduced and follows the available tyre force potential.

hybrid [Gerard 2012] and continuous [Pasillas-Lépine 2012] control designs, provided that the wheel acceleration offset x_2 follows its reference.

In the simulation of Figure 5.5, the control uses the XBS estimation given by the observer. Thanks to the observer performance, the control law (5.23) ensures a good tracking performance of the wheel acceleration x_2 to its pre-defined reference. As a consequence of the robustness added by the closed-loop wheel acceleration control, the brake pressure is automatically increased or decreased to match road conditions.

5.6 Conclusion

In the context of anti-lock brake systems (ABS), we presented in this chapter a new approach to estimate the extended braking stiffness. The first contribution of this work is a new nonlinear wheel acceleration model in which the XBS enters as one of the state variables. This model is obtained using either Burckhardt's model or its linearly parametrized approximation. The second contribution is the design of two stable XBS observers. When the road conditions are known, a three-dimensional observer solves the problem. But, for unknown road conditions, a more complex four-dimensional observer should be used instead. In both cases, the stability of the observers is proved via time-rescaling and LaSalle-like theorems for linear switched systems.

The three-dimensional observer has been tested on experimental data coming from TU-Delft's test-rig [Gerard 2012]. In such tests, the parameters associated to the mounted tyre are known. The experimental results show the effectiveness of this observer. The four-dimensional observer has been tested in simulations in a scenario that includes unkown changes of road conditions. The simulation results show a precise estimation of the XBS even in the case of discontinuous jumps of the road conditions.

The proposed method has nevertheless several limitations. First, it needs a (rough) estimation of the vehicle's speed (see, e.g., [Daiss 1995] and [Corno 2013] for works that consider this problem). Second, the combined convergence of the observer and of the control law has not been proved. One could expect, however, that such a proof is obtainable via cascaded design arguments [Loría 2005]. Third, the vertical load F_z has been considered to be both known and constant. It is true that F_z can be "reconstructed" using the longitudinal and lateral accelerations as inputs. It is also known that hybrid ABS strategies have a certain degree of robustness with respect to vertical load uncertainties (see, e.g., the Appendix A.1 of [Gerard 2012]). Nevertheless, the impact of a time-varying vertical load on the proposed design is clearly a topic that deserves further investigations.

Appendix A - Proof of Theorem 5.1

This section includes a sketch of the proof of Theorem 5.1. The interested reader can find in [Hoàng 2014b] an approach that generalizes this method to a more general class of switched systems that contains, as particular cases, the proposed three and four-dimensional observers.

The characteristic polynomial of the matrix A_+ is given by

$$\eta^3 + (k_1^+ - c)\eta^2 - (ck_1^+ + ak_2^+)\eta - ak_3^+ = 0. \tag{5.24}$$

Using the Routh criterion for (5.24) leads directly to condition (5.15). The same argument, but applied to A_-, gives condition (5.16).

Assume that that the observer gains K^+ and K^- satisfy, respectively, the conditions (5.15) and (5.16). For additional details concerning the following steps, the reader is referred to [Hespanha 2004, Theorem 4]. The objective is to show that there exists a pair $\{P_+, P_-\}$, of symmetric positive definite matrices satisfying all the conditions required by that theorem, for an appropriately defined pair of matrices $\{C_+, C_-\}$.

Define $C_+ = \begin{pmatrix} c_1^+ & 0 & 0 \end{pmatrix}$ and $C_- = \begin{pmatrix} c_1^- & 0 & 0 \end{pmatrix}$, where $c_1^+, c_1^- \neq 0$. It is easy to check that the pairs (A_+, C_+) and (A_-, C_-) are observable. In order to satisfy the conditions of [Hespanha 2004, Theorem 4], one must find a matrix P that satisfies simultaneously the equations $A_+^T P + PA_+ = -C_+^T C_+$ and $A_-^T P + PA_- = -C_-^T C_-$. Observe that P defines a non-strict Lyapunov function only, because the symmetric matrices $C_i^T C_i$ are not strictly positive definite. Denote by (p_{ij}) the elements of P. One can easily deduce from $A_+^T P + PA_+ = -C_+^T C_+$ that

$$\begin{aligned} p_{11} &= \frac{c^2 - (ck_1^+ + ak_2^+)}{a^2} p_{22}, \quad p_{12} = \frac{c}{a} p_{22}, \\ p_{13} &= \frac{1}{a} p_{22}, \quad p_{23} = 0, \quad \text{and} \quad p_{33} = \frac{(c - k_1^+)}{ak_3^+} p_{22}, \end{aligned} \tag{5.25}$$

where $p_{22} > 0$. With the elements of P computed as in (5.25), one obtains

$$c_1^+ = \pm\sqrt{2\frac{(c - k_1^+)(ck_1^+ + ak_2^+) + ak_3^+}{a^2} p_{22}} \neq 0. \tag{5.26}$$

The term in the square root is positive because of (5.15) and $p_{22} > 0$.

Similarly, since P has to satisfy the condition $A_-^T P + PA_- = -C_-^T C_-$, it follows

that the elements of P are also of the form

$$\begin{aligned} p_{11} &= \frac{c^2 - (ck_1^- + ak_2^-)}{a^2} p_{22}, \quad p_{12} = \frac{c}{a} p_{22}, \\ p_{13} &= \frac{1}{a} p_{22}, \quad p_{23} = 0, \quad \text{and} \quad p_{33} = \frac{(c - k_1^-)}{ak_3^-} p_{22}. \end{aligned} \tag{5.27}$$

From (5.25) and (5.27), additional conditions on the observer gains K^+ and K^- can be obtained:

$$\frac{(c - k{-}_1)}{ak_3^-} = \frac{(c - k_1^+)}{ak_3^+} > 0 \quad \text{and} \quad (ck_1^+ + ak_2^+) = (ck_1^- + ak_2^-) < 0. \tag{5.28}$$

The element c_1^- of C_- is also different from zero and, because of (5.16) and $p_{22} > 0$, one obtains

$$c_1^- = \pm \sqrt{-2 \frac{(c - k_1^-)(ck_1^- + ak_2^-) + ak_3^-}{a^2} p_{22}}, \tag{5.29}$$

which ends the proof.

Appendix B - Stability conditions for the four-dimensional observer

This section is devoted to finding the conditions on the observer gains for which the four-dimensional observer is convergent. It has been shown in Section 5.4 that the observer error dynamics is also an autonomous switched linear system. The stability analysis of the four-dimensional observer is then proved thanks to Theorem 4 of [Hespanha 2004] provided that the dwell-time condition is satisfied. The similar steps, as shown in Section 5.6, are taken in order to obtain the stability conditions on the observer gains.

The characteristic polynomial of the matrix A_+ is given by

$$\eta^4 + (k_1^+ - \alpha_2)\eta^3 + (-\alpha_1 - k_1^+\alpha_2 - ak_2^+)\eta^2 + (-k_1^+\alpha_1 + ak_2^+\alpha_2 - ak_3^+)\eta - ak_4^+ = 0. \tag{5.30}$$

η^4	1	$(-\alpha_1 - k_1^+\alpha_2 - ak_2^+)$	$-ak_4^+$
η^3	$(k_1^+ - \alpha_2)$	$(-k_1^+\alpha_1 + ak_2^+\alpha_2 - ak_3^+)$	
η^2	$(-\alpha_1 - k_1^+\alpha_2 - ak_2^+) - \frac{(-k_1^+\alpha_1 + ak_2^+\alpha_2 - ak_3^+)}{(k_1^+ - \alpha_2)}$	$-ak_4^+$	
η	$(-k_1^+\alpha_1 + ak_2^+\alpha_2 - ak_3^+) + \frac{(k_1^+ - \alpha_2)ak_4^+}{(-\alpha_1 - k_1^+\alpha_2 - ak_2^+) - \frac{(-k_1^+\alpha_1 + ak_2^+\alpha_2 - ak_3^+)}{(k_1^+ - \alpha_2)}}$		
1	$-ak_4^+$		

Table 5.2: The Routh criterion

Applying the Routh criterion (see Table 5.2), we must ensure that

$$\begin{aligned}
&(k_1^+ - \alpha_2) > 0 \\
&(-\alpha_1 - k_1^+\alpha_2 - ak_2^+) - \frac{(-k_1^+\alpha_1 + ak_2^+\alpha_2 - ak_3^+)}{(k_1^+ - \alpha_2)} > 0 \\
&(-k_1^+\alpha_1 + ak_2^+\alpha_2 - ak_3^+) + \frac{ak_4^+(k_1^+ - \alpha_2)}{(-\alpha_1 - k_1^+\alpha_2 - ak_2^+) - \frac{(-k_1^+\alpha_1 + ak_2^+\alpha_2 - ak_3^+)}{(k_1^+ - \alpha_2)}} > 0 \\
&-ak_4^+ > 0.
\end{aligned} \tag{5.31}$$

Then, the observer gain $K^+ = \begin{pmatrix} k_1^+ & k_2^+ & k_3^+ & k_4^+ \end{pmatrix}$ satisfies

$$\begin{aligned}
&k_1^+ > \alpha_2 \\
&k_2^+ < \frac{-\alpha_1 - k_1^+\alpha_2}{a} \\
&-\frac{(-\alpha_1 - k_1^+\alpha_2 - ak_2^+)(k_1^+ - \alpha_2)}{a} + \frac{-k_1^+\alpha_1 + ak_2^+\alpha_2}{a} < k_3^+ < \frac{-k_1^+\alpha_1 + ak_2^+\alpha_2}{a} \\
&-\frac{(-k_1^+\alpha_1 + ak_2^+\alpha_2 - ak_3^+)(-\alpha_1 - k_1^+\alpha_2 - ak_2^+)}{a(k_1^+ - \alpha_2)} + \frac{(-k_1^+\alpha_1 + ak_2^+\alpha_2 - ak_3^+)^2}{a(k_1^+ - \alpha_2)^2} < k_4^+ < 0.
\end{aligned} \tag{5.32}$$

The same argument, but applied to A_-, gives the conditions on the observer

gain $K^- = \begin{pmatrix} k_1^- & k_2^- & k_3^- & k_4^- \end{pmatrix}$ as follows

$$\begin{aligned}
&k_1^- < \alpha_2 \\
&k_2^- < \frac{-\alpha_1 - k_1^-\alpha_2}{a} \\
&\frac{-k_1^-\alpha_1 + ak_2^-\alpha_2}{a} < k_3^- < \frac{(-\alpha_1 - k_1^-\alpha_2 - ak_2^-)(\alpha_2 - k_1^-)}{a} + \frac{-k_1^-\alpha_1 + ak_2^-\alpha_2}{a} \\
&- \frac{(k_1^-\alpha_1 - ak_2^-\alpha_2 + ak_3^-)(-\alpha_1 - k_1^-\alpha_2 - ak_2^-)}{a(\alpha_2 - k_1^-)^2} + \frac{(k_1^-\alpha_1 - ak_2^-\alpha_2 + ak_3^-)^2}{a(\alpha_2 - k_1^-)^2} < k_4^- < 0.
\end{aligned} \tag{5.33}$$

Following [Hespanha 2004, Theorem 4], the objective is again to show that there exists a pair $\{P_+, P_-\}$, of symmetric positive definite matrices satisfying all the conditions required by that theorem, for an appropriately defined pair of matrices $\{C_+, C_-\}$. To that aim, let's define $C_+ = \begin{pmatrix} c_1^+ & 0 & 0 & 0 \end{pmatrix}$ and $C_- = \begin{pmatrix} c_1^- & 0 & 0 & 0 \end{pmatrix}$, where $c_1^+, c_1^- \neq 0$. Our first task is to check the observability of the pairs (A_+, C_+) and (A_-, C_-). The observability matrix $\mathcal{O}_{(A_+,C_+)}$ is shown as follows

$$\mathcal{O}_{(A_+,C_+)} = \begin{pmatrix} c_1^+ & 0 & 0 & 0 \\ -k_1^+c_1^+ & -ac_1^+ & 0 & 0 \\ ((k_1^+)^2 + ak_2^+)c_1^+ & ac_1^+k_1^+ & -ac_1^+ & 0 \\ -k_1^+c_1^+((k_1^+)^2 + aK_2^+) - ac_1^+(k_1^+k_2^+ - k_3^+) & -ac_1^+((k_1^+)^2 + ak_2^+ + \alpha_1) & ac_1^+(k_1^+ - \alpha_2) & -ac_1^+ \end{pmatrix} \tag{5.34}$$

The determinant this matrix is equal to $-a^3(c_1^+)^4$ that is clearly different to 0, then the pair (A_+, C_+) is observable. The observability proof of (A_-, C_-) is similar.

The second task is to find a matrix P that satisfies simultaneously the two equations $A_+^TP + PA_+ = -C_+^TC_+$ and $A_-^TP + PA_- = -C_-^TC_-$. Observe that P defines a non-strict Lyapunov function only, because the symmetric matrices $C_i^TC_i$ are not strictly positive definite. Denote by (p_{ij}) the elements of P. One can easily deduce from $A_+^TP + PA_+ = -C_+^TC_+$ the following equations

$$\begin{aligned}
&2(k_1^+p_{11} + k_2^+p_{12} + k_3^+p_{13} + k_4^+p_{14}) = (c_1^+)^2 \\
&- k_1^+p_{12} - k_2^+p_{22} - k_3^+p_{23} - k_4^+p_{24} - ap_{11} + \alpha_1p_{13} = 0 \\
&- k_1^+p_{13} - k_2^+p_{23} - k_3^+p_{33} - k_4^+p_{34} + p_{12} + \alpha_2p_{13} = 0 \\
&- k_1^+p_{14} - k_2^+p_{24} - k_3^+p_{34} - k_4^+p_{44} + p_{13} = 0 \\
&- ap_{12} + \alpha_1p_{23} = 0 \\
&- ap_{13} + \alpha_1p_{33} + p_{22} + \alpha_2p_{23} = 0 \\
&- ap_{14} + \alpha_1p_{34} + p_{23} = 0 \\
&p_{23} + \alpha_2p_{33} = 0 \\
&p_{24} + \alpha_2p_{34} + p_{33} = 0 \\
&p_{34} = 0.
\end{aligned} \tag{5.35}$$

Then, we obtain

$$\begin{aligned}
p_{11} &= \left(\frac{\xi^+}{a}[(-\alpha_1 - ak_2^+ - k_1^+\alpha_2) + (\alpha_2^2 + 2\alpha_1)] + \frac{\alpha_1^2}{a} + k_4^+\right)\frac{p_{33}}{a} \\
p_{12} &= -\frac{\alpha_1\alpha_2}{a}p_{33}, \quad p_{13} = \frac{\xi^+ + \alpha_1}{a}p_{33}, \quad p_{14} = -\frac{\alpha_2}{a}p_{33}, \quad p_{22} = (\xi^+ + \alpha_2^2)p_{33} \\
p_{23} &= -\alpha_2 p_{33}, \quad p_{24} = -p_{33}, \quad p_{34} = 0, \quad p_{44} = -\frac{(-\alpha_1 - k_1^+\alpha_2 - ak_2^+) - \xi^+}{ak_4^+}p_{33}.
\end{aligned} \tag{5.36}$$

where $p_{33} > 0$ and $\xi^+ = \frac{(-k_1^+\alpha_1 + ak_2^+\alpha_2 - ak_3^+)}{(k_1^+ - \alpha_2)} > 0$ thanks to (5.32).

With the element of P computed as in (5.36), one obtain

$$\begin{aligned}
(c_1^+)^2 &= 2\left(k_1^+p_{11} + k_2^+p_{12} + k_3^+p_{13} + k_4^+p_{14}\right) \\
&= 2\left(k_1^+p_{11} + \left((\xi^+ + \alpha_1)k_3^+ - \alpha_1\alpha_2k_2^+ - \alpha_2k_4^+\right)\frac{1}{a}p_{33}\right) \\
&= \frac{2p_{33}}{a}\left(k_1^+\left(\frac{\xi^+}{a}[(-\alpha_1 - ak_2^+ - k_1^+\alpha_2) + (\alpha_2^2 + 2\alpha_1)] + \frac{\alpha_1^2}{a} + k_4^+\right) + \left((\xi^+ + \alpha_1)k_3^+ - \alpha_1\alpha_2k_2^+ - \alpha_2k_4^+\right)\right) \\
&= \frac{2p_{33}}{a}\left(\frac{k_1^+\xi^+}{a}[(-\alpha_1 - ak_2^+ - k_1^+\alpha_2) + (\alpha_2^2 + 2\alpha_1)] - \frac{\alpha_1\xi^+(K_1^+ - \alpha_2)}{a} + k_4^+(k_1^+ - \alpha_2) + k_3^+\xi^+\right).
\end{aligned} \tag{5.37}$$

Thanks to the conditions of observer gain K^+, as shown in (5.32), expression $(c_1^+)^2 > 0$. Indeed, from the condition of k_4^+, we have

$$k_4^+(k_1^+ - \alpha_2) > \frac{-\xi^+(-\alpha_1 - ak_2^+ - k_1^+\alpha_2)(k_1^+ - \alpha_2)}{a} + \frac{(\xi^+)^2(k_1^+ - \alpha_2)}{a}.$$

This leads to

$$\begin{aligned}
(c_1^+)^2 &> \frac{2p_{33}}{a}\Big(\frac{k_1^+\xi^+(-\alpha_1 - ak_2^+ - k_1^+\alpha_2)}{a} + \frac{k_1^+\xi^+(\alpha_2^2 + 2\alpha_1)}{a} - \frac{\alpha_1\xi^+(k_1^+ - \alpha_2)}{a} \\
&\quad - \frac{\xi^+(-\alpha_1 - ak_2^+ - k_1^+\alpha_2)(k_1^+ - \alpha_2)}{a} + \frac{(\xi^+)^2(k_1^+ - \alpha_2)}{a} + k_3^+\xi^+\Big) \\
&> \frac{2\xi^+p_{33}}{a^2}\left(k_1^+(\alpha_2^2 + 2\alpha_1) - \alpha_1(k_1^+ - \alpha_2) + \alpha_2(-\alpha_1 - ak_2^+ - k_1^+\alpha_2) + \xi^+(k_1^+ - \alpha_2) + ak_3^+\right) \\
&> \frac{2\xi^+p_{33}}{a^2}\left(\alpha_1k_1^+ - aK_2^+\alpha_2 + ak_3^+ + (-aK_3^+ + ak_2^+\alpha_2 - \alpha_1k_1^+)\right) \\
&> 0.
\end{aligned} \tag{5.38}$$

Similarly, since P has to satisfy the condition $A_-^TP + PA_- = -C_-^TC_-$, it follows

that the elements of P are also of the form

$$\begin{aligned}
&-2(k_1^- p_{11} + k_2^- p_{12} + k_3^- q_{13} + k_4^- p_{14}) = (c_1^-)^2 \\
&k_1^- p_{12} + k_2^- p_{22} + k_3^- p_{23} + k_4^- p_{24} + a p_{11} - \alpha_1 p_{13} = 0 \\
&k_1^- p_{13} + k_2^- p_{23} + k_3^- p_{33} + k_4^- p_{34} - p_{12} - \alpha_2 p_{13} = 0 \\
&k_1^- p_{14} + k_2^- p_{24} + k_3^- p_{34} + k_4^- p_{44} - p_{13} = 0 \\
&a p_{12} - \alpha_1 p_{23} = 0 \\
&a p_{13} - \alpha_1 p_{33} - p_{22} - \alpha_2 p_{23} = 0 \\
&a p_{14} - \alpha_1 p_{34} - p_{23} = 0 \\
&-p_{23} - \alpha_2 p_{33} = 0 \\
&-p_{24} - \alpha_2 p_{34} - p_{33} = 0 \\
&p_{34} = 0.
\end{aligned} \tag{5.39}$$

Thus,

$$\begin{aligned}
&p_{11} = \left(\frac{\xi^-}{a}[(-\alpha_1 - a k_2^- - k_1^- \alpha_2) + (\alpha_2^2 + 2\alpha_1)] + \frac{\alpha_1^2}{a} + k_4^- \right) \frac{p_{33}}{a} \\
&p_{12} = -\frac{\alpha_1 \alpha_2}{a} p_{33}, \quad p_{13} = \frac{\xi^- + \alpha_1}{a} p_{33}, \quad p_{14} = -\frac{\alpha_2}{a} p_{33}, \quad p_{22} = (\xi^- + \alpha_2^2) p_{33} \\
&p_{23} = -\alpha_2 p_{33}, \quad p_{24} = -p_{33}, \quad p_{34} = 0, \quad p_{44} = -\frac{(-\alpha_1 - k_1^- \alpha_2 - a k_2^-) - \xi^-}{a k_4^-} p_{33}.
\end{aligned} \tag{5.40}$$

where $\xi^- = \frac{(k_1^- \alpha_1 - a k_2^- \alpha_2 + a k_3^-)}{(\alpha_2 - k_1^-)} > 0$ thanks to (5.33).

From (5.36) and (5.40), additional conditions on the observer gains K^+ and K^- can be obtained

$$\begin{aligned}
&\xi^+ = \frac{(-k_1^+ \alpha_1 + a k_2^+ \alpha_2 - a k_3^+)}{(k_1^+ - \alpha_2)} = \frac{(k_1^- \alpha_1 - a k_2^- \alpha_2 + a k_3^-)}{(\alpha_2 - k_1^-)} = \xi^- = \xi \\
&\frac{\xi}{a}(-\alpha_1 - a k_2^+ - k_1^+ \alpha_2) + k_4^+ = \frac{\xi}{a}(-\alpha_1 - a k_2^- - k_1^- \alpha_2) + k_4^- \\
&\frac{(-\alpha_1 - k_1^+ \alpha_2 - a k_2^+) - \xi}{a k_4^+} = \frac{(-\alpha_1 - k_1^- \alpha_2 - a k_2^-) - \xi}{a k_4^-}.
\end{aligned} \tag{5.41}$$

The proof is ended by showing that c_1^- of C_- is also different from zero. From

the first equation of (5.39), we have

$$\begin{aligned}
(c_1^-)^2 &= -2\left(k_1^- p_{11} + k_2^- p_{12} + k_3^- p_{13} + k_4^- p_{14}\right) \\
&= -2\left(k_1^- p_{11} + \left((\xi^- + \alpha_1)k_3^- - \alpha_1\alpha_2 k_2^- - \alpha_2 k_4^-\right)\frac{1}{a}p_{33}\right) \\
&= -\frac{2p_{33}}{a}\left(k_1^-\left(\frac{\xi^-}{a}[(-\alpha_1 - ak_2^- - k_1^-\alpha_2) + (\alpha_2^2 + 2\alpha_1)] + \frac{\alpha_1^2}{a} + k_4^-\right) + \left((\xi^- + \alpha_1)k_3^- - \alpha_1\alpha_2 k_2^- - \alpha_2 k_4^-\right)\right) \\
&= -\frac{2p_{33}}{a}\left(\frac{k_1^-\xi^-}{a}[(-\alpha_1 - ak_2^- - k_1^-\alpha_2) + (\alpha_2^2 + 2\alpha_1)] + \frac{\alpha_1\xi^-(\alpha_2 - k_1^-)}{a} + k_4^-(k_1^- - \alpha_2) + k_3^-\xi^-\right) \\
&= \frac{2p_{33}}{a}\left(-\frac{k_1^-\xi^-}{a}[(-\alpha_1 - ak_2^- - k_1^-\alpha_2) + (\alpha_2^2 + 2\alpha_1)] - \frac{\alpha_1\xi^-(\alpha_2 - k_1^-)}{a} + k_4^-(\alpha_2 - k_1^-) - k_3^-\xi^-\right).
\end{aligned} \tag{5.42}$$

Using

$$k_4^-(\alpha_2 - k_1^-) > \frac{-\xi^-(-\alpha_1 - ak_2^- - k_1^-\alpha_2)(\alpha_2 - k_1^-) + (\xi^-)^2(\alpha_2 - k_1^-)}{a},$$

we obtain

$$\begin{aligned}
(c_1^-)^2 &> \frac{2p_{33}}{a}\Big(-\frac{k_1^-\xi^-(-\alpha_1 - ak_2^- - k_1^-\alpha_2)}{a} - \frac{k_1^-\xi^-(\alpha_2^2 + 2\alpha_1)}{a} - \frac{\alpha_1\xi^-(\alpha_2 - k_1^-)}{a} \\
&\qquad \frac{\xi^-(-\alpha_1 - ak_2^- - k_1^-\alpha_2)(\alpha_2 - k_1^-)}{a} + \frac{(\xi^-)2(\alpha_2 - k_1^-)}{a} - k_3^-\xi^-\Big) \\
&> \frac{2\xi_2 p_{33}}{a^2}\left(-k_1^-(\alpha_2^2 + 2\alpha_1) - \alpha_1(\alpha_2 - k_1^-) - \alpha_2(-\alpha_1 - ak_2^- - k_1^-\alpha_2) + \xi_2(\alpha_2 - k_1^-) - ak_3^-\right) \\
&> \frac{2\xi^- p_{33}}{a^2}\left(-\alpha_1 k_1^- + ak_2^-\alpha_2 - ak_3^- + (ak_3^- - ak_2^-\alpha_2 + \alpha_1 k_1^-)\right) \\
&> 0.
\end{aligned} \tag{5.43}$$

Part II

Input-delay compensation for linearizable systems

Chapter 6

Output tracking for restricted feedback linearizable systems with input time-delay

---

The content of this chapter is strongly based on :

W. Pasillas-Lépine, A. Loría, and T.-B. Hoang. Output tracking for restricted feedback linearizable systems with input delay. In *Proceedings of the IEEE Conference on Decision and Control*, Florence (Italy), 2013.

The proof of Theorem 6.2 is due to Antonio Loria.

Abstract: We propose a new method for input delay compensation of nonlinear systems that can be linearized using restricted feedback. Our approach is based on an inversion procedure that finds the input that tracks asymptotically the desired output. This kind of inversion schemes, typically, needs an estimate of the future of the system's state. In order to compute this estimate, instead of integrating the original system (which might be nonlinear or unstable), we integrate the desired error dynamics (which is both linear and stable, at least asymptotically). Our approach is validated numerically on an academic nonlinear pendulum example.

6.1 Introduction

The list of available methods for input delay compensation is not short [Krstic 2009]. The simplest is probably the Smith predictor [Smith 1959], designed for stable linear systems. This method, based on frequency domain techniques, is widely used in industrial applications. For more general (possibly unstable) linear systems, other solutions based on a state-space representation are available (see, e.g., [Manitius 1979] and [Artstein 1982]). But it is only recently that methods have been proposed for several classes of nonlinear systems (see, e.g., [Mazenc 2006], [Georges 2007], [Besançon 2007], [Krstic 2010], [Mazenc 2011b], [Koo 2012], and the references therein). A more complete overview on time-delay control systems can be found, for example, in the surveys [Richard 2003] and [Sipahi 2011], and in the books [Niculescu 2001] and [Krstic 2009].

In order to compensate input delays, most methods use either the exact value or an estimation of the future of the system's state. Consider, for example, the linear system

$$\dot{x}(t) = Ax(t) + Bu(t-h), \quad x \in \mathbb{R}^n, \tag{6.1}$$

for which we want the origin to be asymptotically stable. Since the dynamics of this system can be integrated explicitly, a closed-form prediction is available. A classical trick (see, e.g., [Manitius 1979] and [Artstein 1982], or [Richard 2003] for a more recent account), based on this prediction, is to use the variable

$$z(t) = x(t) + \int_{t-h}^{t} e^{A(t-h-s)} Bu(s) ds, \tag{6.2}$$

which satisfies the differential equation

$$\dot{z}(t) = Az(t) + e^{-Ah} Bu(t). \tag{6.3}$$

When the pair (A, B) is stabilizable, one can always find a gain K such that $u = -Kz(t)$ stabilizes (6.3). Unfortunately, the exponential stability of (6.3) does not imply that of (6.1), because the operator associated to (6.2) is not necessarily stable. We refer the reader to [Mazenc 2011a] for a discussion on this problem and for an alternative choice of this operator. In the nonlinear case, several approaches have been proposed in order to generalize this idea (see, e.g., [Krstic 2009]). Nevertheless, even in the linear case, it is well known that the numerical implementation of such predictor techniques might lead to an unstable behavior (see, e.g., [Engelborghs 2001] and [Mondié 2003]), at least when the original system is unstable. At the opposite, when the original system is both linear and stable, a very recent result [Mazenc 2012] shows that such schemes admit a stable numerical implementation.

Oversimplifying the previous observations, one could deduce a simple but probably abusive conclusion: a prediction of the future of the system's state based on the integration of a stable and linear system is likely to lead to a stable numerical scheme; while the integration of an unstable or nonlinear system might be confronted with a more delicate numerical implementation. Nevertheless, if our aim is to find a control law that tracks a given reference for the system's output, the reference model for the error dynamics can be considered as a part of the control design. Even in the case of an unstable and/or nonlinear plant, one can always chose a tracking error dynamics that is both stable and linear, at least asymptotically. Since the evolution of such a system can be predicted more easily, it is tempting to use this prediction in order to compensate input delays. The aim of this chapter is to explore this simple idea, to propose a control law based on it, and to show its stability (in continuous time). In order to follow this program, we consider a class of systems that is contained in the class of feedback-linearizable systems (we assume, additionally, that the vector-field

associated to the control input is rectified [Brockett 1979]). Our main objective is the input-output inversion of the system, for the feedback linearizing output, with a compensation of the input delays. Observe that more general classes of systems have been considered before (see, e.g., [Mazenc 2006], [Krstic 2010], and [Mazenc 2011b]), but with different objectives that lead to different control laws.

Notation. For a square matrix β we use β_m and β_M to denote, respectively, the lower and the upper bounds on its spectral norm, which is induced by the Euclidean norm on vectors. For $t_\circ \in \mathbb{R}_{\geq 0}$ and any absolutely continuous $\phi : [0, h] \to \mathbb{R}^n$, the solutions of a functional differential equation

$$\dot{z}(t) = f(t, z(t), z(t-h)) \tag{6.4}$$

with $f(t, \cdot)$ locally Lipschitz and $f(\cdot, z)$ locally integrable, are absolutely continuous functions z that satisfy, additionally to (6.4) for $t \geq t_\circ$, the initial condition

$$z(t_\circ - s) = \phi(s) \quad \forall\, s \in [0, h].$$

We say that the trivial solution $z(t) \equiv 0$ is uniformly exponentially stable if there exist κ, $\lambda > 0$ such that, for any absolutely continuous initial condition ϕ,

$$|z(t)| \leq \kappa \, \|\phi\| \, \mathrm{e}^{-\lambda(t-t_\circ)} \quad \forall\, t \geq t_\circ$$

where

$$\|\phi\| := \Big(|\phi(0)|^2 + \sup_{s \in [0,h]} |\phi(s)|^2 \Big)^{1/2}.$$

6.2 Scalar systems

In the absence of input delays, the tracking problem for a scalar nonlinear system

$$\dot{x}(t) = f\big(x(t)\big) + u(t), \text{ for } x(t) \in \mathbb{R}, \tag{6.5}$$

is a trivial task. Indeed, if we want $x(t)$ to converge towards a continuously differentiable reference $x^*(t)$, one can define the tracking error

$$e(t) = x(t) - x^*(t) \tag{6.6}$$

and apply the linearizing control input

$$u(t) = -f(x(t)) - \alpha e(t) + \dot{x}^*(t), \tag{6.7}$$

which stabilizes the origin of the error dynamics

$$\dot{e}(t) = -\alpha e(t) \tag{6.8}$$

globally and exponentially, for any control gain $\alpha > 0$.

In the presence of input delays, that is for a system described by the functional differential equation

$$\dot{x}(t) = f\big(x(t)\big) + u(t-h), \text{ for } x(t) \in \mathbb{R}, \tag{6.9}$$

this task is more complex since the closed-loop system's trajectories are generated by

$$\dot{x}(t) - \dot{x}^*(t-h) = -\alpha e(t-h) + f\big(x(t)\big) - f\big(x(t-h)\big),$$

as opposed to the "ideal" error dynamics (6.8), in the absence of delay.

One way to compensate the delay is to use, if possible, the *future* values of x and $\dot{x}^*$, at the instant $t+h$. But, since the future state values are unknown, they must be estimated or predicted. Moreover, the reference trajectory might be unknown in advance as, for example, in the case when a human operator fixes it in real-time. Therefore, when implementing (6.7), we shall set the control goal to

$$\lim_{t\to\infty} e(t) = 0, \quad \text{for} \quad e(t) := x(t) - x^*(t-h), \tag{6.10}$$

and introduce a *state prediction* denoted by x^P. More precisely, we denote by $x^P(t,h)$ an estimate value of $x(t+h)$, computed at the instant t. Then, with the control goal (6.10) in mind, we define the control input as

$$u(t) = -f\big(x^P(t,h)\big) - \alpha e(t) + \dot{x}^*(t) \tag{6.11}$$

so that, in closed loop with (6.9), we have

$$\dot{e}(t) = -\alpha e(t-h) + f(x(t)) - f(x^P(t-h,h)). \tag{6.12}$$

By construction, when the prediction x^P is perfect, we recover the error dynamics

$$\dot{e}(t) = -\alpha e(t-h), \tag{6.13}$$

whose origin is known (see, e.g., [Niculescu 2001, Proposition 3.15]) to be exponentially stable if $0 < \alpha < \pi/2h$. For this reason, we consider (6.13) as the *target error dynamics*.

When the error follows its reference dynamics (6.13), a prediction of the future error evolution may be obtained by a direct integration of (6.13). Otherwise, if the target error dynamics is not followed exactly, one can add an integral term to this

prediction, in order to damp the perturbation coming from the mismatch between the ideal and the actual error dynamics. We thus define the *error prediction* as

$$e^P(t,s) := e(t) - \alpha \int_t^{t+s} e(\tau - h)d\tau - \beta \int_{-\infty}^{t+s} p(\tau - h)d\tau, \tag{6.14}$$

for $s \in [0, h]$, where the *prediction bias* is defined by

$$p(t) := e^P(t - h, h) - e(t). \tag{6.15}$$

The meaning of this bias is clarified if we observe that the error prediction $e^P(t-h, h)$ corresponds to the estimate of $e(t)$ computed at the instant $t-h$. Another important point is that, in our estimation, the *past* values of the error $e(t - s)$, for $s \in [0, h]$, are needed in order to estimate its *future* values $e^P(t, s)$, for $s \in [0, h]$.

We emphasize that the real-time implementation of such prediction schemes is straightforward. This implementation has however the drawback that at each instant t the past values of all variables, for the instants $s \in [t - h, t]$, must be stored in a memory buffer. We consider, nevertheless, that this drawback is compensated by the numerical stability of the proposed approach.

Our interest in this error prediction comes from the fact that an estimate of the future values of the system's state can be deduced from it, by taking

$$x^P(t,s) := x^*(t + s - h) + e^P(t,s), \quad \forall\, s \in [0, h], \tag{6.16}$$

which completes the definition of the control law in (6.11). Observe that, as we have already said, the estimation of $x^P(t, s)$ is not obtained by an integration of the system's dynamics but by an integration of the target-error dynamics.

Next, for the purpose of analysis, it is convenient to rewrite the closed-loop equation (6.12) as

$$\dot{e}(t) = -\alpha e(t - h) + f\big(x(t)\big) - f\big(x(t) + p(t)\big) \tag{6.17}$$

and to compute the dynamics of the prediction bias $p(t)$. To that end, we differentiate on both sides of (6.15), we use (6.12) and (6.14) and, to compact the notation, we introduce

$$\psi(s) := f\big(x(s)\big) - f\big(x(s) + p(s)\big),$$

which leads to

$$\dot{p}(t) = -\beta p(t - h) - \psi(t) + \psi(t - h). \tag{6.18}$$

Note that, if f is Lipschitz, we have $|\psi(s)| \leq \gamma\, |p(s)|$, where γ is the Lipschitz constant of the function f.

A first property of this equation is that, via the Lyapunov-Krasovskĭi method, one

may establish exponential stability of $\{p = 0\}$ for sufficiently large β, and this result is global if so is the Lipschitz property. A second property of the closed-loop system dynamics, given by equations (6.17) and (6.18), is that it consists in the *cascade* of two exponentially stable systems; as a matter of fact, it may also be shown that (6.17) is input-to-state-stable from the input $p(t)$.

The following proposition, whose proof is a direct consequence of our main result (Theorem 6.1), formalizes the previous developments.

Proposition 6.1. *Consider the scalar input-delay system (6.9). Assume that there exists γ such that the function f satisfies*

$$|f(x) - f(y)| \leq \gamma\,|x - y|\,, \qquad \forall\ x,\, y \in \mathbb{R}.$$

For any given $h^* > 0$, if the gains α and β satisfy the relations

$$\alpha < 1/h^* \quad \textit{and} \quad \beta \geq (9/4)\gamma + \beta(\beta + 2\gamma)h^*, \tag{6.19}$$

the origin of the closed-loop system, given by (6.9) with the control $u(t)$ defined by (6.11) and (6.14)–(6.16), is globally exponentially stable for any constant delay $h \in [0,\, h^*]$.

Observe that the constraint on β imposed by condition (6.19) is sufficient for the exponential stability of $\{p = 0\}$, for (6.18). Additionally, in the absence of the nonlinearities, one may take $\gamma = 0$ and, hence, for the system $\dot{p}(t) = -\beta p(t - h)$ we obtain the condition $\beta < 1/h^*$ which is slightly more conservative than the well known condition $\beta < \pi/2h^*$.

The simple ideas followed in this section, in order to compensate input-delays for scalar systems, are generalizable to a particular class of systems in triangular form, to which we devote our attention in the next section.

6.3 Restricted-feedback linearizable systems

Following the streamlines laid in the previous section for the control of (6.9), let us consider the class of systems that can be linearized using a change of coordinates and a restricted-feedback transformation [Brockett 1979]. When an input-delay is introduced, after a change of coordinates these systems can be written in the following form:

$$\begin{aligned}
\dot{x}_1(t) &= f_1\big(x_1(t)\big) + x_2(t) \\
\dot{x}_2(t) &= f_2\big(x_1(t), x_2(t)\big) + x_3(t) \\
&\vdots \\
\dot{x}_{n-1}(t) &= f_{n-1}\big(x_1(t), \ldots, x_{n-1}(t)\big) + x_n(t) \\
\dot{x}_n(t) &= f_n\big(x(t)\big) + u(t - h),
\end{aligned} \tag{6.20}$$

where $x(t) := [x_1(t) \cdots x_n(t)]^\top \in \mathbb{R}^n$ and $y(t) = x_1(t)$ is the system's output, for which we have a reference $y^*(t)$.

One of the characteristics of this class of systems is that conditions for the existence of a *global* transformation into this triangular form are available (see, e.g., [Dayawansa 1985] and [Respondek 1986]). For a more recent reference, we refer the reader to the lecture notes [Respondek 2002, Theorem 4.12]. Another property of these systems is that they belong to the family of p-normal forms [Cheng 2003] (see also [Respondek 2003]).

Since the control input is subject to a constant delay h, as for the first-order counterpart of (6.20), the control goal is reset to (6.10) where

$$e_i(t) = x_i(t) - x_i^*(t-h), \qquad \forall\, i \in \{1, \ldots, n\}.$$

Following the classical backstepping procedure (see [Krstic 1995] and [Marino 1995]), the variable x_i is viewed as a virtual control input to the $\dot{x}_{i-1}$-equation. Analogously to (6.11), we start with $x_1^*(t) = y^*(t)$ and define

$$\begin{aligned} x_i^*(t) \;:=\; & -f_{i-1}(x_1^P(t,h), \ldots, x_{i-1}^P(t,h)) \\ & - \alpha_{i-1} e_{i-1}(t) + \dot{x}_{i-1}^*(t), \end{aligned}$$

for $2 \leq i \leq n$. The terms $x_i^P(t,h)$, for $1 \leq i \leq n$, denote the prediction of $x_i(t+h)$ computed at the instant t. These terms are constructed below.

The reference error dynamics is naturally imposed to have a *cascaded* structure

$$\begin{aligned} \dot{e}_1(t) &= -\alpha_1 e_1(t-h) + e_2(t) \\ \dot{e}_2(t) &= -\alpha_2 e_2(t-h) + e_3(t) \\ &\vdots \\ \dot{e}_{n-1}(t) &= -\alpha_{n-1} e_{n-1}(t-h) + e_n(t) \\ \dot{e}_n(t) &= -\alpha_n e_n(t-h), \end{aligned} \tag{6.21}$$

which corresponds to the ideal case in which $x_i^P(t,h) = x_i(t+h)$. Note that (6.21) consists in a chain of input-to-state stable systems, driven by the n-th system, whose origin is exponentially stable. This is the rationale which leads to our main statement.

Theorem 6.1. *Consider the restricted-feedback linearizable system (6.20) and assume that, for each $1 \leq i \leq n$, there exists γ_i such that*

$$|f_i(z) - f_i(y)| \leq \gamma_i |z - y|, \qquad \forall\; z,\, y \in \mathbb{R}^i. \tag{6.22}$$

At each instant t, for $s \in [0,h]$, construct the error prediction starting with

$$e_n^P(t,s) = e_n(t) - \alpha_n \int_t^{t+s} e_n(\tau - h)d\tau - \beta_n \int_{-\infty}^{t+s} p_n(\tau - h)d\tau \tag{6.23}$$

and, from $i = n-1$ down to 1, with

$$\begin{aligned} e_i^P(t,s) = e_i(t) - \alpha_i \int_t^{t+s} e_i(\tau - h)d\tau - \beta_i \int_{-\infty}^{t+s} p_i(\tau - h)d\tau \\ + \int_t^{t+s} e_{i+1}^P(\tau - h, h)d\tau, \end{aligned} \tag{6.24}$$

where

$$e_i(t) = x_i(t) - x_i^*(t-h), \qquad \forall\, i \in \{1, \dots, n\}. \tag{6.25}$$

and

$$p_i(t) = e_i^P(t-h, h) - e_i(t). \tag{6.26}$$

Construct the state prediction, starting with $x_1^*(t) = y^*(t)$, and, from $i = 1$ up to n, with

$$x_i^P(t,h) = x_i^*(t) + e_i^P(t,h), \tag{6.27}$$

where

$$\begin{aligned} x_i^*(t) \;=\; & - f_{i-1}(x_1^P(t,h), \dots, x_{i-1}^P(t,h)) \\ & - \alpha_{i-1} e_{i-1}(t) + \dot{x}_{i-1}^*(t), \end{aligned} \tag{6.28}$$

and consider the controller

$$u(t) = -f_n(x^P(t,h)) - \alpha_n e_n(t) + \dot{x}_n^*(t). \tag{6.29}$$

Then, given any $h^* > 0$, if the norms of the control gains α and β satisfy

$$\alpha_m \;\geq\; 4 + \alpha_M(\alpha_M + 2)h^* \tag{6.30}$$

$$\beta_m \;\geq\; 4\gamma + \beta_M(\beta_M + 2\gamma)h^*, \tag{6.31}$$

the origin of the closed-loop system is uniformly globally exponentially stable for all constants $h \in [0, h^*]$.

The proof of Theorem 6.1 relies on the following statement on stability of cascades of functional differential equations which, to the best of our knowledge, is also original. A sketch of proof is provided in the Appendix.

Theorem 6.2. *Consider the system*

$$\dot{z}_1(t) \;=\; -\alpha z_1(t-h) + B z_1(t) + \Psi(t) \tag{6.32a}$$

$$\dot{z}_2(t) \;=\; -\beta z_2(t-h) + d_1\Phi(t) + d_2\Phi(t-h), \tag{6.32b}$$

where $z_1(t)$, $z_2(t) \in \mathbb{R}^n$ and d_1, $d_2 \in \mathbb{R}$. Assume that α and β are diagonal positive matrices of dimension n, that $\Psi : [-h, \infty) \to \mathbb{R}^n$ and $\Phi : [-h, \infty) \to \mathbb{R}^n$ are

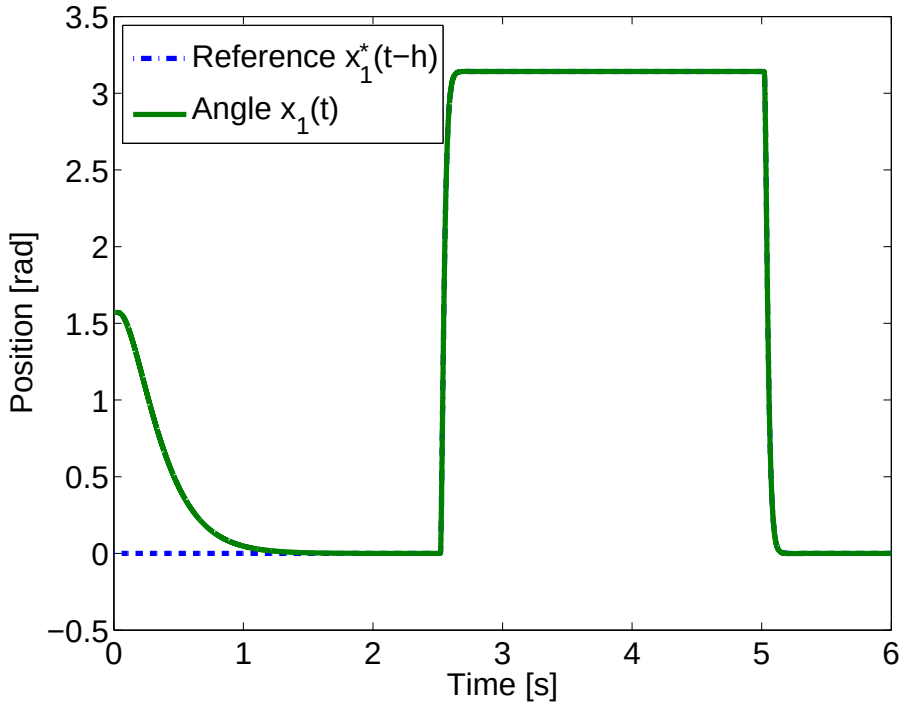

Figure 6.1: Numerical simulation of our delay compensation scheme (6.38), on the simple example given by an academic pendulum.

absolutely continuous, and that there exist $\gamma_1,\ \gamma_2 > 0$ *such that*

$$|\Psi(s)| \leq \gamma_1 \, |z_2(s)| \quad \textit{and} \quad |d_j \Phi(s)| \leq \gamma_2 \, |z_2(s)| \,, \tag{6.33}$$

for $j \in \{1, 2\}$. *Then, given any* $h^* > 0$, *the origin is uniformly globally exponentially stable for all* $h \in [0, h^*]$ *if (6.31) and*

$$\alpha_m \geq 4 b_M + \alpha_M (\alpha_M + 2 b_M) h^* \tag{6.34}$$

hold.

In order to invoke Theorem 6.2 we proceed to show that the closed-loop dynamics of (6.20) with the controller (6.29) has the form (6.32) with $z_1 = e$, $z_2 = p$, $\alpha :=$

$\text{diag}\{\alpha_1 \cdots \alpha_n\}$, $\beta := \text{diag}\{\beta_1 \cdots \beta_n\}$ and

$$B = \begin{bmatrix} 0 & 1 & 0 & \cdots & 0 \\ & & & \ddots & \vdots \\ \vdots & & \ddots & & 0 \\ & & & & 1 \\ 0 & & \cdots & & 0 \end{bmatrix}$$

hence, $b_M = 1$. By differentiating on both sides of Equation (6.25) and using (6.20), we obtain

$$\begin{aligned} \dot{e}_1(t) &= f_1(x_1(t)) + x_2(t) - \dot{x}_1^*(t-h) \\ \dot{e}_2(t) &= f_2(x_1(t), x_2(t)) + x_3(t) - \dot{x}_2^*(t-h) \\ &\vdots \\ \dot{e}_{n-1}(t) &= f_{n-1}(x_1(t), \ldots, x_{n-1}(t)) + x_n(t) - \dot{x}_{n-1}^*(t-h) \\ \dot{e}_n(t) &= f_n(x(t)) + u(t-h) - \dot{x}_n^*(t-h). \end{aligned}$$

Then, using (6.28) and (6.29), we obtain

$$\begin{aligned} \dot{e}_1(t) &= -\alpha_1 e_1(t-h) + e_2(t) \\ &\quad +[f_1(x_1(t)) - f_1(x_1^P(t-h,h))] \\ \dot{e}_2(t) &= -\alpha_2 e_2(t-h) + e_3(t) + [f_2(x_1(t), x_2(t)) \\ &\quad -f_2(x_1^P(t-h,h), x_2^P(t-h,h))] \\ &\vdots \\ \dot{e}_{n-1}(t) &= -\alpha_{n-1} e_{n-1}(t-h) + e_n(t) \\ &\quad +[f_{n-1}(x_1(t), \ldots, x_{n-1}(t)) \\ &\quad -f_{n-1}(x_1^P(t-h,h), \ldots, x_{n-1}^P(t-h,h))] \\ \dot{e}_n(t) &= -\alpha_n e_n(t-h) \\ &\quad +[f_n(x(t)) - f_n(x^P(t-h,h))] \end{aligned} \tag{6.35}$$

where, in view of (6.27), we have for each $1 \le i \le n$,

$$\begin{aligned} x_i^P(t-h,h) &= x_i^*(t-h) + e_i^P(t-h,h) \pm x_i(t) \\ &= -e_i(t) + e_i^P(t-h,h) + x_i(t) \\ &= p_i(t) + x_i(t). \end{aligned}$$

Now, to compact the notation, we introduce

$$\begin{aligned}\psi_i(s) &:= f_i(\bar{x}_i(s)) - f_i(\bar{x}_i(s) + \bar{p}_i(s)),\\ \bar{x}_i &:= [x_1 \cdots x_i]^\top, \quad \bar{x}_n = x,\\ \bar{p}_i &:= [p_1 \cdots p_i]^\top, \quad \bar{p}_n = p\end{aligned}$$

so, for each $1 \leq i \leq n$,

$$\dot{e}_i(t) = -\alpha_i e_i(t-h) + e_{i+1}(t) + \psi_i(t) \tag{6.36}$$

which is of the form (6.32a) with

$$\Psi(s) := [\psi_1(s) \cdots \psi_n(s)]^\top.$$

Next, we compute the prediction bias dynamics. For this, we differentiate on both sides of (6.26) and use (6.24) and (6.36) to obtain, for $1 \leq i \leq n-1$,

$$\begin{aligned}\dot{p}_i(t) = -\beta_i p_i(t-h) + \psi_i(t-h) - \psi_i(t)\\ +p_{i+1}(t) - p_{i+1}(t-h)\\ \dot{p}_n(t) = -\beta_n p_n(t-h) + \psi_n(t-h) - \psi_n(t).\end{aligned}$$

Thus, defining

$$\Phi(s) := [-\psi_1(s) + p_2(s), \cdots -\psi_{n-1}(s) + p_n(s), \ -\psi_n(s)]^\top$$

we see that the closed-loop dynamics takes the cascaded form

$$\begin{aligned}\dot{e}(t) &= -\alpha e(t-h) + Be(t) + \Psi(t)\\ \dot{p}(t) &= -\beta p(t-h) + \Phi(t) - \Phi(t-h)\end{aligned}$$

which corresponds to (6.32) with $d_1 = 1$ and $d_2 = -1$. Therefore, the result follows invoking Theorem 6.2 with $b_M = 1$, $\gamma_1 = \max\{\gamma_i\}$ – (see (6.22)) and $\gamma_2 = \gamma_1 + 1$.

6.4 Simulations on a simple example

In this section, we illustrate Theorem 6.1. We consider the pendulum equation

$$\begin{aligned}\dot{x}_1(t) &= x_2(t)\\ \dot{x}_2(t) &= -a \sin x_1(t) - bx_2(t) + u(t-h),\end{aligned} \tag{6.37}$$

where $a, b \in \mathbb{R}$ and $h \geq 0$. The control goal is to track a desired reference $x_1^*(t-h)$ with the system's output $x_1(t)$.

This restricted-feedback linearizable system is already, in its original coordinates, in the form (6.20). The functions $f_2(x(t)) = -a \sin x_1(t) - bx_2(t)$ and $f_1(x_1(t)) = 0$ are, moreover, Lipschitz continuous. We can thus apply Theorem 6.1, in order to construct a control law that solves the asymptotic output tracking problem.

In order to achieve our control goal $\lim_{t\to\infty} e(t) = 0$, we computed the error prediction $e^P(t,s)$ and the state prediction $x^P(t,s)$, for $s \in [0,h]$, based on the equations from (6.23) to (6.27) in Theorem 6.1, which gives the control input

$$u(t) = a \sin x_1^P(t,h) + bx_2^P(t,h) - \alpha_2 e_2(t) + \dot{x}_2^*(t), \tag{6.38}$$

where the gain matrices α and β satisfy conditions (6.30) and (6.31).

A simulation of the system's dynamics, where the output tracks the desired reference x_1^* is shown in Figure 6.1. In this simulation, the desired reference x_1^* is a filtered square wave that oscillates between 0 (a stable equilibrium point) and π (an unstable equilibrium point). For the system's parameters, we take the following values $a = 1$, $b = 1$, $h = 0.02$. For the controller, we take $\alpha_1 = \alpha_2 = 5$ and $\beta_1 = \beta_2 = 10$. When $t < h$, due to the input delay h, the control has no impact on the closed-loop system. The system output changes freely. At the time instant $t = h$, the control kicks in. After that, the control compensates the input delay and leads the system's output exponentially towards its desired reference. The good tracking performance confirms that the origin of the closed-loop system is asymptotically stable when the conditions imposed on the gains α and β are satisfied, as predicted by Theorem 6.1.

If we linearize the pendulum's equations (6.37) in a neighborhood of either a stable or an unstable equilibrium point, the finite spectrum assignment method presented shortly in the introduction — (see equations (6.1) to (6.3)) — can be applied. Once implemented numerically, this method only works for the stable equilibrium. For the unstable equilibrium, it fails unless some extra tricks are used in order to filter the unstable eigenvalues generated by the numerical implementation [Mondié 2003].

In comparison, our method works around both equilibria because our predictor technique is based on the choice of a stable and linear reference model for the tracking error. For the sake of brevity, the detailed computations of the system's linearization, of the application of the finite spectrum assignment method, as well as its simulation results are omitted.

6.5 Conclusion

In this chapter, we proposed a new method for input delay compensation of restricted feedback linearizable systems. Our approach inverts the system, computing the input that tracks asymptotically the desired output. In order to compute an estimate of the future of the system's state, instead of integrating the original system (which is nonlinear and might be unstable), we integrate the desired error dynam-

ics (which is both linear and stable, at least asymptotically). The results of our simulations show the effectiveness of this method for the pendulum equation.

Appendix: Proof of the main results

The rationale behind the proof of Theorem 6.2 follows the usual reasoning to establish stability for cascaded systems of ordinary differential equations. First, we show that the origin of (6.32a) with $z_2 \equiv 0$ is exponentially stable, then we show that $z_2 \equiv 0$ is exponentially stable for (6.32b) and finally, we show that the solutions of (6.32a) under the vanishing perturbation $\Psi(t)$ are bounded and converge exponentially to zero. For this purpose we first present some preliminary results for perturbed functional differential equations.

Lemma 6.1 (Output injection)**.** *The trivial solution of*

$$\dot{z} = -\beta z(t-h) + d_1\Phi(t) + d_2\Phi(t-h), \quad d_1,\, d_2 \in \mathbb{R}, \tag{6.39}$$

with $t_\circ = 0$ and $\beta > 0$ is diagonal, is globally exponentially stable if there exists $\gamma > 0$ such that $|d_j\Phi(s)| \leq \gamma\,|z(s)|$, $j \in \{1, 2\}$ and (6.31) holds.

Proof of Lemma 6.1 (Sketch) We denote by ϕ the initial condition of (6.39), defined in the Notation paragraph of Section 6.1, let β_i be the ith element of the main diagonal of β and let β_M be the largest of β_is. The proof may be constructed (it is removed here due to page constraints) using the Lyapunov-Krasovskĭi functional $V : \mathbb{R}_{\geq 0} \to \mathbb{R}_{\geq 0}$,

$$\begin{aligned} V(t) \;:=\; & V_1(t) + V_2(t) + V_3(t) + V_4(t) \\ & V_1(t) := \frac{1}{2}\sum_{i=1}^{n}\left[z_i(t) - \beta_i\int_{-h}^{0} z_i(t+\theta)d\theta\right]^2 \\ & V_2(t) := \frac{\beta_M(\beta_M + 2\gamma)}{2}\int_{-h}^{0}\int_{t+\theta}^{t} |z(s)|^2\, ds\, d\theta \\ & V_3(t) := \frac{\gamma\beta_M}{2}\left[\int_{-h}^{0} |z(t+\theta)|\, d\theta\right]^2 \\ & V_4(t) := \gamma\int_{t-h}^{t} |z(s)|^2\, ds, \end{aligned} \tag{6.40}$$

which satisfies

$$V(0) \;\leq\; \max\left\{1,\; c_\circ\right\}\|\phi\|^2$$

where

$$c_\circ := \frac{(\beta_M^2 + \delta_1)h^2 + (\delta_2 + \gamma)h}{2}.$$

and, under (6.31),

$$\dot{V}(t) \leq -(\beta_m/2)\,|z(t)|^2 \leq 0. \tag{6.41}$$

Lemma 6.2 (Vanishing perturbation)**.** *Consider the system*

$$\dot{z}(t) = -\alpha z(t-h) + Bz(t) + \varepsilon(t), \quad z \in \mathbb{R}^n, \tag{6.42}$$

starting at $t_\circ = 0$*, where* α *satisfies (6.34). Let* $\phi_\varepsilon : [0, h] \to \mathbb{R}^n$ *and* $\varepsilon : [-h, \infty) \to \mathbb{R}^n$ *be absolutely continuous functions satisfying* $\varepsilon(-s) = \phi(s)$ *for all* $s \in [0, h]$*. Assume that there exists* $c_\varepsilon > 0$ *such that*

$$\max\left\{ \sup_{t \geq -h} |\varepsilon(t)|\,,\ \left(\int_0^\infty |\varepsilon(t)|^2 \right)^{1/2} \right\} \leq c_\varepsilon \,\|\phi_\varepsilon\|\,. \tag{6.43}$$

Then, there exist κ*,* $\lambda > 0$ *such that*

$$|z(t)| \leq \kappa\big[\,\|\phi_z\| + \|\phi_\varepsilon\|\,\big]\, e^{-\lambda t}, \tag{6.44}$$

where ϕ_z *is the initial condition of (6.42).*

The proof of Lemma 6.2 follows similar lines as [Panteley 2001, Lemma 3].

Proof of Theorem 6.2 We denote by ϕ_1 and ϕ_2 the initial condition of (6.32a) and (6.32b), respectively, as defined in the Notation paragraph of Section 6.1. We invoke Lemma 6.1 with $z = z_2$ and $t_\circ = 0$ to obtain that there exist κ_2 and λ_2 such that

$$|z_2(t)| \leq \kappa_2 \,\|\phi_2\|\, \mathrm{e}^{-\lambda_2 t}$$

therefore, there exists $c_\varepsilon > 0$ such that (6.43) holds with $\varepsilon = \Psi$. By Lemma 6.2 with $z = z_1$ and (6.33), there exist κ_1 and λ_1 such that

$$|z_1(t)| \leq \kappa_1\big[\,\|\phi_1\| + \|\phi_2\|\,\big]\mathrm{e}^{-\lambda_1 t}.$$

Chapter 7

Actuator delay compensation for ABS systems

The aim of this chapter is purely ILLUSTRATIVE. We show, using simulations, that different results proposed in this thesis can be combined in order to design a new ABS control law. It has not been submitted for publication to any journal or conference.

Abstract: The objective of this chapter is to compensate the delay induced by actuators for ABS systems. The benefit of the actuator delay compensation is twofold. On the one hand, it improves the robustness of theoretical ABS systems with respect to the actuator delay, and thus ensures their good working when implemented on the test bench, since the actuator delay has been identified as the main cause of failure [Gerard 2012]. On the other hand, standard ABS algorithms, which are designed for today's hydraulic actuators in brake systems, can be adapted to other actuators, like those of in-wheel motor based electric vehicles (with a quicker response time) or heavy-duty trucks (with a slower response). In the context of wheel acceleration control, our goal is achieved by providing a control law that is based on the prediction of the system's state.

The chapter starts with a brief modelling of the extended braking stiffness dynamics with the presence of a constant input delay h, which is based on the one without the input delay that was shown in Chapter 5. Then, the two prediction states, which are needed in the control law, are estimated. While the first one, denoted by $z_1^P(t,h)$, can be computed using the results obtained in Chapter 6, the computation of the second one, denoted by $z_2^P(t,h)$, is more difficult. The stability analysis of the control law hasn't been proved theoretically, but simulation results show that the proposed control law compensates the effect of the actuator delay and fulfils the control goal.

7.1 System modelling

We recall here the extended braking stiffness dynamics (5.7) that was derived in Section 5.3.2

$$\begin{aligned}\frac{dz_1}{dt} &= -\frac{a}{v_x(t)}z_1(t)z_2(t) + bu(t)\\ \frac{dz_2}{dt} &= (cz_2(t) + z_3(t))\frac{z_1(t)}{v_x(t)}\\ \frac{dz_3}{dt} &= 0,\end{aligned} \tag{7.1}$$

where the state variable z_1 is the wheel acceleration offset, z_2 is the XBS, and z_3 is the unknown product of parameters of Burckhardt's model. The control variable $u = dP_b(t)/dt$ is the derivative of the brake pressure and the system parameters a, b, and c are known constants. For more details of this system modelling, we refer the reader to Chapter 5.

In the presence of actuator delays, equation (7.1) becomes

$$\frac{dz_1}{dt} = -\frac{a}{v_x(t)}z_1(t)z_2(t) + bu(t-h) \tag{7.2a}$$

$$\frac{dz_2}{dt} = (cz_2(t) + z_3(t))\frac{z_1(t)}{v_x(t)} \tag{7.2b}$$

$$\frac{dz_3}{dt} = 0, \tag{7.2c}$$

where the input delay h is a positive constant. This model can be seen as a generalization of the model (2.1) described in Section 2.1 since the XBS is no longer considered constant, but variable.

7.2 Control design

The control objective is to make the wheel acceleration offset $z_1(t)$ converge towards a continuously differentiable reference $z_1^*(t-h)$, provided that the brake pressure is delayed by h seconds. We define the tracking error

$$e_1(t) = z_1(t) - z_1^*(t-h)., \tag{7.3}$$

and set the control goal such that

$$\lim_{t\to\infty} e_1(t) = 0. \tag{7.4}$$

In the absence of input delays, one can achieve the control goal by taking the following control law (which is similar to 5.23 of Section 5.5)

$$u(t) = \frac{1}{b}\left(\frac{a}{v_x} z_1(t)\hat{z}_2(t) + \frac{dz_1^*(t)}{dt} - \alpha e_1(t)\right), \tag{7.5}$$

where $\alpha > 0$ is the control gain and $\hat{z}_2(t)$ is an estimation of the extended braking stiffness $z_2(t)$. The value of XBS can be estimated thanks to the observer (5.8) that has been proposed in Section 5.3.3. In what follows, we assume that the XBS estimation is perfect, or in other words, that there is no estimation error, the tracking error then converges exponentially to zero, provided that the control gain α is taken big enough.

One might be surprised that only the variable z_1 is chosen to be controlled. But, as explained in Section 5.5, when the acceleration offset z_1 follows its reference, it appears that the stability of all other variables actually comes from the fact that they are bounded functions of the wheel slip x_1, which remains bounded both for hybrid [Gerard 2012] and continuous [Pasillas-Lépine 2012] control designs.

Now, in the presence of input delays, we define a similar control law that is, however, based on the prediction of the system states $z_1^P(t,h)$ and $z_2^P(t,h)$ as follows

$$u(t) = \frac{1}{b}\left(\frac{a}{v_x} z_1^P(t,h) z_2^P(t,h) + \frac{dz_1^*(t)}{dt} - \alpha e_1(t)\right). \tag{7.6}$$

Thus, we get the tracking error dynamics

$$\dot{e}_1(t) = -\alpha e_1(t-h) - \frac{a}{v_x}\left(z_1(t)z_2(t) - z_1^P(t-h,h)z_2^P(t-h,h)\right). \tag{7.7}$$

If the two state predictions are estimated perfectly, then we obtain the ideal error dynamics

$$\dot{e}_1(t) = -\alpha e_1(t-h), \tag{7.8}$$

which is exponentially stable if $0 < \alpha < \pi/2h$. If this dynamics is the target error dynamics, then the state prediction $z_1^P(t,h)$ can be computed by using the method proposed in Section 6.2. Indeed, the error prediction is computed by integrating the target error dynamics as follows

$$e_1^P(t,s) = e_1(t) - \alpha \int_t^{t+s} e(\tau - h)d\tau - \beta \int_{-\infty}^{t+s} p_1(\tau - h)d\tau, \tag{7.9}$$

for $s \in [0,h]$, where the prediction bias $p_1(t) = e_1^P(t-h,h) - e_1(t)$ is used to damp the mismatch between the actual and the target error dynamics, i.e. (7.7) and (7.8).

The state prediction $z_1^P(t,s)$ is then computed thanks to the error prediction

$$z_1^P(t,s) = z_1^*(t+s-h) + e_1^P(t,s), \text{for } s \in [0,h]. \tag{7.10}$$

The computation of the state prediction $z_2^P(t,h)$ is, however, different to that of $z_1^P(t,h)$ since the proposed method is no longer applicable. It is computed through the resolution, at each time instant t and for an interval $[t, t+h]$, of the two equations (7.2b) and (7.2c). Let's consider thus the following dynamics

$$\begin{aligned} \frac{d\overline{z}_2}{dr} &= \big(c\overline{z}_2(r) + \overline{z}_3(r)\big)\frac{\overline{z}_1(r)}{v_x} \\ \frac{d\overline{z}_3}{dr} &= 0, \end{aligned} \tag{7.11}$$

where $0 \leq r \leq h$ and the state variables $\overline{z}_i$, for $1 \leq i \leq 3$, are defined as

$$\overline{z}_i(r) := z_i(t+r). \tag{7.12}$$

The dynamics (7.11) is in fact the dynamics (7.2b) and (7.2c) in the time interval $[t, t+h]$. From (7.12), it can be noticed that the initial states of (7.11) are $\overline{z}_i(0) = z_i(t)$, which are given by the observer (see Section 5.3.3), and the states of (7.11) at the time instant h are $\overline{z}_i(h) = z_i(t+h)$, which are the values of z_i at the time instant $t+h$.

The resolution of (7.11) isn't a trivial task due to the term $z_1(r)/v_x$. Nevertheless, one can see that without $z_1(r)/v_x$, the dynamics (7.11) is in the form of a linear system for which the solutions are available in the literature. Our aim is thus to cancel this nonlinear term. To that aim, let's define a new time scale as

$$\tau(r) := \int_0^r \frac{|\overline{z}_1(\sigma)|}{v_x} d\sigma, , \tag{7.13}$$

which ensures that $dr/d\tau > 0$, independently of the value of $\overline{z}_1(r)$. In the new time scale, (7.11) can be written as follows

$$\frac{d}{d\tau}\begin{pmatrix}\overline{z}_2\\ \overline{z}_3\end{pmatrix} = \begin{cases} \begin{pmatrix} c & 1\\ 0 & 0\end{pmatrix}\begin{pmatrix}\overline{z}_2\\ \overline{z}_3\end{pmatrix} & \text{if } \overline{z}_1 > 0 \\ \\ \begin{pmatrix} -c & -1\\ 0 & 0\end{pmatrix}\begin{pmatrix}\overline{z}_2\\ \overline{z}_3\end{pmatrix} & \text{if } \overline{z}_1 < 0. \end{cases} \tag{7.14}$$

The solution of (7.14) is

$$\begin{pmatrix}\overline{z}_2(\tau)\\ \overline{z}_3(\tau)\end{pmatrix} = \begin{cases} e^{\begin{pmatrix}c & 1\\ 0 & 0\end{pmatrix}\tau}\begin{pmatrix}\overline{z}_2(0)\\ \overline{z}_3(0)\end{pmatrix} = \begin{pmatrix}e^{c\tau} & \frac{e^{c\tau}-1}{c}\\ 0 & 1\end{pmatrix}\begin{pmatrix}\overline{z}_2(0)\\ \overline{z}_3(0)\end{pmatrix} & \text{if } \overline{z}_1 > 0 \\ e^{\begin{pmatrix}-c & -1\\ 0 & 0\end{pmatrix}\tau}\begin{pmatrix}\overline{z}_2(0)\\ \overline{z}_3(0)\end{pmatrix} = \begin{pmatrix}e^{-c\tau} & \frac{e^{-c\tau}-1}{c}\\ 0 & 1\end{pmatrix}\begin{pmatrix}\overline{z}_2(0)\\ \overline{z}_3(0)\end{pmatrix} & \text{if } \overline{z}_1 < 0. \end{cases} \tag{7.15}$$

Since we need compute the state prediction of $z_2^P(t,h)$, then only the variable $\overline{z}_2(\tau)$ is considered

$$\overline{z}_2(\tau) = \begin{cases} e^{c\tau}\overline{z}_2(0) + \frac{e^{c\tau}-1}{c}\overline{z}_3(0) & \text{if } \overline{z}_1 > 0 \\ e^{-c\tau}\overline{z}_2(0) + \frac{e^{-c\tau}-1}{c}\overline{z}_3(0) & \text{if } \overline{z}_1 < 0. \end{cases} \tag{7.16}$$

In the time scale r, the value of $\overline{z}_2(r)$, for $0 \le r \le h$, is equal to that of $\overline{z}_2(\tau(r))$ in the time scale τ, or in other words

$$\overline{z}_2(r)_{\text{in } r} = \overline{z}_2(\tau(r))_{\text{in } \tau}. \tag{7.17}$$

And besides, by the definition (7.12), we have, for $0 \le r \le h$

$$z_2(t+r)_{\text{in } t} = \overline{z}_2(r)_{\text{in } r}. \tag{7.18}$$

This leads to the following expression

$$z_2(t+h)_{\text{in } t} = \overline{z}_2(\tau(h))_{\text{in } \tau} = \begin{cases} e^{c\tau(h)}z_2(t) + \frac{e^{c\tau(h)}-1}{c}z_3(t) & \text{if } \overline{z}_1 > 0 \\ e^{-c\tau(h)}z_2(t) + \frac{e^{-c\tau(h)}-1}{c}z_3(t) & \text{if } \overline{z}_1 < 0. \end{cases} \tag{7.19}$$

We compute $\tau(h)$ based on (7.13)

$$\begin{aligned} \tau(h) &= \int_0^h \frac{|\overline{z}_1(\sigma)|}{v_x} d\sigma \\ &= \int_0^h \frac{|z_1(t+\sigma)|}{v_x} d\sigma \\ &= \int_t^{t+h} \frac{|z_1(\sigma)|}{v_x} d\sigma. \end{aligned} \tag{7.20}$$

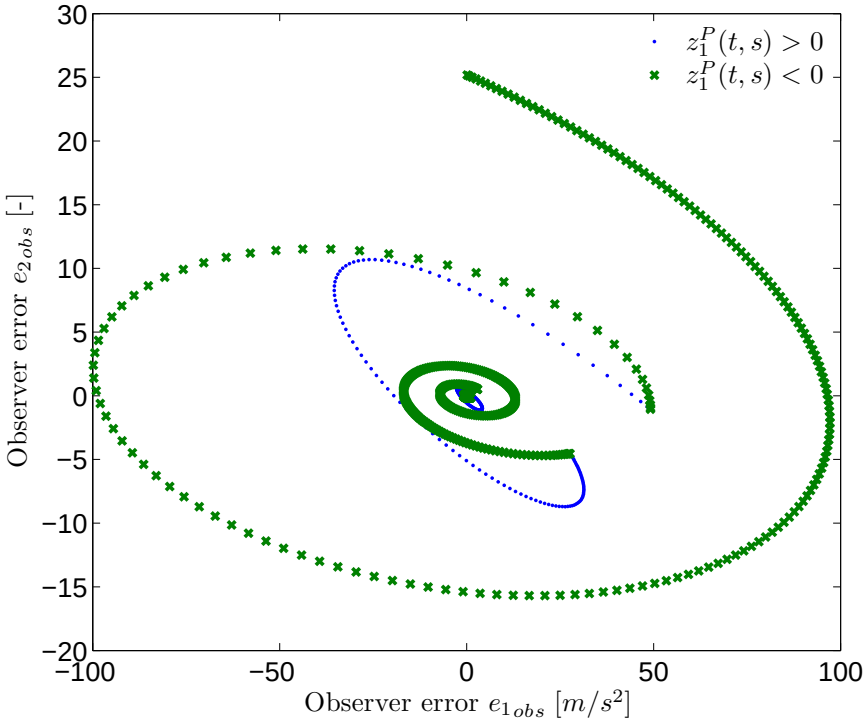

Figure 7.1: Phase-plane evolution of the observer error, obtained by a projection of the three-dimensional error dynamics on the (e_{1obs}, e_{2obs}) plane.

Combining equations (7.3) and (7.10), one can obtain

$$z_1^P(t-h,h) = z_1(t) + p_1(t). \tag{7.21}$$

We replace (7.21) into (7.20)

$$\begin{aligned} \tau(h) &= \int_t^{t+h} \frac{|z_1^P(\sigma-h,h) - p_1(\sigma)|}{v_x} d\sigma \\ &= \left| \int_t^{t+h} \frac{z_1^P(l-h,h)}{v_x} dl - \int_t^{t+h} \frac{p_1(l)}{v_x} dl \right| \end{aligned} \tag{7.22}$$

We do not know the future values of $p_1(\sigma)$, with $t \leq \sigma \leq (t+h)$, but if all the state predictions are estimated perfectly, then the prediction bias $\lim_{t\to\infty} p_1(t) = 0$. The expression of p_1 in (7.22) is thus neglected

$$\tau(h) = \int_t^{t+h} \frac{\left|z_1^P(l-h,h)\right|}{v_x} dl. \tag{7.23}$$

Furthermore, we define the prediction bias $p_2(t)$ in order to damp the mismatch

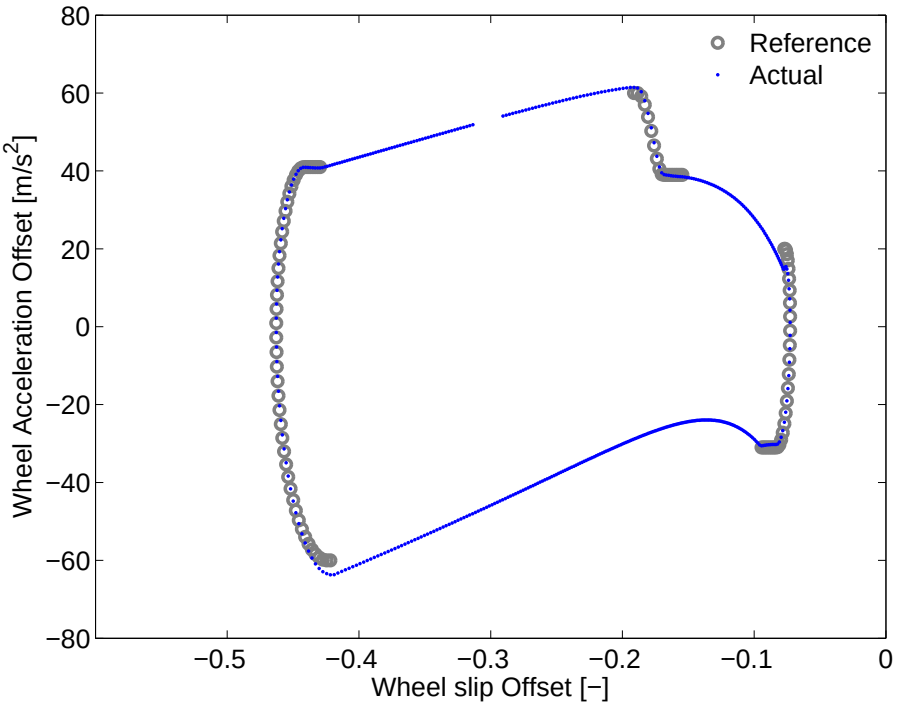

Figure 7.2: A cycle of the five-phase ABS algorithm with of the wheel acceleration tracking, during phases 1, 3, and 4.

between $z_2^P(t-h,h)$ and $z_2(t)$

$$p_2(t) = z_2^P(t-h,h) - z_2(t). \tag{7.24}$$

And finally, the state prediction $z_2^P(t,h)$ is computed as follows

$$z_2^P(t,h) = \begin{cases} e^{c\tau(h)} z_2(t) + \frac{e^{c\tau(h)}-1}{c} z_3(t) - \beta_2 \int_{-\infty}^{t+h} p_2(r-h)dr & \text{if } z_1^P(t,s) > 0 \\ e^{-c\tau(h)} z_2(t) + \frac{e^{-c\tau(h)}-1}{c} z_3(t) - \beta_2 \int_{-\infty}^{t+h} p_2(r-h)dr & \text{if } z_1^P(t,s) < 0, \end{cases} \tag{7.25}$$

where $s \in [0,h]$.

With the value of $z_1^P(t,h)$ and $z_2^P(t,h)$, computed as in (7.10) and (7.25), the control law (7.6) can be implemented. The stability analysis of the control law (7.6), however, hasn't been theoretically proved in the thesis due to its complexity. But, we will show, in Section 7.3, through numerical simulations that the proposed control law can compensate the input delay and stabilize the system around a given reference.

7.3 Simulation results

In order to illustrate the effectiveness of the control law (7.6), the case of a simple academic ABS is considered [Pasillas-Lépine 2006]. A brief description of this ABS algorithm has been shown in Section 5.5. The control law (7.6) is used to regulate the wheel acceleration offset to track a given reference on the phases for which the brake pressure is modified. The reference trajectories during these phases have been discussed in Section 5.5. We suppose that the ABS algorithm is affected by a constant delay $h = 10$ms.

It is worth mentioning that to get the value of the variable z_2 (the XBS), we use the observer (5.8), as proposed in Section 5.3. We define the observer errors

$$e_{iobs} := z_i(t) - \hat{z}_i(t), \tag{7.26}$$

for $1 \leq i \leq 3$, and $\hat{z}_i$ are the observer states. The delay has no effect on the observer convergence, the observer gains are then chosen following Theorem 5.1, as shown in Section 5.3. Figure 7.1 shows that the observer errors converge toward zero when the time goes toward infinity.

The control gains are chosen as follows

$$\alpha = \frac{\pi}{4h}, \ \beta_1 = \frac{\pi}{10h}, \text{ and } \beta_2 = \frac{\pi}{10h}. \tag{7.27}$$

Since equation (7.2a) can be considered as a scalar system, the values of α and β_1 are chosen based on Proposition 6.1, presented in Section 6.2. The value of β_2 is then taken such that it is equal to that of β_1. The simulation results are shown from Figure 7.2 to Figure 7.4. It can be seen that the wheel acceleration tracks the given reference and the input delay h is compensated by the control law (7.6). It should be stressed that Figures 7.2 and 7.3 are in fact two different ways to represent the tracking results. While the former shows us the wheel acceleration tracking in a cycle of the five-phase ABS algorithm, the latter represents this tracking in the time domain. The brake pressure during the tracking control associated to Figure 7.3 is shown in Figure 7.4.

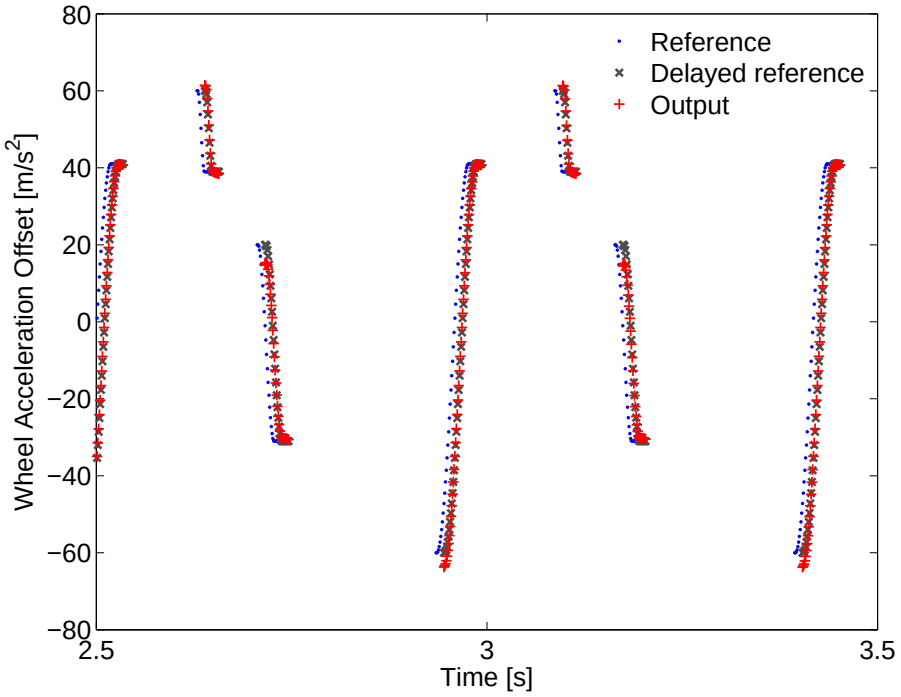

Figure 7.3: Wheel acceleration tracking, during phases 1, 3, and 4 of the five-phase ABS algorithm.

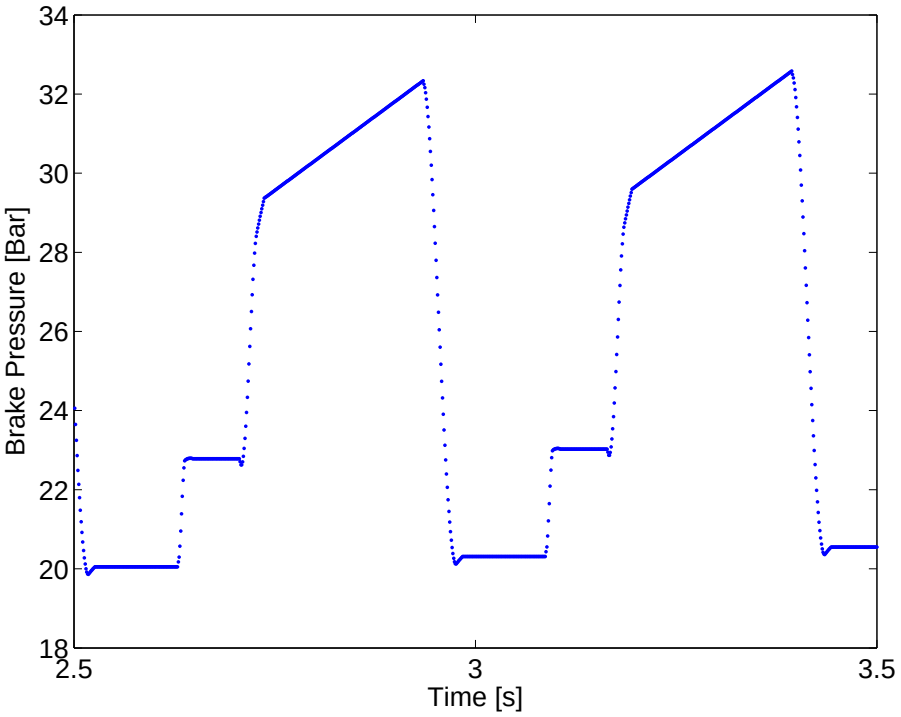

Figure 7.4: Brake pressure of five-phase ABS algorithm.

Chapter 8

Dynamic notch filter

The content of this chapter is strongly based on :

T.-B. Hoang, W. Pasillas-Lépine, and A. De Bernardinis. Reducing the impact of wheel-frequency oscillations in continuous and hybrid ABS strategies. In *Proceedings of the International Symposium on Advanced Vehicle Control*, Seoul (Korea), 2012.

In the published paper, Appendices A and B were not included because of the length restrictions imposed on papers by this conference.

Abstract: In this chapter, a stable dynamic notch filter is presented. This filter is able to eliminate the disturbance of the wheel acceleration, even when the vehicle speed is variable. This new filter is used, in two applicative examples, to improve ABS performance. Simulations results show that our notch filter might be helpful for both continuous and hybrid ABS algorithms.

The subject of this chapter is, somehow, intermediate between Parts I and II of the thesis. On the one hand, filtering wheel-frequency oscillations is a problem that is directly connected to the XBS observation problem considered in Part I. Indeed, the most important measure in this context is the wheel acceleration, which must be filtered using the appropriate techniques before being exploited by an observer. On the other hand, the main subject of this conference paper is the impact of such filters on the delay margin of a simple control loop, a theme that is clearly closer to Part II. Actually, this small paper was the starting point of the thesis. Even if its results are clearly not the most important, it gives an indication of the road that lead to the two main parts of this dissertation.

8.1 Introduction

In the area of traction and brake control, several algorithms use wheel acceleration measurements in order to control the wheel slip (see, e.g., [Leiber 1979], [Kiencke 2000], [Pasillas-Lépine 2010], and [Savaresi 2010, Chapter 6]). But these measurements are often corrupted by noise. Typically, changes in the properties of the rubber along the circumference of the tire (as the change in the wheel diameter, stiffness of the belt, wear, etc.) are a source of disturbances for wheel acceleration measurements. These disturbances, which are periodic with a period of one wheel

rotation, can trigger the ABS control logic with an inappropriate timing. Thus, the design of a filter to eliminate this disturbance is necessary.

In this chapter, we propose a stable dynamic notch filter that is able to eliminate the disturbance of the wheel acceleration, even when the vehicle speed is variable (Section 8.2). This new filter is used, in two applicative examples, to improve the ABS performance. Simulation results show that our notch filter might be helpful for both continuous and hybrid ABS algorithms (Section 8.3). Nevertheless, adding a notch filter to the ABS braking control system may decrease the phase margin as well as the delay margin. But a computation of the delay margin of these control laws, when combined with the filter, shows that it does not destroy the robustness of the closed-loop systems (Section 8.4).

8.2 Modelling of the dynamic notch filter

The use of a notch filter to eliminate the effects of the periodic disturbances on the wheel acceleration has two advantages: it removes a particular frequency, but with a very low impact on other frequencies of the input signal.

If $x(t)$ and $y(t)$ are the input and output signals of a notch filter, then its transfer function can be written as

$$N(s) = \frac{Y(s)}{X(s)} = \frac{(\frac{s}{\omega_n})^2 + \frac{2\zeta_n s}{\omega_n} + 1}{(\frac{s}{\omega_n})^2 + \frac{2\zeta_d s}{\omega_n} + 1}, \tag{8.1}$$

where ω_n denotes the notch frequency, ζ_n and ζ_d (with $\zeta_n \ll \zeta_d < 1$) are the filter's quality factors. We consider as the notch frequency ω_n the frequency ω_p of the disturbance that we want to eliminate. We define the ratio

$$R_\zeta := \frac{\zeta_n}{\zeta_d}. \tag{8.2}$$

The filter's quality factors decide the attenuation level, which is equal to $20 \log |R_\zeta|$ at ω_p. Furthermore, the bandwidth of the filter depends on its quality factors. For an unchanged ratio R_ζ, the smaller ζ_d is, the smaller the bandwidth of the filter (at -3dB) will be. Figure 8.1 shows the Bode plots of the notch filter with the same ratio $R_\zeta = 0.01$, for three different values of ζ_d (0.01, 0.1 and 1).

By observing Figure 8.1, we should clearly choose a small value of ζ_d to have a good and performing notch filter, which not only filters accurately the disturbance but also has a small effect on the delay margin of the system (see Section 8.4). Nevertheless, via numerical simulations, we notice that the response time of the filter depends also on the value of ζ_d. The smaller ζ_d is, the longer the response time of the filter will be. Therefore, if the time response is an important factor in filtering, we cannot take

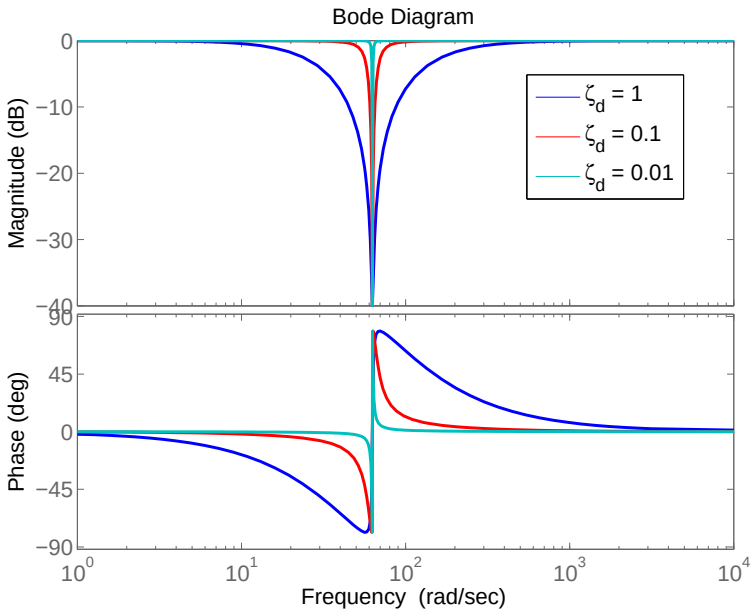

Figure 8.1: Bode plot of the notch filter.

a too small value of ζ_d.

As a first step, let us assume that the speed of the vehicle is constant and equal to v_0. Then the disturbance frequency is: $\omega_p = f(v_0) = v_0/R$, where R is the radius of the wheel. Transforming (8.1) into the time domain, we obtain the following notch filter in the form of second order differential equation

$$\frac{1}{f^2(v_0)}\frac{d^2y}{dt^2} + \frac{2\zeta_d}{f(v_0)}\frac{dy}{dt} + y = \frac{1}{f^2(v_0)}\frac{d^2x}{dt^2} + \frac{2\zeta_n}{f(v_0)}\frac{dx}{dt} + x. \tag{8.3}$$

We define two state variables

$$y_1 = f(v_0)y \quad \text{and} \quad y_2 = \frac{dy}{dt}, \tag{8.4}$$

and we obtain

$$\begin{aligned} \frac{dy_1}{dt} &= f(v_0)y_2 \\ \frac{dy_2}{dt} &= f(v_0)[(-y_1 - \alpha y_2) + x^0_{ref}], \end{aligned} \tag{8.5}$$

where $\alpha = 2\zeta_d$ and $\beta = 2\zeta_n$ are positive constants, and

$$x^0_{ref} := f(v_0)x + \beta\frac{dx}{dt} + \frac{1}{f(v_0)}\frac{d^2x}{dt^2} \tag{8.6}$$

is the input signal.

We apply a change of time-scale

$$s(t) = \int_0^t \frac{v_x(\tau)}{R} d\tau, \tag{8.7}$$

where $v_x(t) = v_0$. For a constant velocity, this new time-scale $s(t)$ is just the wheel angle.

Consequently, for any state-space trajectory $\phi : \mathbb{R} \to \mathbb{R}^n$, we have

$$\frac{d\phi}{ds} = \frac{R}{v_x}\frac{d\phi}{dt}. \tag{8.8}$$

Therefore, we obtain

$$\begin{aligned} \frac{dy_1}{ds} &= y_2 \\ \frac{dy_2}{ds} &= -y_1 - \alpha y_2 + x^0_{ref}. \end{aligned} \tag{8.9}$$

In the new time scale, the eigenvalues of (8.9) are $(-\alpha \pm \sqrt{\alpha^2 - 4})/2$. Since all eigenvalues have negative real parts, the notch filter is stable (in the sense that any bounded input $x^0_{ref}(t)$ will result in a bounded output).

Now, in a second step, we can take an arbitrary vehicle speed $v_x(t) \geq v_\varepsilon > 0$, which might be non-constant. Clearly, the new time-scale $s(t)$ is always well-defined since $ds/dt > 0$. The state space representation of the filter in the new time scale is described by the following dynamics

$$\begin{aligned} \frac{dy_1}{ds} &= y_2 \\ \frac{dy_2}{ds} &= -y_1 - \alpha y_2 + x^1_{ref}, \end{aligned}$$

where

$$x^1_{ref} := f(v_x)x + \beta\frac{dx}{dt} + \frac{1}{f(v_x)}\frac{d^2x}{dt^2} \tag{8.10}$$

denotes the filter's input, the two state variables

$$y_1 = f(v_x)y \quad \text{and} \quad y_2 = \frac{dy}{dt}, \tag{8.11}$$

and the perturbation frequency is $\omega_p = f(v_x) = v_x/R$. The filter's stability is preserved since neither the filter's input nor the time-scaling (with $ds/dt > 0$) has an impact on it.

8.3 Application to ABS

In the literature, there exist two different kinds of anti-lock brake system designs: those based on logic switching from wheel deceleration thresholds [Leiber 1979] and those based on wheel slip regulation [Pasillas-Lépine 2010]. In this section, we present the application of the notch filter for both anti-lock brake system approaches.

8.3.1 Wheel dynamics

We recall the evolution of wheel slip and wheel acceleration of the simple single-wheel model that has been derived in Section 5.2.

The states x_1 and x_2 are defined as

$$\begin{aligned} x_1 &= \lambda \\ x_2 &= R\frac{d\omega}{dt} - a_x(t), \end{aligned} \tag{8.12}$$

where λ denotes the wheel slip, ω its angular velocity, and $a_x(t)$ the vehicle's acceleration.

We obtain the following dynamics

$$\begin{aligned} \frac{dx_1}{dt} &= \frac{1}{v_x(t)}\left(-a_x(t)x_1 + x_2\right) \\ \frac{dx_2}{dt} &= -\frac{a\mu'(x_1)}{v_x(t)}\left(-a_x(t)x_1 + x_2\right) + \frac{u}{v_x(t)}, \end{aligned} \tag{8.13}$$

where

$$a = \frac{R^2}{I}F_z \quad \text{and} \quad u = v_x(t)\frac{R}{I}\frac{dT}{dt}. \tag{8.14}$$

The variable I denotes the wheel's inertia, F_z the vertical load, and T the torque applied to the wheel.

8.3.2 Continuous wheel-slip control

Assume that the given time-dependent wheel-slip setpoint $\lambda^*(t)$ and $a_x(t)$ are piecewise constant functions. We define the dynamic reference for each of the system's states:

$$x_1^* = \lambda^*(t) \quad \text{and} \quad x_2^* = -\gamma z_1 + a_x x_1, \tag{8.15}$$

and the corresponding error variables

$$z_1 = x_1 - x_1^* \quad \text{and} \quad z_2 = x_2 - x_2^*, \tag{8.16}$$

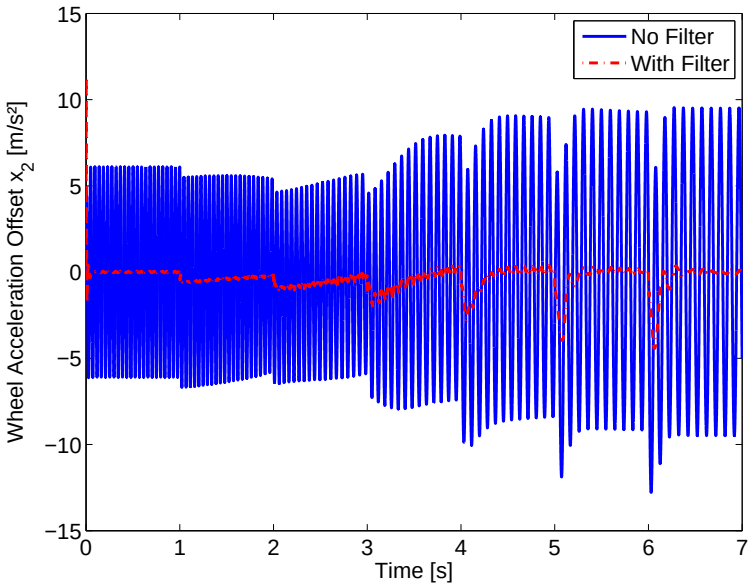

Figure 8.2: Filtering properties of the notch filter, for a manoeuvre at variable speed during which the frequency of the perturbation is not constant.

where γ is a positive constant. While x_1^* is equal to $\lambda^*(t)$, the setpoint x_2^* is dynamic. The steady state part is $a_x x_1$, while the other term is used to decrease the error on z_1, using feedback $-\gamma z_1$. Thanks to this dynamic setpoint, the system will converge to exactly the desired wheel slip, irrespectively from the tyre characteristic [Pasillas-Lépine 2010].

We define the feedback control law as

$$u = -K z_2, \tag{8.17}$$

where $K > 0$ is a positive gain. The main result of [Pasillas-Lépine 2010] states that the control law (8.17) gives global exponential stability towards the desired setpoint for the system defined by equations (8.13), provided that the gain K is large enough and that the setpoint reference $\lambda^*(t)$ is constant.

In simulations, the notch filter is used to filter the wheel acceleration offset x_2. The ABS braking system is active for 7 seconds. In the first and last seconds of the braking manoeuvre, the speed is constant at 150 km/h and at 80 km/h. For 5 seconds in the middle, the vehicle velocity decreases from 150 km/h to 80 km/h. We observe that the perturbation of the wheel acceleration is eliminated (Figure 8.2). It can be noticed that the filtering of the perturbation when the vehicle speed is constant is better than when speed is variable; and the smaller the vehicle's speed, the worse the filtering effect. Thanks to the filter applied to the disturbance, the brake pressure is less noisy (Figure 8.3). The elimination of the noise on the control

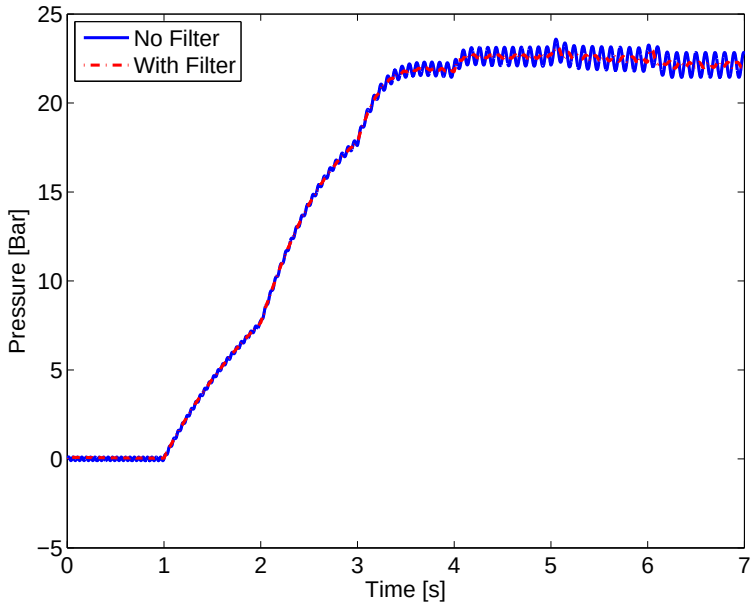

Figure 8.3: Continuous wheel-slip control, with and without notch filtering. The brake pressure oscillations are reduced by the filter.

is desired because there's less impact on the actuator.

8.3.3 Hybrid ABS control

A five-phase hybrid algorithm that uses the wheel acceleration logic-based switching is presented in [Pasillas-Lépine 2006]. Each of the five phases of the algorithm defines the control action $u = \dot{P}_b$ that should be applied to the brake. The value of $\dot{P}_b$ is either kept constant or changed very quickly. The switch between these phases will be triggered by given thresholds based on the value of the wheel acceleration offset x_2. The purpose of the algorithm is to keep the wheel slip in a small neighborhood of the optimal value λ_0, where the longitudinal tyre force is maximal, with the aim of minimizing the braking distances while keeping steerability at a reasonable level, without using explicitly the value of the optimal setpoint.

The algorithm is applied when the wheel starts locking. The cycling between the different phases will generate a repetitive trajectory. The cycle amplitude determines the braking performance: The smaller the cycle amplitude, the smaller the vehicle's braking distance. If there is perturbation on the wheel acceleration, the control action can be triggered at the inappropriate moments, which can cause the failure of the hybrid algorithm or make the wheel slip far from the optimal value. Thus, filtering the perturbation is unavoidable to make the algorithm more robust.

The aim of our simulations is to observe the performance of the notch filter in

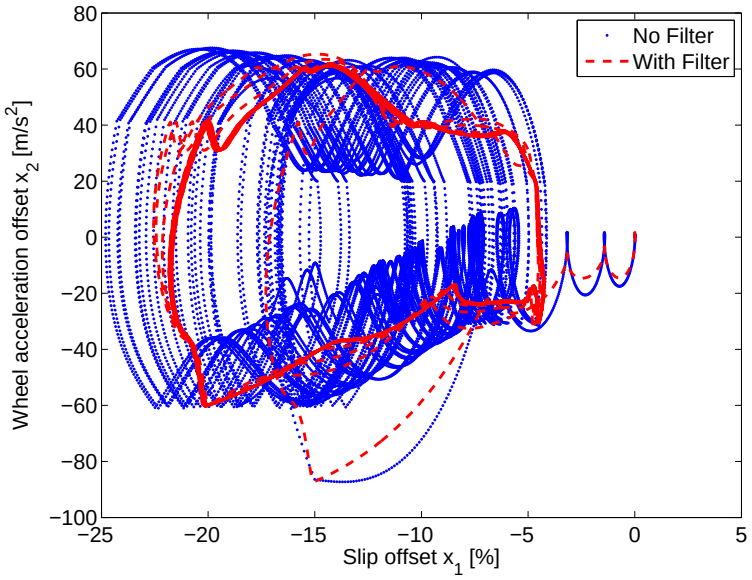

Figure 8.4: Hybrid ABS limit cycles, with and without notch filtering. When the filter is not active, the system does not converge to the optimal cycle.

eliminating the perturbation during the activation of the ABS algorithm. As one can see in Figure 8.4, when the notch filter is not used the algorithm still works but the optimal cycle is not obtained. The wheel slip varies in a large interval, thus the brake distance is large. If we add the notch filter to the system, we observe that it improves the ABS algorithm performance. The wheel slip varies in a smaller interval, thus the braking distance is smaller, and the system converges to the optimal cycle.

8.4 Delay margin analysis

When implementing the control laws of the previous section, one should take into account that a discrete time delay (of around 10 ms) might be introduced in the feedback loop (due to tyre dynamics, actuator limitations, etc.). The control law should thus be robust with respect to discrete time delays. Introducing a notch filter into the control law modifies the delay margin of the system. The aim of this section is to observe the notch filter impact on the delay margin of the control law.

8.4.1 Computing the delay margin

Let us begin with equation (8.13). We have to find out the transfer function between the acceleration offset x_2 and the acceleration offset reference x_2^*. In order to obtain this transfer function, we consider some following assumptions. The first one is

that we take a constant vehicle speed. This leads to the fact that $(-a_x x_1 + x_2) = x_2$ since $a_x = 0$. Besides, it is important to highlight that our aim is to establish a relation between the delay margin and each vehicle speed varied from 0 to 180 (see Section 8.4.2). The second one is that the derivative of the tyre characteristic $\mu'(\lambda)$ is assumed to be constant. It is zero when λ is equal to the maximal value of wheel slip λ_0; positive when the wheel slip λ belongs to the stable region of the tyre ($|\lambda| < \lambda_0$); and negative when λ is on the unstable region ($|\lambda| > \lambda_0$).

With these assumptions, the second equation of (8.13) becomes

$$\frac{dx_2}{dt} = -\frac{\theta}{v_x} x_2 + \frac{u}{v_x}, \tag{8.18}$$

where $\theta = a\mu'(x_1)$ is constant.

With the control law (8.17), the transfer function of the open loop system without the notch filter is obtained by using the Laplace transform

$$G(s) = \frac{K}{(v_x s + \theta)}. \tag{8.19}$$

And the open loop transfer function with the notch filter is

$$L(s) = G(s)N(s) = \frac{K}{(v_x s + \theta)} \frac{(\frac{s}{\omega_n})^2 + \frac{2\zeta_n s}{\omega_n} + 1}{(\frac{s}{\omega_n})^2 + \frac{2\zeta_d s}{\omega_n} + 1}. \tag{8.20}$$

In order to fully understand the impact of the notch filter on the delay margin of our control law, we have to obtain the analytical expression of the delay margin.

To any transfer function $H(s)$ one can associate its gain $\gamma_H(\omega)$, at a given frequency, which is defined by the relation

$$\gamma_H(\omega) = 20 \log |H(j\omega)|. \tag{8.21}$$

The gain crossover frequency $\omega_c(H)$ is defined as the solution of the equation $\gamma_H(\omega) = 0$. This frequency can be used to define $\phi_c(H)$ as the argument of $H(j\omega_c(H))$, and the delay margin $\Delta(H)$ by the relation

$$\Delta(H) = \frac{\pi + \phi_c(H)}{\omega_c(H)}. \tag{8.22}$$

If there are several gain crossover frequencies, the delay margin is

$$\Delta(H) = \min_i \frac{\pi + [\phi_c(H)]_i}{[\omega_c(H)]_i}. \tag{8.23}$$

When there is no gain crossover frequency we define $\Delta(H) = +\infty$.

Without the notch filter, one can easily obtain the gain crossover frequency of $G(s)$

$$\omega_c(G) = \frac{\sqrt{K^2 - \theta^2}}{v_x}, \tag{8.24}$$

and the delay margin:

$$\Delta(G) = \frac{\pi + \phi_c(G)}{\omega_c(G)}, \tag{8.25}$$

where $\phi_c(G) = \arctan(\frac{-v_x\omega_c(G)}{\theta})$.

Nevertheless, it is much more difficult to find the delay margin expression of the system with notch filter from $L(s)$. Assume that the gain crossover frequencies of $L(s)$ and $G(s)$ are close. Then, we can approximate $L(s)$ in the neighborhood of the crossover frequency $\omega_c(G)$ in order to get a simpler transfer function of $L(s)$. In the next paragraph, we will see that the delay margin given by the approximative transfer function of $L(s)$ is quite accurate.

Our first approximation is the Padé approximation, a very good approximation of a function by a rational function of a given order. However, the calculation of the necessary components for the Padé approximation is complex. Therefore, a second approximation which is less accurate but simpler, is carried out. Based on the Taylor series, we approximate separately the numerator

$$N_L(s) = K(s^2 + 2\zeta_n\omega_n s + \omega_n^2) \tag{8.26}$$

and the denominator

$$D_L(s) = (v_x s + \theta)(s^2 + 2\zeta_d\omega_n s + \omega_n^2) \tag{8.27}$$

of $L(s)$ in the neighborhood of $\omega_c(G)$. The approximation of $L(j\omega)$ is given by these two approximations of the numerator and denominator

$$\tilde{L}(j\omega) = \frac{N_L(j\omega_c(G)) + j(\omega - \omega_c(G))\frac{dN_L}{ds}(j\omega_c(G))}{D_L(j\omega_c(G)) + j(\omega - \omega_c(G))\frac{dD_L}{ds}(j\omega_c(G))}, \tag{8.28}$$

or equivalently

$$\tilde{L}(j\omega) = \frac{a + j\omega c}{c + j\omega d}, \tag{8.29}$$

where a, b, c, d are complex coefficients

$$\begin{aligned} a &= N_L(j\omega_c(G)) - j\omega_c(G)\frac{dN_L}{ds}(j\omega_c(G)) \\ b &= \frac{dN_L}{ds}(j\omega_c(G)) \\ c &= D_L(j\omega_c(G)) - j\omega_c(G)\frac{dD_L}{ds}(j\omega_c(G)) \\ d &= \frac{dN_L}{ds}(j\omega_c(G)), \end{aligned} \tag{8.30}$$

with

$$\begin{aligned} \frac{dN_L}{ds}(j\omega_c(G)) &= K(2s + 2\zeta_n\omega_n) \\ \frac{dD_L}{ds}(j\omega_c(G)) &= v_x(s^2 + 2\zeta_d\omega_n s + \omega_n^2) + (v_x s + \theta)(2s + 2\zeta_n\omega_n). \end{aligned} \tag{8.31}$$

Now we can describe the gain crossover frequency expression of $\tilde{L}(j\omega)$:

$$\omega_c(\tilde{L}) = \frac{-((a_i b_r - a_r b_i) - (c_i d_r - c_r d_i)) - \Delta'}{(|b|^2 - |d|^2)}, \tag{8.32}$$

where $a_r, a_i, b_r, b_i, c_r, c_i, d_r, d_i$ are respectively the real and imaginary parts of a, b, c, d; and

$$\Delta' = ((a_i b_r - a_r b_i) - (c_i d_r - c_r d_i))^2 - (|b|^2 - |d|^2)(|a|^2 - |c|^2). \tag{8.33}$$

The phase of $\tilde{L}$ is:

$$\phi_c(\tilde{L}) = \arctan\left(\frac{\tilde{L}_i}{\tilde{L}_r}\right), \tag{8.34}$$

where

$$\tilde{L}_i = (a_i + b_r\omega)(c_r - d_i\omega) - (a_r - b_i\omega)(c_i + d_r\omega), \tag{8.35}$$

and

$$\tilde{L}_r = (a_r - b_i\omega)(c_r - d_i\omega) + (a_i + b_r\omega)(c_i + d_r\omega). \tag{8.36}$$

Therefore, at the end, the expression for the approximate delay margin of $\tilde{L}(j\omega)$ is given by

$$\Delta(\tilde{L}) = \frac{\pi + \phi_c(\tilde{L})}{\omega_c(\tilde{L})}. \tag{8.37}$$

8.4.2 Robustness of the notch-filtered feedback

In order to ensure the stability of the closed loop system, the delay margin of the control law has to be superior than the total delay in the loop (which, is typically,

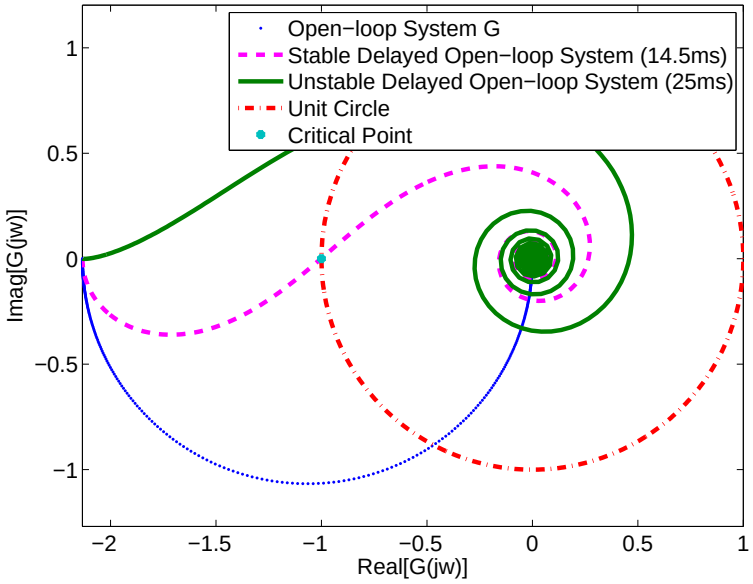

Figure 8.5: The Nyquist plot of $G(j\omega)$, in the unstable region, where $\mu'(x_1) < 0$. The vehicle speed is 33 km/h and the control gain $K = 800$.

around 15 ms). And this constraint should be respected for every vehicle speed, from 0 to 180 km/h.

A natural idea to study the impact of using the notch filter in the control law is thus to try to keep a constant delay margin $\Delta(G) = D$ for the system, independently of the vehicle's speed (in our study, we fix $D = 25$ ms.). But this is possible only when $\mu'(x_1) \leq 0$. Indeed, when $\mu'(x_1) > 0$ the stability of the system produces an infinite delay margin $\Delta(G) = +\infty$, when the speed of the vehicle is low. That is, the stability of the system is maintained independently of the value of the loop delays.

When $\mu'(x_1) = 0$, taking a gain of the form

$$K = K_a v_x$$

gives a constant delay margin for $G(s)$, independently of the speed. But when $\mu'(x_1) \neq 0$ the situation is more complicated. For $\mu'(x_1) > 0$ one can still take $K = K_b v_x$, but the delay margin will increase (which is not a bad thing) when the speed of the vehicle decreases. For $\mu'(x_1) < 0$ one can obtain a constant delay margin if we compute numerically the value of $K(v_x)$ that gives the correct margin, for each v_x. But, this, only when the speed is big enough. Indeed, when the vehicle's speed v_x is too small, it might be impossible to obtain the prescribed delay margin of 25 ms.

Once the value of K fixed, for each speed v_x, we compared the difference between the delay margin of the original system $G(s)$ to that of the system that uses our notch

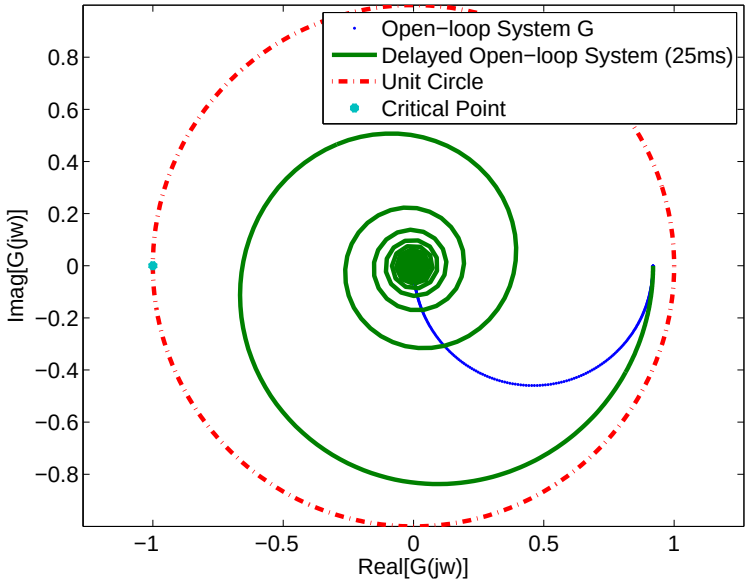

Figure 8.6: The Nyquist plot of $G(j\omega)$, in the stable region, where $\mu'(x_1) > 0$. The vehicle speed is 70 km/h and the control gain $K = 1723$.

filter $L(s)$. The results are plotted in Figures 8.7 - 8.12. One can observe that there are some speeds for which the corresponding delay margins are not represented. For these speeds, either: (a) the system is stable independently of the delay magnitude (the delay margin is infinite) or (b) it is impossible to obtain the prescribed delay margin of 25 ms. The Nyquist plots corresponding to those two different situations are shown of Figures 8.5 and 8.6.

8.5 Conclusion

In this chapter, we proposed a stable dynamic notch filter that is able to eliminate periodic disturbances on the wheel acceleration, even when the vehicle speed is variable. We showed, in two applicative examples, that this filter improves the ABS performance. An inconvenient of using the notch filter is that the control law is less robust with respect to delay. In the near future, we will test the notch filter effect for both continuous and hybrid ABS algorithms on an experimental setup.

Appendix A - Alternative modelling of the notch filter

We present here an alternative modelling of the notch filter. The main difference of this modelling is that it doesn't use the second and the third derivatives of the input signal $x(t)$, but only $x(t)$. This alternative modelling is also taken in two steps: the constant vehicle speed in the first step and the variable vehicle speed in the second one.

We develop (8.1)

$$\begin{aligned} Y(s) &= \frac{[(\frac{s}{\omega_n})^2 + \frac{2\zeta_d s}{\omega_n} + 1] + \frac{2(\zeta_n - \zeta_d)s}{\omega_n}}{(\frac{s}{\omega_n})^2 + \frac{2\zeta_d s}{\omega_n} + 1} X(s) \\ &= X(s) + \frac{\frac{2(\zeta_n - \zeta_d)s}{\omega_n}}{(\frac{s}{\omega_n})^2 + \frac{2\zeta_d s}{\omega_n} + 1} X(s) \\ &= X(s) + sZ(s), \end{aligned} \tag{8.38}$$

where

$$Z(s) = \frac{\frac{2(\zeta_n - \zeta_d)}{\omega_n}}{(\frac{s}{\omega_n})^2 + \frac{2\zeta_d s}{\omega_n} + 1} X(s). \tag{8.39}$$

In the first step when the vehicle speed is constant, we can transform (8.39) into the time domain

$$\frac{1}{f^2(v_0)} \frac{d^2 z}{dt^2} + \frac{2\zeta_n}{f(v_0)} \frac{dz}{dt} + z = \frac{2(\zeta_n - \zeta_d)}{f(v_0)} x, \tag{8.40}$$

with $\omega_n = f(v_0) = v_0/R$. Then we obtain

$$\frac{d^2 z}{dt^2} = -f^2(v_0) z - 2\zeta_d f(v_0) \frac{dz}{dt} + 2(\zeta_n - \zeta_d) f(v_0) x. \tag{8.41}$$

For two states defined as

$$z_1 = f(v_0) z \quad \text{and} \quad z_2 = \frac{dz}{dt}, \tag{8.42}$$

we obtain the following state space representation

$$\begin{aligned} \frac{dz_1}{dt} &= f(v_0) z_2 \\ \frac{dz_2}{dt} &= f(v_0)(-z_1 - 2\zeta_d z_2 + 2(\zeta_n - \zeta_d) x). \end{aligned} \tag{8.43}$$

In the new time scale s defined by (8.7), the dynamics (8.43) becomes

$$\begin{aligned} \frac{dz_1}{ds} &= z_2 \\ \frac{dz_2}{ds} &= -z_1 - \alpha z_2 + 2(\zeta_n - \zeta_d)x, \end{aligned} \tag{8.44}$$

with $\alpha = 2\zeta_d$. The eigenvalues of (8.43) in the new time scale are $(-\alpha \pm \sqrt{\alpha^2 - 4})/2$. Therefore, the dynamics (8.43) is stable.

From (8.38), we get

$$y = x + \frac{dz}{dt}. \tag{8.45}$$

We define then the output of (8.43) as $z_2 = dz/dt$ to get the filtered signal $y(t)$.

In the second step when the vehicle longitudinal speed v_x is variable, the state space representation becomes

$$\begin{aligned} \frac{dz_1}{ds} &= z_2 \\ \frac{dz_2}{ds} &= -z_1 - \alpha z_2 + 2(\zeta_n - \zeta_d)x. \end{aligned} \tag{8.46}$$

where the two states are

$$z_1 = f(v_x)z \quad \text{and} \quad z_2 = \frac{dz}{dt}, \tag{8.47}$$

and the output signal is

$$y = x + z_2. \tag{8.48}$$

Appendix B - Padé approximation

The Padé approximation is a very good approximation of a function by a rational function of a given order. In this technique, the approximant's power series agree with the power series of the function it is approximating. We recall here the principle of the Padé approximation [Baker 1996].

Given a formal series expansion

$$f(z) = \sum_{i=0}^{\infty} c_i z^i, \tag{8.49}$$

the [L/M] Padé approximant to $f(z)$ is a rational function of the form

$$[L/M] = \frac{a_0 + a_1 z + a_2 z^2 + ... + a_L z^L}{b_0 + b_1 z + b_2 z^2 + ... + b_M z^M}, \tag{8.50}$$

that satisfies

$$f(z) = \sum_{i=0}^{\infty} c_i z^i = \frac{a_0 + a_1 z + a_2 z^2 + ... + a_L z^L}{b_0 + b_1 z + b_2 z^2 + ... + b_M z^M} + O(z^{L+M+1}) \tag{8.51}$$

with $b_0 = 1$.

By cross-multiplying, we find that

$$(1 + b_1 z + b_2 z^2 + ... + b_M z^M)(c0 + c_1 z + ...) = a_0 + a_1 z + a_2 z^2 + ... + a_L z^L. \tag{8.52}$$

Equaling the coefficients of $1, z, ..., z^L$, we obtain immediately the L following equations where the unknown coefficients are $a_1, a_2, ..., a_L$

$$\begin{aligned} a_0 &= c_0 \\ a_1 &= c_1 + b_1 c_0 \\ &\vdots \\ a_L &= c_L + \sum_{i=1}^{min(L,M)} b_i c_{L-i}, \end{aligned} \tag{8.53}$$

while equating the coefficients of $z^{L+1}, z^{L+2}, ..., z^{L+M}$, we get M equations where the unknown coefficients are $b_1, b_2, ..., b_M$.

Now, we try to get [1/1] Padé approximation of $L(s)$ in the neighborhood of the crossover frequency $\omega_c(G)$ of $G(s)$. We define

$$\varepsilon = (\omega - \omega_c(G)). \tag{8.54}$$

Firstly, we need to have the Taylor series of $L(s)$ in the neighborhood of $\omega_c(G)$, to at least the second order

$$\begin{aligned} L(j\omega) &= L(j\omega_c(G)) + j\varepsilon L'(j\omega_c(G)) + \frac{(j\varepsilon)^2}{2!} L''(j\omega_c(G)) + O((j\omega)^3) \\ &= f(j\varepsilon), \end{aligned} \tag{8.55}$$

where

$$L(j\omega_c(G)) = \frac{K}{(j\omega_c(G)v_x + \theta)} \frac{(j\omega_c(G))^2 + 2\zeta_n j\omega_c(G)\omega_n + \omega_n^2}{(j\omega_c(G))^2 + 2\zeta_d j\omega_c(G)\omega_n + \omega_n^2}, \tag{8.56}$$

$$\begin{aligned} L'(j\omega_c(G)) =& \frac{-K}{(j\omega_c(G)v_x+\theta)^2}\,\frac{1}{((j\omega_c(G))^2+2\zeta_d j\omega_c(G)\omega_n+\omega_n^2)^2}\times \\ & \Big(j\omega_c(G))^4+2(j\omega_c(G))^2\omega_n^2+4\zeta_n\omega_n(j\omega_c(G))^3+ \\ & 4\omega_n^3\zeta_d j\omega_c(G)+4\zeta_n\zeta_d\omega_n^2(j\omega_c(G))^2+\omega_n^4\Big), \end{aligned} \tag{8.57}$$

and

$$\begin{aligned} L''(j\omega_c(G)) =& \frac{2k}{(j\omega_c(G)v_x+\theta)^3}\,\frac{1}{((j\omega_c(G))^2+2\zeta_d j\omega_c(G)\omega_n+\omega_n^2)^3}\times \\ & \Big((j\omega_c(G))^6+\omega_n^6+12\zeta_n\zeta_d\omega_n^2(j\omega_c(G))^4+8\zeta_n\zeta_d^2\omega_n^3(j\omega_c(G))^3+ \\ & 3(j\omega_c(G))^4\omega_n^2+3(j\omega_c(G))^2\omega_n^4+14(j\omega_c(G))^3\omega_n^3\zeta_d+6\zeta_n(j\omega_c(G))^5\omega_n \\ & -2\zeta_n(j\omega_c(G))^3\omega_n^3+12\omega_n^4\zeta_d^2(j\omega_c(G))^2+6\omega_n^5\zeta_d j\omega_c(G)\Big). \end{aligned} \tag{8.58}$$

The [1/1] Padé approximation of $L(s)$ (or, in other words, of $f(j\varepsilon)$) is

$$L_P(j\varepsilon)=\frac{a_0+a_1(j\varepsilon)}{1+b1(j\varepsilon)} \tag{8.59}$$

The coefficients of the [1/1] Padé approximant of L are then computed as follows

$$\begin{aligned} a_0 &= L(j\omega_c(G)) \\ b_1 &= \frac{-L''(j\omega_c(G))}{2L'(j\omega_c(G))} \\ a_1 &= L'(j\omega_c(G))+b_1L(j\omega_c(G)). \end{aligned} \tag{8.60}$$

It is obvious that $a_0,\ a_1,\ b_1$ could be complex numbers. We denote $a_{0r},\ a_{1r}$ and b_{1r} the real parts of a_0, a_1 and b_1, respectively; and a_{0i}, a_{1i}, and b_{1i} the imaginary parts of a_0, a_1, and b_1, respectively.

The crossover frequency of $L_P(j\varepsilon)$ is computed by the following equation

$$\left|\frac{a_0+a_1j\varepsilon}{1+b_1j\varepsilon}\right|=1, \tag{8.61}$$

or,

$$\left|\frac{(a_{0r}-a_{1i}\varepsilon)+j(a_{0i}+a_{1r}\varepsilon)}{(1-b_{1i}\varepsilon)+jb_{1r}\varepsilon}\right|=1, \tag{8.62}$$

and we obtain the second order equation

$$(|a_1|^2 - |b_1|^2)\varepsilon^2 + 2(a_{0i}a_{1r} - a_{0r}a_{1i} + b_{1i})\varepsilon + (|a_0|^2 - 1) = 0. \tag{8.63}$$

The solutions of this equation are

$$\varepsilon_{1,2} = \frac{-(a_{0i}a_{1r} - a_{0r}a_{1i} + b_{1i}) \pm \sqrt{(a_{0i}a_{1r} - a_{0r}a_{1i} + b_{1i})^2 - (|a_1|^2 - |b_1|^2)(|a_0|^2 - 1)}}{(|a_1|^2 - |b_1|^2)}. \tag{8.64}$$

By using Matlab, we notice that the right root is

$$\varepsilon_2 = \frac{-(a_{0i}a_{1r} - a_{0r}a_{1i} + b_{1i}) - \sqrt{(a_{0i}a_{1r} - a_{0r}a_{1i} + b_{1i})^2 - (|a_1|^2 - |b_1|^2)(|a_0|^2 - 1)}}{(|a_1|^2 - |b_1|^2)}, \tag{8.65}$$

thus, the crossover frequency of L_P is

$$\omega_c(L_P) = \omega_c(G) + \varepsilon_2. \tag{8.66}$$

We rewrite the [1/1] Padé approximation (8.59) as

$$L_P(j\varepsilon) = \frac{(a_{0r} - a_{1i}\varepsilon) + j(a_{0i} + a_{1r}\varepsilon)}{(1 - b_{1i}\varepsilon) + jb_{1r}\varepsilon}. \tag{8.67}$$

Based on this frequency formula, we can compute the argument of $L_P(j\varepsilon)$

$$\phi_c(L_P) = \arctan\left(\frac{(a_{0i} + a_{1r}\varepsilon_2)(1 - b_{1i}\varepsilon_2) - (a_{0r} - a_{1i}\varepsilon_2)b_{1r}\varepsilon_2}{(a_{0r} - a_{1i}\varepsilon_2)(1 - b_{1i}\varepsilon_2) + (a_{0i} + a_{1r}\varepsilon_2)b_{1r}\varepsilon_2}\right). \tag{8.68}$$

Therefore, the time delay margin of the [1/1] Padé approximation of $L(s)$ is expressed as

$$\Delta(L_P) = \frac{\pi + \phi_c(L_P)}{\omega_c(L_P)} \qquad (s). \tag{8.69}$$

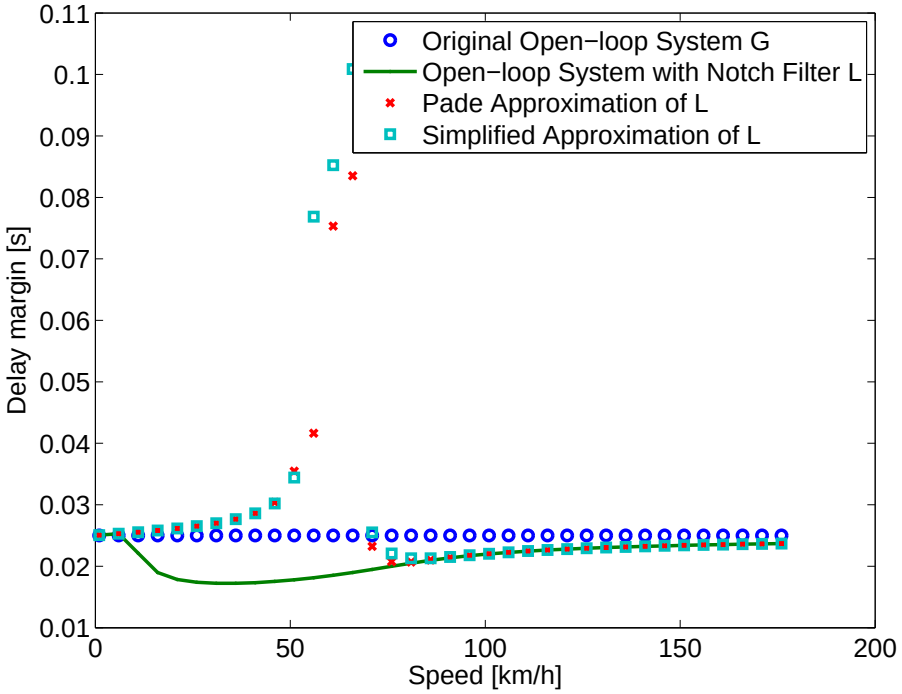

Figure 8.7: For an optimal wheel slip, when $\mu'(x_1) = 0$. The delay margin is constant $\Delta(G) = 25\,\text{ms}$ and $K = 63\,v_x$. The filter's quality factor is $\zeta_d = 0.1$.

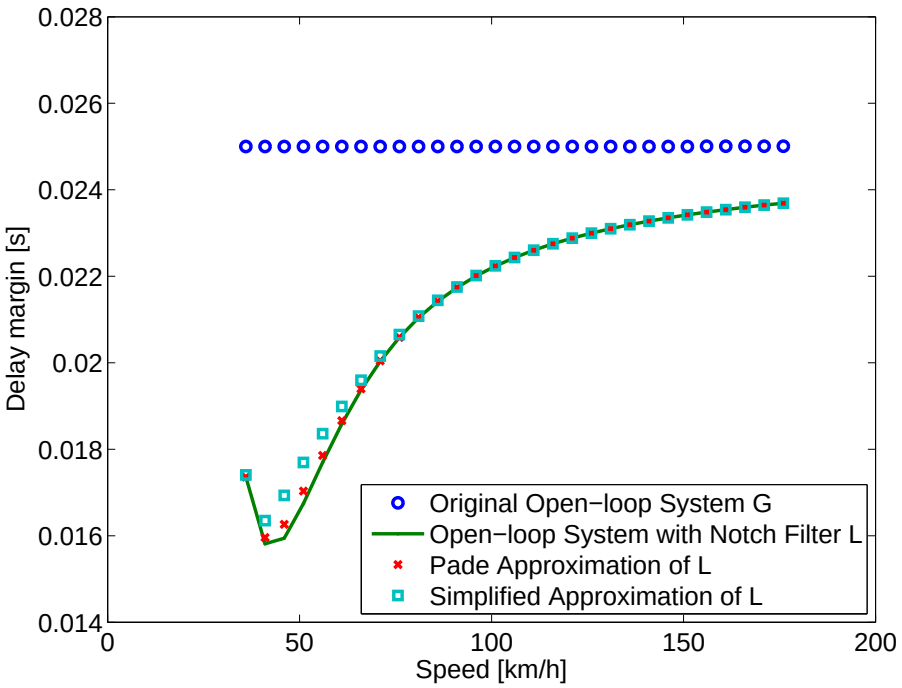

Figure 8.8: In the unstable region, when $\mu'(x_1) < 0$. The delay margin is constant $\Delta(G) = 25\,\text{ms}$. The filter's quality factor is $\zeta_d = 0.1$.

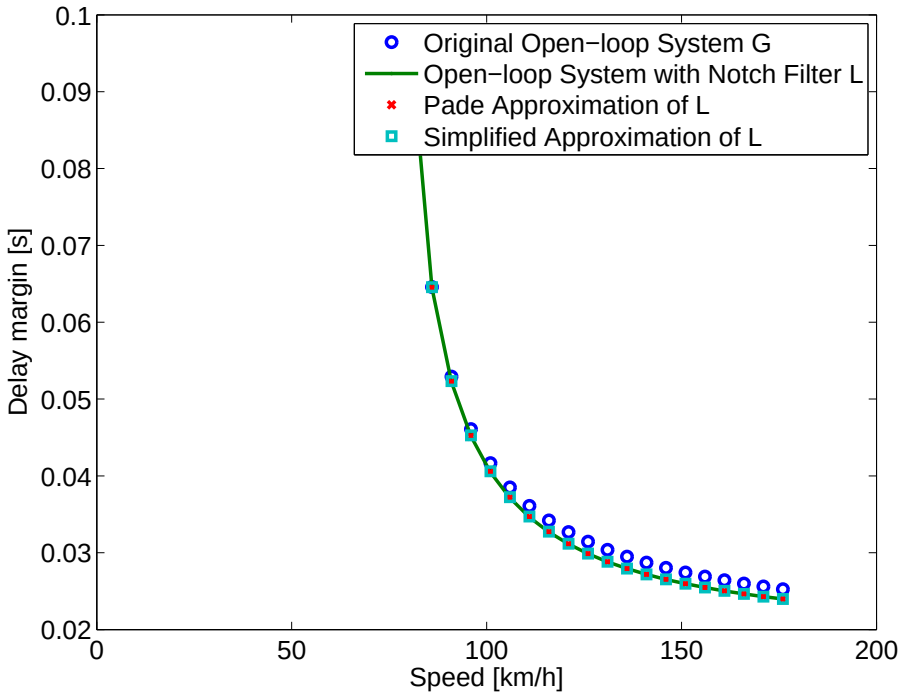

Figure 8.9: In the stable region, when $\mu'(x_1) > 0$. The delay margin is $\Delta(G) \geq 25$ms for the control gain $K = 89\, v_x$. The filter's quality factor is $\zeta_d = 0.1$.

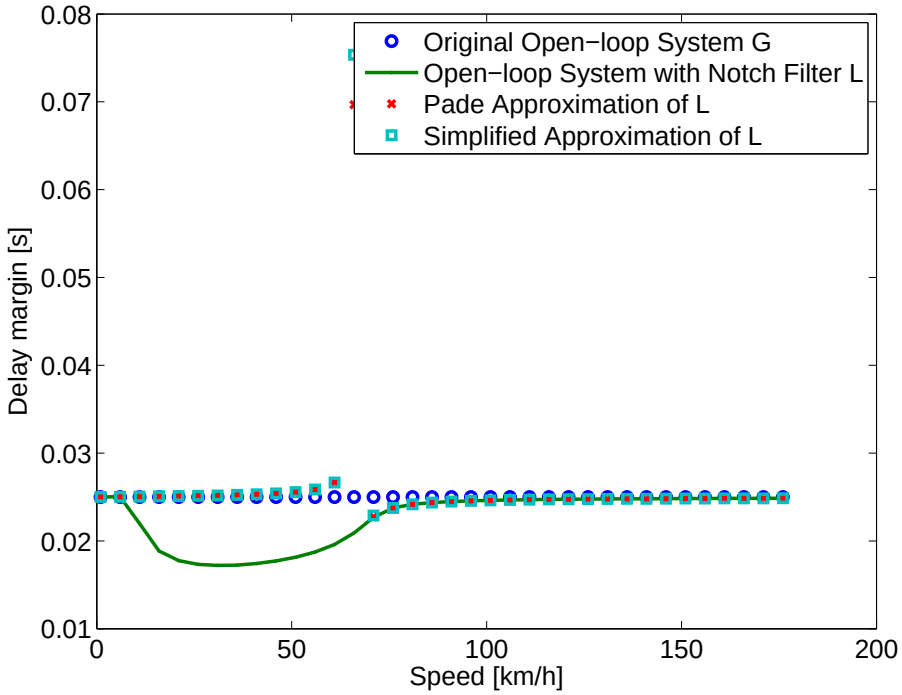

Figure 8.10: For an optimal wheel slip, when $\mu'(x_1) = 0$. The delay margin is constant $\Delta(G) = 25\,\text{ms}$ and $K = 63\, v_x$. The filter's quality factor is $\zeta_d = 0.01$.

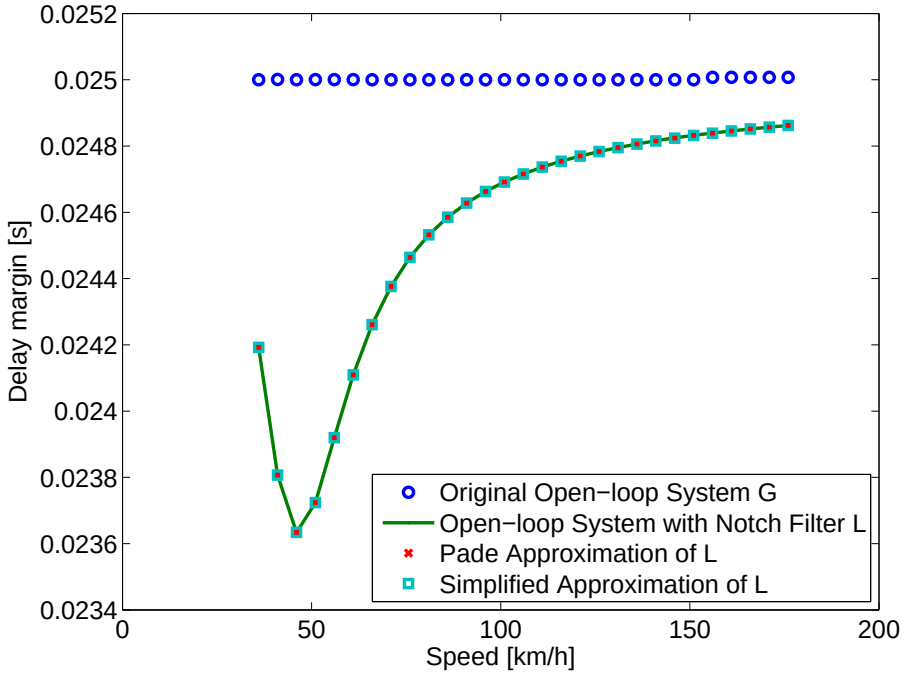

Figure 8.11: In the unstable region, when $\mu'(x_1) < 0$. The delay margin is constant $\Delta(G) = 25\,\text{ms}$. The filter's quality factor is $\zeta_d = 0.01$.

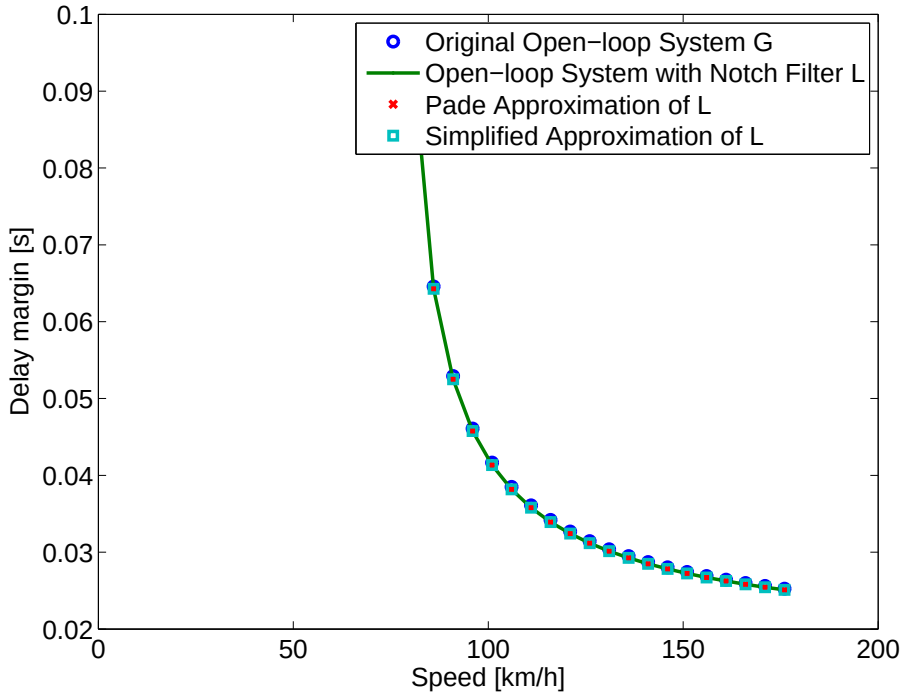

Figure 8.12: In the stable region, when $\mu'(x_1) > 0$. The delay margin is $\Delta(G) \geq 25\text{ms}$ for the control gain $K = 89\,v_x$. The filter's quality factor is $\zeta_d = 0.01$.

Conclusion & Perspectives

Conclusion

In this thesis, several theoretical and practical issues associated to ABS systems have been investigated, such as the estimation of unmeasured parameters, the compensation of input delays induced by actuators, and the reduction of disturbances in the wheel acceleration.

The objective of the thesis has been to improve the robustness of current ABS systems with respect to actuator delays or changes in the environment (as changes in the road conditions, brake properties, tyre properties, etc.), and adapt them (for instance the Bosch ABS algorithm) to other advanced actuators like electric in-wheel motors. To that aim, two general methods for the observation and delay compensation of two particular classes of nonlinear systems have been provided. By using these theoretical results, the issues of interest in the thesis, in the context of ABS systems, have then been solved.

In Part I, a systematic technique to construct a time-rescaling based switching observer that can estimate the state of a class of singular systems with scalar output has been presented. Our first main contribution is devoted to analyzing the observer stability, which is proved in Theorems 4.1 and 4.2 of Section 4.2. The proof of Theorem 4.1 has been presented in Section 4.5 ; while Theorem 4.2 is a direct consequence of Theorem 4.1 and Theorem 4 of [Hespanha 2004].

A concrete application of the observation of singular systems is the extended braking stiffness estimation in the case of ABS systems, which is our second main contribution. The observer has been validated on data coming from the tyre-in-the-loop experimental facility of TU Delft, acquired in the context of ABS research [Gerard 2012]. We would like to stress that this result is original, since to our knowledge, the idea of exploiting the nonlinear XBS in a model-based observer has not been considered in the literature, at least in the case of the longitudinal stiffness.

The third main contribution of this thesis, which is related to the input delay compensation for restricted feedback linearizable systems in the context of the output tracking problem, has been shown in Chapter 6 of Part II. A control law that can compensate the input delays and achieve the tracking control goal has been provided. This control law uses the prediction of the future of the system's state, which are estimated based on a stable procedure, through the integration of a desired error dynamics that can be chosen to be both stable and linear.

We will describe in the following some limitations of the present work. First, the compensation of the input delay for ABS systems hasn't been completely theoretically handled. Applying the theoretical results obtained in Chapter 6, a simple scheme

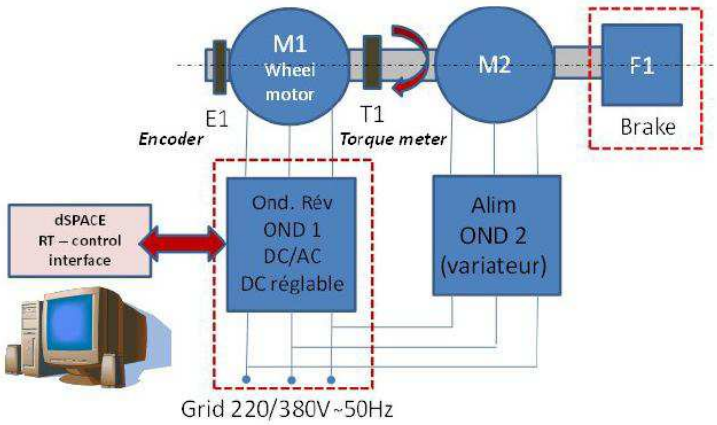

Figure 8.13: Synoptic of the modular test bench in IFSTTAR LTN.

for compensating the input delays has been shown in Chapter 7, but a theoretical analysis of the control law stability was lacked due to its complexity. The proposed method has been tested by numerical simulations to show it effectiveness, and real experiments are part of the future work.

Second, the combined convergence of the observer and of the control law, which are presented in the wheel acceleration control in Chapter 5, has not been proved. The main reason is that this convergence proof is not our main interest in the thesis, but rather the design of the observer and its stability analysis and its application in the wheel acceleration control has been done only for illustration purposes.

Third, several experimental tests couldn't be performed during the time span of the thesis. The validation of the dynamic notch filter could not yet be done on the LTN test bench within the thesis time. Nevertheless, the next step (at the beginning 2014) will be the validation of the notch filter on an assembly : electrical asynchronous motor with its position encoder - converter - electromagnetic power brake at LTN laboratory, and managed by FPGA-based Real-Time dSPACE prototyping interface. A short description of the system is given in the perspective section. The experiments of the input delay compensation and of the observation with changes of road conditions were planned to be tested in the test-rig of TU Delft. While the first one hasn't been done due to the lack of theoretical proof of the stability analysis of the proposed method, the second one hasn't been realized since changes of road conditions are not possible in the test-rigs of TU Delft.

Perspectives

Several possible directions can be proposed for future research of this thesis. First, the theoretical results obtained in the thesis should be tested in test-rigs. As said above, a test bench is being developed in IFSTTAR-LTN for the validation of the notch filter for both hybrid and continuous ABS algorithms. Nevertheless, the main interest of the test bench is that it will permit to test drive functionalities of an electric vehicle (EV) traction chain and linked with driving assistance concepts (ABS, TCS, regenerative braking). The test bench will be basically composed of an electronic converter supplying an electrical AC motor, a load (generator or electromagnetic brake) and having a position encoder for the control strategy (position rotor tops). The whole system is managed using a modular FPGA-based dSPACE Real-Time prototyping interface which will permit to control the AC motor in the torque/speed frame. The transmitted power of the test bench is envisaged between $4-10$kW. The test bench prototype is shown in Figure 8.13. The construction of this test bench is expected to be finished at the end of 2014, but it needs only the AC motor, the position encoder and the electronic converter in order to validate the effect of the notch filter. Therefore, these experiments are expected to be realized at the beginning of 2014.

The validation of the proposed observer, when there are changes in road conditions, is impossible in test-rigs like those of TU Delft due to their configuration. One possible direction is to carry out experiments on a test vehicle that can be found either in LIVIC or at TU Delft.

Future research on delay compensation for ABS is required in order to obtain a theoretical proof of the stability of the proposed method. Besides, since the dynamics (7.2) isn't in the form of restricted feedback linearizable systems (6.20), an alternative choice is therefore to extend our approach to a more general class of systems.

Second, future research should prove the combined convergence between the observer and the control in wheel acceleration control. Such a proof can be expected to be obtained via cascaded design arguments [Loría 2005]. Indeed, the closed-loop system is composed of the tracking error dynamics and the observer error dynamics. Conditions for which the observer error dynamics is exponentially stable have been shown in Theorem 5.1. Without the observer error, the tracking error dynamics is stable if the control gain is taken big enough. Since both the real and estimated XBS are bounded, the closed-loop system then can be proved to be exponentially stable, with the help of cascade arguments. The main delicate point is, however, the switching property of the observer since there exists no theoretical results in the literature on cascade arguments associated to the switches.

Finally, it is worth mentioning that the achievement of the objective of Part I is not equivalent to the fact that the problem of observing the class of singular

systems (2.10) is totally solved. This problem is, in fact, much more complex, due to the interaction between the controller and the observer. In order to completely solve this problem, three different problems with an increasing order of complexity must be considered. The first problem is the objective of Part I, which is the observation of singular systems around a reference trajectory that is generated by an appropriate (open-loop) control $u(t)$. The second problem is the observation of singular systems around a reference trajectory that is generated by a closed-loop control $u(t)$. The third problem involves the use of the observer to stabilize singular systems around of an equilibrium point.

Bibliography

[Ait-Hammouda 2008] I. Ait-Hammouda and W. Pasillas-Lépine. *Jumps and synchronization in anti-lock brake algorithms*. In Proceedings of the International Symposium on Advanced Vehicle Control, Kobe (Japan), 2008. (Cited on pages 79 and 93.)

[Andrieu 2006] V. Andrieu and L. Praly. *On the existence of a Kazantzis–Kravaris/Luenberger observer*. SIAM Journal on Control and Optimization, vol. 45, no. 2, pages 432–456, 2006. (Cited on pages 29 and 50.)

[Angeli 1999] D. Angeli. *A note on stability of arbitrarily switched homogeneous systems*. Nonlinear Control Abstracts, vol. 1, no. 13, 1999. (Cited on pages 53 and 85.)

[Arcak 2001] M. Arcak and P. Kokotović. *Nonlinear observers: A circle criterion design and robustness analysis*. Automatica, vol. 37, no. 12, pages 1923–1930, 2001. (Cited on page 30.)

[Artstein 1982] Z. Artstein. *Linear systems with delayed controls: A reduction*. IEEE Transactions on Automatic Control, vol. 27, no. 4, pages 869–879, 1982. (Cited on pages 42, 105 and 106.)

[Baker 1996] G.A. Baker and P.R. Graves-Morris. Padé approximants, volume 59. Cambridge University Press, 1996. (Cited on page 143.)

[Balde 2009] M. Balde, U. Boscain and P. Mason. *A note on stability conditions for planar switched systems*. International Journal of Control, vol. 82, no. 10, pages 1882–1888, 2009. (Cited on page 22.)

[Bernard 2002] O. Bernard and J.L. Gouzé. *State estimation for bioprocesses*. In ICTP Lecture Notes Series — Summer School on Mathematical Control Theory. 2002. (Cited on pages 27 and 49.)

[Besançon 2007] G. Besançon, D. Georges and Z. Benayache. *Asymptotic state prediction for continuous-time systems with delayed input and application to control*. In Proceedings of the European Control Conference, Kos (Grece), 2007. (Cited on page 105.)

[Besançon 1996] G. Besançon and H. Hammouri. *On uniform observation of non-uniformly observable systems*. Systems and Control Letters, vol. 29, no. 1, pages 9–19, 1996. (Cited on page 30.)

[Besançon 2000] G. Besançon. *Remarks on nonlinear adaptive observer design*. Systems and Control Letters, vol. 41, no. 4, pages 271–280, 2000. (Cited on pages 30 and 83.)

[Besançon 2007] G. Besançon and A. Ticlea. *An immersion-based observer design for rank-observable nonlinear systems*. IEEE Transactions on Automatic Control, vol. 52, no. 1, pages 83–88, 2007. (Cited on page 30.)

[Besançon 2013] G. Besançon, I. Rubio Scola and D. Georges. *About input selection in observer design for non-uniformly observable systems*. In Proceedings of the IFAC Symposium on Nonlinear Control Systems, Toulouse (France), 2013. (Cited on pages 30 and 50.)

[Bestle 1983] D. Bestle and M. Zeitz. *Canonical form observer design for nonlinear time-variable systems*. International Journal of Control, vol. 38, no. 2, pages 419–431, 1983. (Cited on page 28.)

[Bornard 1991] G. Bornard and H. Hammouri. *A high gain observer for a class of uniformly observable systems*. In Proceedings of the IEEE Conference on Decision and Control, pages 1494–1496, Brighton (England), 1991. (Cited on pages 20, 26, 28 and 50.)

[Bosch Automotive Technology 2013] Siteweb of Bosch Automotive Technology. *Driving-safety systems for passenger cars: Active safety*. http://www.bosch-automotivetechnology.com/en/de/driving_safety/driving_safety_systems_for_passenger_cars_1/active_safety/active_safety_2.html, 2013. (Cited on page 9.)

[Bosch 2004] R. Bosch. Bosch Automotive Handbook, volume 74. Bentley, Cambridge, 2004. (Cited on pages 11, 13, 37 and 77.)

[Brockett 1979] R.W. Brockett. *Feedback invariants for nonlinear systems*. In Proceedings of the IFAC World Congress, Helsinki (Finland), 1979. (Cited on pages 4, 107 and 110.)

[Burckhardt 1993] M. Burckhardt. Fahrwerktechnik: Radschlupf-Regelsysteme. Vogel-Verlag, Germany, 1993. (Cited on pages 16, 34, 57 and 82.)

[Cheng 2003] D. Cheng and W. Lin. *On p-normal forms of nonlinear systems*. IEEE Transactions on Automatic Control, vol. 48, no. 7, pages 1242–1248, 2003. (Cited on page 111.)

[Choi 2008] S.B. Choi. *Antilock brake system with a continuous wheel slip control to maximize the braking performance and the ride quality*. IEEE Transactions on Control Systems Technology, vol. 16, no. 5, pages 996–1003, 2008. (Cited on pages 13 and 78.)

[Corno 2012] M. Corno, M. Gerard, M. Verhaegen and E. Holweg. *Hybrid ABS Control Using Force Measurement*. IEEE Transactions on Control Systems Technology, vol. 20, no. 5, pages 1223–1235, 2012. (Cited on page 78.)

[Corno 2013] M. Corno, G. Panzani and S.M. Savaresi. *Traction-control-oriented state estimation for motorcycles*. IEEE Transactions on Control Systems Technology, vol. 21, no. 6, pages 2400–2407, 2013. (Cited on page 95.)

[Daiss 1995] A. Daiss and U. Kiencke. *Estimation of vehicle speed: Fuzzy-estimation in comparison with Kalman-filtering*. In Proceedings of the IEEE Conference on Control Applications, pages 281–284, Albany (USA), 1995. (Cited on pages 83 and 95.)

[Dayawansa 1985] W. Dayawansa, W.M. Boothby and D.L. Elliott. *Global state and feedback equivalence of nonlinear systems*. Systems and Control Letters, vol. 6, no. 4, pages 229–234, 1985. (Cited on pages 44 and 111.)

[Daytona Tin Tec 2013] Siteweb of Daytona Tin Tec. `http://www.daytona-twintec.com/tech_twin_scan3.html`, 2013. (Cited on page 10.)

[de Castro 2010] R. de Castro, R.E. Araujo, J.S. Cardoso and D. Freitas. *A new linear parametrization for peak friction coefficient estimation in real time*. In Proceedings of the IEEE Vehicle Power and Propulsion Conference, pages 1–6, Lille (France), 2010. (Cited on page 32.)

[de Castro 2012] R. de Castro, R.E. Araujo and D. Freitas. *Real-time estimation of tyre-road friction peak with optimal linear parameterisation*. IET Control Theory and Applications, vol. 6, no. 14, pages 2257–2268, 2012. (Cited on pages 36 and 89.)

[Dufour 2010] P. Dufour, S. Flila and H. Hammouri. *Nonlinear observers synthesis based on strongly persistent inputs*. In Proceedings of the IEEE Chinese Control Conference, pages 316–320, Beijing (China), 2010. (Cited on page 50.)

[Engelborghs 2001] K. Engelborghs, M. Dambrine and D. Roose. *Limitations of a class of stabilization methods for delay systems*. IEEE Transactions on Automatic Control, vol. 46, no. 2, pages 336–339, 2001. (Cited on pages 42, 44 and 106.)

[Eykhoff 1974] P. Eykhoff and P. Eykhoff. System identification: Parameter and state estimation. Wiley-Interscience London, 1974. (Cited on page 27.)

[Fan 2003] X. Fan and M. Arcak. *Observer design for systems with multivariable monotone nonlinearities*. Systems and Control Letters, vol. 50, no. 4, pages 319–330, 2003. (Cited on page 30.)

[Farza 2004] M. Farza, M. M'Saad and L. Rossignol. *Observer design for a class of MIMO nonlinear systems*. Automatica, vol. 40, no. 1, pages 135–143, 2004. (Cited on page 28.)

[Farza 2009] M. Farza, M. M'Saad, T. Maatoug and M. Kamoun. *Adaptive observers for nonlinearly parameterized class of nonlinear systems*. Automatica, vol. 45, no. 10, pages 2292–2299, 2009. (Cited on page 30.)

[Funahashi 1979] Y. Funahashi. *Stable state estimator for bilinear systems*. International Journal of Control, vol. 29, no. 2, pages 181–188, 1979. (Cited on page 30.)

[Gauthier 1981] J.P. Gauthier and G. Bornard. *Observability for any u(t) for a Class of Nonlinear Systems*. IEEE Transactions on Automatic Control, vol. 26, no. 4, pages 922–926, 1981. (Cited on pages 20, 25, 26 and 28.)

[Gauthier 1992] J.P. Gauthier, H. Hammouri and S. Othman. *A simple observer for nonlinear systems applications to bioreactors*. IEEE Transactions on Automatic Control, vol. 37, no. 6, pages 875–880, 1992. (Cited on pages 20, 26, 28 and 50.)

[Gauthier 1994] J.P. Gauthier and I. Kupka. *Observability and observers for nonlinear systems*. SIAM Journal on Control and Optimization, vol. 32, no. 4, pages 975–994, 1994. (Cited on pages 20, 26, 28 and 50.)

[Georges 2007] D. Georges, G. Besançon, Z. Benayache and E. Witrant. *A nonlinear state feedback design for nonlinear systems with input delay*. In Proceedings of the European Control Conference, Kos (Greece), 2007. (Cited on pages 43 and 105.)

[Gerard 2012] M. Gerard, W. Pasillas-Lépine, E.J.H. De Vries and M. Verhaegen. *Improvements to a five-phase ABS algorithm for experimental validation*. Vehicle System Dynamics, vol. 50, no. 10, pages 1585–1611, 2012. (Cited on pages 3, 14, 16, 17, 35, 37, 78, 79, 80, 81, 86, 91, 93, 95, 119, 121 and 151.)

[Guay 2002] M. Guay. *Observer linearization by output-dependent time-scale transformations*. IEEE Transactions on Automatic Control, vol. 47, no. 10, pages 1730–1735, 2002. (Cited on pages 4, 29 and 50.)

[Gustafsson 1997] F. Gustafsson. *Slip-based tire-road friction estimation*. Automatica, vol. 33, no. 6, pages 1087–1099, 1997. (Cited on page 31.)

[Gustafsson 1998] F. Gustafsson. *Monitoring tire-road friction using the wheel slip*. IEEE Control Systems Magazines, vol. 18, no. 4, pages 42–49, 1998. (Cited on pages 14 and 78.)

[Hammouri 2003] H. Hammouri and M. Farza. *Nonlinear observers for locally uniformly observable systems*. ESAIM: Control, Optimisation and Calculus of Variations, vol. 9, no. 1, pages 353–370, 2003. (Cited on pages 20 and 26.)

[Hara 1976] S. Hara and K. Furuta. *Minimal order state observers for bilinear systems*. International Journal of Control, vol. 24, no. 5, pages 705–718, 1976. (Cited on page 30.)

[Hespanha 1999] J.P. Hespanha and A.S. Morse. *Stability of switched systems with average dwell-time*. In Proceedings of the IEEE Conference on Decision and Control, volume 3, pages 2655–2660, Phoenix (USA), 1999. (Cited on page 22.)

[Hespanha 2004] J.P. Hespanha. *Uniform stability of switched linear systems: Extensions of LaSalle's invariance principle*. IEEE Transactions on Automatic

Control, vol. 49, no. 4, pages 470–482, 2004. (Cited on pages 22, 33, 34, 35, 50, 52, 53, 54, 79, 85, 86, 96, 97, 99 and 151.)

[Hildebrand 1974] F.B. Hildebrand. Introduction to numerical analysis — second edition. Dover Publications, 1974. (Cited on page 89.)

[Hoàng 2012] T.B. Hoàng, W. Pasillas-Lépine and A. De Bernardinis. *Reducing the impact of wheel-frequency oscillations in continuous and hybrid ABS strategies*. In Proceedings of the International Symposium on Advanced Vehicle Control, Seoul (Korea), 2012. (Cited on pages 78 and 93.)

[Hoàng 2013] T.B. Hoàng, W. Pasillas-Lépine and M. Netto. *Closed-loop wheel-acceleration control based on an extended braking stiffness observer*. In Proceedings of the American Control Conference, pages 2133–2138, Washington DC (USA), 2013. (Cited on pages 57, 58 and 59.)

[Hoàng 2014a] T.B. Hoàng, W. Pasillas-Lépine, A. De Bernardinis and M. Netto. Extended braking stiffness estimation based on a switched observer. Submitted to *IEEE Transactions on Control Systems Technology* (accepted), 2014. (Cited on page 57.)

[Hoàng 2014b] T.B. Hoàng, W. Pasillas-Lépine and W. Respondek. A switching observer for systems with linearizable error dynamics via singular time-scaling. Submitted to *Mathematical Theory of Networks and Systems* (under review), 2014. (Cited on pages 83, 86, 87 and 96.)

[Isidori 1995] A. Isidori. Nonlinear control systems. Springer Verlag, 1995. (Cited on page 56.)

[Johansen 2003] T.A. Johansen, I. Petersen, J. Kalkkuhl and J. Ludemann. *Gain-scheduled wheel slip control in automotive brake systems*. IEEE Transactions on Control Systems Technology, vol. 11, no. 6, pages 799–811, 2003. (Cited on pages 13 and 78.)

[Johnson 2001] A. Johnson. *From dynamometers to simulations: transforming brake testing technology into antilock braking systems*. In Instrumentation between Science, State and Industry, volume 22 of *Sociology of the Sciences*, pages 199–218. Springer, 2001. (Cited on page 9.)

[Johnson 2009] A. Johnson. Hitting the brakes: Engineering design and the production of knowledge. Duke University Press Books, 2009. (Cited on page 9.)

[Kalman 1960] R. Kalman. *A new approach to linear filtering and prediction problems*. Journal of Basic Engineering, vol. 82, no. 1, pages 35–45, 1960. (Cited on page 49.)

[Karafyllis 2006] I. Karafyllis. *Finite-time global stabilization by means of time-varying distributed delay feedback*. SIAM Journal on Control and Optimization, vol. 45, no. 1, pages 320–342, 2006. (Cited on page 43.)

[Kazantzis 1998] N. Kazantzis and C. Kravaris. *Nonlinear observer design using Lyapunov's auxiliary theorem*. Systems and Control Letters, vol. 34, no. 5, pages 241–247, 1998. (Cited on pages 29 and 50.)

[Kiencke 2000] U. Kiencke and L. Nielsen. Automotive Control Systems. Springer-Verlag New York, Inc., 2000. (Cited on pages 11, 12, 13, 77, 81, 82 and 129.)

[Kienhöfer 2008] F.W. Kienhöfer, J.I. Miller and D. Cebon. *Design concept for an alternative heavy vehicle ABS system*. Vehicle System Dynamics, vol. 46, no. S1, pages 571–583, 2008. (Cited on pages 17 and 37.)

[Koo 2012] M.S. Koo, H.L. Choi and J.T. Lim. *Global regulation of a class of feedforward and non-feedforward nonlinear systems with a delay in the input*. Automatica, vol. 48, no. 10, pages 2607–2613, 2012. (Cited on page 105.)

[Kou 1975] S.R. Kou, D.L. Elliott and T.J. Tarn. *Exponential observers for nonlinear dynamic systems*. Information and Control, vol. 29, no. 3, pages 204–216, 1975. (Cited on page 28.)

[Krener 1983] A.J. Krener and A. Isidori. *Linearization by output injection and nonlinear observers*. Systems and Control Letters, vol. 3, no. 1, pages 47–52, 1983. (Cited on pages 4, 28, 49 and 56.)

[Krener 1985] A.J. Krener and W. Respondek. *Nonlinear observers with linearizable error dynamics*. SIAM Journal on Control and Optimization, vol. 23, no. 2, pages 197–216, 1985. (Cited on pages 29, 49 and 56.)

[Krener 2002a] A.J. Krener and M.Q. Xiao. *Nonlinear observer design in the Siegel domain*. SIAM Journal on Control and Optimization, vol. 41, no. 3, pages 932–953, 2002. (Cited on pages 29 and 50.)

[Krener 2002b] A.J. Krener and M.Q. Xiao. *Observers for linearly unobservable nonlinear systems*. Systems and Control Letters, vol. 46, no. 4, pages 281–288, 2002. (Cited on page 29.)

[Krstic 1995] M. Krstic, I. Kanellakopoulos and P.V. Kokotovic. Nonlinear and adaptive control design. John Wiley and Sons New York, 1995. (Cited on page 111.)

[Krstic 2009] M. Krstic. Delay compensation for nonlinear, adaptive, and PDE systems. Birkhauser Boston, MA, 2009. (Cited on pages 43, 105 and 106.)

[Krstic 2010] M. Krstic. *Input delay compensation for forward complete and strict-feedforward nonlinear systems*. IEEE Transactions on Automatic Control, vol. 55, no. 2, pages 287–303, 2010. (Cited on pages 43, 105 and 107.)

[Kuo 1992] CY Kuo and EC Yeh. *A four-phase control scheme of an anti-skid brake system for all road conditions*. IMechE Part D: Journal of Automobile Engineering, vol. 206, no. 4, pages 275–283, 1992. (Cited on pages 13 and 77.)

[Leiber 1979] H. Leiber and A. Czinczel. *Antiskid system for passenger cars with a digital electronic control unit*. SAE paper, no. 790458, 1979. (Cited on pages 13, 77, 129 and 133.)

[Liberzon 1999] D. Liberzon and A.S. Morse. *Basic problems in stability and design of switched systems*. IEEE Control Systems Magazine, vol. 19, no. 5, pages 59–70, 1999. (Cited on page 85.)

[Liberzon 2003] D. Liberzon. Switching in systems and control. Springer, 2003. (Cited on pages 52 and 85.)

[Limpert 1992] R. Limpert. Brake design and safety. Society of Automotive Engineers, 1992. (Cited on page 9.)

[Lin 2009] H. Lin and P.J. Antsaklis. *Stability and stabilizability of switched linear systems: a survey of recent results*. IEEE Transactions on Automatic control, vol. 54, no. 2, pages 308–322, 2009. (Cited on page 22.)

[Ljung 1987] L. Ljung. System identification: theory for the user. Prentice Hall, 1987. (Cited on page 31.)

[Loría 2005] A. Loría and E. Panteley. *Cascaded Nonlinear Time-Varying Systems: Analysis and Design*. In F. Lamnabhi-Lagarrigue, A. Loría and E. Panteley, editeurs, Advanced Topics in Control Systems Theory, pages 579–579. Springer, 2005. (Cited on pages 95 and 153.)

[Luenberger 1964] D. Luenberger. *Observing the state of a linear system*. IEEE Transactions on Military Electronics, vol. 8, no. 2, pages 74–80, 1964. (Cited on pages 27 and 49.)

[Lyapunov 1992] A.M. Lyapunov. *The general problem of the stability of motion*. International Journal of Control, vol. 55, no. 3, pages 531–534, 1992. (Cited on page 29.)

[Madison 1969] R.H. Madison and H.E. Riordan. Evolution of sure-track brake system. Society of Automotive Engineers, 1969. (Cited on page 9.)

[Manitius 1979] A. Manitius and A. Olbrot. *Finite spectrum assignment problem for systems with delays*. IEEE Transactions on Automatic Control, vol. 24, no. 4, pages 541–552, 1979. (Cited on pages 42, 105 and 106.)

[Marino 1990] R. Marino. *Adaptive observers for single output nonlinear systems*. IEEE Transactions on Automatic Control, vol. 35, no. 9, pages 1054–1058, 1990. (Cited on pages 29 and 49.)

[Marino 1995] R. Marino and P. Tomei. Nonlinear control design: geometric, adaptive and robust. Prentice Hall International (UK) Ltd., 1995. (Cited on page 111.)

[Mazenc 2004] F. Mazenc, S. Mondie and R. Francisco. *Global asymptotic stabilization of feedforward systems with delay in the input*. IEEE Transactions on Automatic Control, vol. 49, no. 5, pages 844–850, 2004. (Cited on page 43.)

[Mazenc 2006] F. Mazenc and P.A. Bliman. *Backstepping design for time-delay nonlinear systems*. IEEE Transactions on Automatic Control, vol. 51, no. 1, pages 149–154, 2006. (Cited on pages 43, 105 and 107.)

[Mazenc 2011a] F. Mazenc and S.I. Niculescu. *Generating positive and stable solutions through delayed state feedback*. Automatica, vol. 47, no. 3, pages 525–533, 2011. (Cited on pages 42 and 106.)

[Mazenc 2011b] F. Mazenc, S.I. Niculescu and M. Bekaik. *Stabilization of nonlinear systems with delay in the input through backstepping*. In Proceedings of the IEEE Conference on Decision and Control and the European Control Conference, pages 7605–7610, Orlando (USA), 2011. (Cited on pages 43, 105 and 107.)

[Mazenc 2012] F. Mazenc and D. Normand-Cyrot. *Stabilization of linear input delayed dynamics under sampling*. In Proceedings of the IEEE Conference on Decision and Control, pages 7523–7528, Hawaii (USA), 2012. (Cited on page 106.)

[Mboup 2009] M. Mboup, C. Join and M. Fliess. *Numerical differentiation with annihilators in noisy environment*. Numerical Algorithms, vol. 50, no. 4, pages 439–467, 2009. (Cited on page 32.)

[Miller 2013] J.I. Miller and D. Cebon. *An investigation of the effects of pneumatic actuator design on slip control for heavy vehicles*. Vehicle System Dynamics, vol. 51, no. 1, pages 139–164, 2013. (Cited on pages 4 and 37.)

[Moler 2003] C. Moler and C.V. Loan. *Nineteen dubious ways to compute the exponential of a matrix, twenty-five years later*. SIAM Review, vol. 45, no. 1, pages 3–49, 2003. (Cited on page 68.)

[Mom 1932] W. Mom. *An Improved Safety Device for Preventing the Jamming of the Running Wheels of Automobiles when Braking*. UK Patent No. 382241A, 1932. (Cited on page 9.)

[Mondié 2003] S. Mondié and W. Michiels. *Finite spectrum assignment of unstable time-delay systems with a safe implementation*. IEEE Transactions on Automatic Control, vol. 48, no. 12, pages 2207–2212, 2003. (Cited on pages 42, 44, 106 and 116.)

[Morse 1995] A.S. Morse. *Control using logic-based switching*. In Trends in Control: A European Perspective, pages 69–113. Springer, 1995. (Cited on page 77.)

[Moya 2002] P. Moya, R. Ortega, M. Netto, L. Praly and J. Picó. *Application of nonlinear time-scaling for robust controller design of reaction systems*. International Journal of Robust and Nonlinear Control, vol. 12, no. 1, pages 57–69, 2002. (Cited on page 50.)

[M'sirdi 2006] N.K. M'sirdi, A. Rabhi, L. Fridman, J. Davila and Y. Delanne. *Second order sliding mode observer for estimation of velocities, wheel sleep, radius and stiffness*. In Proceedings of the American Control Conference, pages 3316–3321, Minneapolis (USA), 2006. (Cited on page 32.)

[Niculescu 2001] S.I. Niculescu. Delay effects on stability: A robust control approach. Springer, 2001. (Cited on pages 105 and 108.)

[Nijmeijer 1990] H. Nijmeijer and A.J. Van der Schaft. Nonlinear dynamical control systems. Springer, 1990. (Cited on page 56.)

[Ohyay 2011] A. Ohyay. Sliding mode control algorithm development for anti-lock brake system. Master's thesis, Middle East Technical University, Çankaya Ankara (Turquie), 2011. (Cited on page 9.)

[Olson 2003] B.J. Olson, S.W. Shaw and G. Stépán. *Nonlinear dynamics of vehicle traction*. Vehicle System Dynamics, vol. 40, no. 6, pages 377–399, 2003. (Cited on page 79.)

[Ono 2003] E. Ono, K. Asano, M. Sugai, S. Ito, M. Yamamoto, M. Sawada and Y. Yasui. *Estimation of automotive tire force characteristics using wheel velocity*. Control Engineering Practice, vol. 11, no. 12, pages 1361–1370, 2003. (Cited on pages 3, 14, 15, 19, 31, 78, 79 and 83.)

[Pacejka 2005] H. Pacejka. Tyre and vehicle dynamics. Elsevier, 2005. (Cited on pages 82, 86 and 87.)

[Panteley 2001] E. Panteley, A. Loría and A. Teel. *Relaxed persistency of excitation for uniform asymptotic stability*. IEEE Transactions on Automatic Control, vol. 46, no. 12, pages 1874–1886, 2001. (Cited on page 118.)

[Pasillas-Lépine 2006] W. Pasillas-Lépine. *Hybrid modeling and limit cycle analysis for a class of five-phase anti-lock brake algorithms*. Vehicle System Dynamics, vol. 44, no. 2, pages 173–188, 2006. (Cited on pages 14, 59, 79, 82, 88, 91, 93, 126 and 135.)

[Pasillas-Lépine 2010] W. Pasillas-Lépine and A. Loría. *A new mixed wheel slip and acceleration control based on a cascaded design*. In Proceedings of the IFAC Symposium on Nonlinear Control System, Bologna (Italy), 2010. (Cited on pages 129, 133 and 134.)

[Pasillas-Lépine 2012] W. Pasillas-Lépine, A. Loría and M. Gerard. *Design and experimental validation of a nonlinear wheel slip control algorithm*. Automatica, vol. 48, no. 8, pages 1852–1859, 2012. (Cited on pages 13, 16, 78, 95 and 121.)

[Prony 1795] R. Prony. *Essai expérimental et analytique: sur les lois de la dilatabilité de fluides élastique et sur celles de la Force expansive de la vapeur de l'eau et de la vapeur de l'alkool, à différentes températures*. Journal de l'Ecole Polytechnique (Paris), vol. 1, no. 2, pages 24–76, 1795. (Cited on page 89.)

[Raghavan 1994] S. Raghavan and J.K. Hedrick. *Observer design for a class of nonlinear systems*. International Journal of Control, vol. 59, no. 2, pages 515–528, 1994. (Cited on pages 28 and 30.)

[Rajamani 2012] R. Rajamani. Electronic stability control. Springer, 2012. (Cited on pages 10 and 11.)

[Respondek 1986] W. Respondek. *Global aspects of linearization, equivalence to polynomial forms and decomposition of nonlinear control systems.* In Algebraic and Geometric Methods in Nonlinear Control Theory, pages 257–284. Springer, 1986. (Cited on pages 44 and 111.)

[Respondek 2001] W. Respondek, A. Pogromsky and H. Nijmeijer. *Time-scaling for linearization of observable dynamics.* In Proceedings of the IFAC Symposium on Nonlinear Control Systems, pages 563–568, St. Petersburg (Russia), 2001. (Cited on page 29.)

[Respondek 2002] W. Respondek. *Introduction to Geometric Nonlinear Control: Linearization, Observability, Decoupling.* In ICTP Lecture Notes Series — Summer School on Mathematical Control Theory, volume 1, pages 169–222. 2002. (Cited on pages 26, 44 and 111.)

[Respondek 2003] W. Respondek. *Transforming a single-input system to a p-normal form via feedback.* In Proceedings of the IEEE Conference on Decision and Control, pages 1574–1579, Maui (USA), 2003. (Cited on page 111.)

[Respondek 2004] W. Respondek, A. Pogromsky and H. Nijmeijer. *Time scaling for observer design with linearizable error dynamics.* Automatica, vol. 40, no. 2, pages 277–285, 2004. (Cited on pages 4, 28, 29, 50, 51 and 56.)

[Richard 2003] J.P. Richard. *Time-delay systems: an overview of some recent advances and open problems.* Automatica, vol. 39, no. 10, pages 1667–1694, 2003. (Cited on pages 42, 105 and 106.)

[Robert Bosch GmbH Press Release 2013] Siteweb of Robert Bosch GmbH Press Release. *From innovation to standard equipment 30 years of safe braking with Bosch ABS.* http://www.bosch.co.jp/en/press/group-0807-05.asp, 2013. (Cited on page 10.)

[Savaresi 2007] S.M. Savaresi, M. Tanelli and C. Cantoni. *Mixed slip-deceleration control in automotive braking systems.* ASME Journal of Dynamic Systems, Measurement, and Control, vol. 129, no. 1, pages 20–31, 2007. (Cited on pages 13 and 78.)

[Savaresi 2010] S.M. Savaresi and M. Tanelli. Active braking control systems design for vehicles. Springer, 2010. (Cited on pages 9, 10, 11 and 129.)

[Schinkel 2002] M. Schinkel. *Nondeterministic hybrid dynamical systems.* PhD thesis, University of Glasgow, Scotland (UK), 2002. (Cited on page 9.)

[Shida 2010] Z. Shida, R. Sakurai, M. Watanabe, Y. Kano and M. Abe. *A study on effects of tire characteristics on stop distance of abs braking with simplified model.* In Proceedings of the International Symposium on Advanced Vehicle Control, Loughborough (UK), 2010. (Cited on pages 3 and 78.)

[Sipahi 2011] R. Sipahi, S.I. Niculescu, C.T. Abdallah, W. Michiels and K. Gu. *Stability and stabilization of systems with time delay*. IEEE Control Systems Magazine, vol. 31, no. 1, pages 38–65, 2011. (Cited on page 105.)

[Smith 1959] O.J.M. Smith. *A controller to overcome dead time*. ISA Journal, vol. 6, no. 2, pages 28–33, 1959. (Cited on pages 41 and 105.)

[Solyom 2003] S. Solyom, A. Rantzer and J. Kalkkuhl. *A benchmark for control of Anti-lock Braking Systems*. Lund Institute of Technology, Lund (Sweden), 2003. (Cited on pages 17 and 37.)

[Solyom 2004] S. Solyom, A. Rantzer and J. Lüdemann. *Synthesis of a model-based tire slip controller*. Vehicle System Dynamics, vol. 41, no. 6, pages 475–499, 2004. (Cited on pages 17 and 37.)

[Sugai 1999] M. Sugai, H. Yamaguchi, M. Miyashita, T. Umeno and K. Asano. *New control technique for maximizing braking force on antilock braking system*. Vehicle System Dynamics, vol. 32, no. 4-5, pages 299–312, 1999. (Cited on pages 3, 14, 78 and 79.)

[Tanelli 2009] M. Tanelli, L. Piroddi and S.M. Savaresi. *Real-time identification of tire-road friction conditions*. Control Theory and Applications, vol. 3, no. 7, pages 891–906, 2009. (Cited on pages 32, 36, 79 and 89.)

[Thau 1973] F.E. Thau. *Observing the state of nonlinear dynamic systems*. International Journal of Control, vol. 17, no. 3, pages 471–479, 1973. (Cited on page 28.)

[Thomas 1936] F.B. Thomas and P. Irwin. *Apparatus for Preventing Wheel Sliding*. US Patent No. 2038144, 1936. (Cited on page 9.)

[Tsinias 1989] J. Tsinias. *Observer design for nonlinear systems*. Systems and Control Letters, vol. 13, no. 2, pages 135–142, 1989. (Cited on page 28.)

[Tsinias 1993] J. Tsinias. *Sontag's input to state stability condition and global stabilization using state detection*. Systems and Control Letters, vol. 20, no. 3, pages 219–226, 1993. (Cited on page 28.)

[Umeno 2002] T. Umeno. *Estimation of Tire-Road Friction by Tire Rotational Vibration Model*. Research and Development Review Toyota CRDL, vol. 37, pages 53–58, 2002. (Cited on page 31.)

[Unsal 1999] C. Unsal and P. Kachroo. *Sliding mode measurement feedback control for antilock braking systems*. IEEE Transactions on Control Systems Technology, vol. 7, no. 2, pages 271–281, 1999. (Cited on pages 13 and 78.)

[Van Assche 1999] V. Van Assche, M. Dambrine, J.F. Lafay and J.P. Richard. *Some problems arising in the implementation of distributed-delay control laws*. In Proceedings of the IEEE Conference on Decision and Control, volume 5, pages 4668–4672, Phoenix (USA), 1999. (Cited on page 42.)

[Van Zanten 2002] A.T. Van Zanten. *Evolution of electronic control systems for improving the vehicle dynamic behavior*. In Proceedings of the International Symposium on Advanced Vehicle Control, pages 1–9, Hiroshima (Japan), 2002. (Cited on page 78.)

[Villagra 2011] J. Villagra, B. d'Andréa Novel, M. Fliess and H. Mounier. *A diagnosis-based approach for tire-road forces and maximum friction estimation*. Control engineering practice, vol. 19, no. 2, pages 174–184, 2011. (Cited on pages 32 and 79.)

[Walcott 1987] B. Walcott and S. Zak. *State observation of nonlinear uncertain dynamical systems*. IEEE Transactions on Automatic Control, vol. 32, no. 2, pages 166–170, 1987. (Cited on page 30.)

[Wang 1998] Q.G. Wang, T.H. Lee and K.K. Tan. Finite-spectrum assignment for time-delay systems, volume 239. Springer Verlag, 1998. (Cited on page 42.)

[Watanabe 1981] K. Watanabe and M. Ito. *A process-model control for linear systems with delay*. IEEE Transactions on Automatic Control, vol. 26, no. 6, pages 1261–1269, 1981. (Cited on page 42.)

[Wellstead 1997] P.E. Wellstead and N.B.O.L. Pettit. *Analysis and redesign of an antilock brake system controller*. IEE Proceedings — Control Theory and Applications, vol. 144, no. 5, pages 413–426, 1997. (Cited on page 9.)

[Zegelaar 1998] P.W.A. Zegelaar. *The dynamic response of tyres to brake torque variations and road unevennesses*. PhD thesis, Delft University of Technology, Delft (Netherlands), 1998. (Cited on page 87.)

[Zeitz 1987] M. Zeitz. *The extended Luenberger observer for nonlinear systems*. Systems and Control Letters, vol. 9, no. 2, pages 149–156, 1987. (Cited on page 27.)

[Zhang 2002] Q. Zhang. *Adaptive observer for multiple-input multiple-output (MIMO) linear time-varying systems*. IEEE Transactions on Automatic Control, vol. 47, no. 3, pages 525–529, 2002. (Cited on page 31.)